Enhancing the Solar Still Performance Using Nanofluid-Based Volumetric Absorption Solar Collector and Solar Pond: An Experimental Investigation

A thesis

submitted on partial fulfillment of the requirement for the award of the degree of

Doctor of Philosophy

in

Mechanical Engineering

by

Jagteshwar Singh

(Reg. No. 951708003)

MECHANICAL ENGINEERING DEPARTMENT

THAPAR INSTITUTE OF ENGINEERING AND TECHNOLOGY,

PATIALA-147004, INDIA

(Declared as Deemed-to-be University u/s of the UGC Act, 1956 Vide Notification No. F9-12-84-U.3 of G.O.I)

OCTOBER – 2023

DECLARATION

I, **Jagteshwar Singh** hereby certify that the work presented in this thesis report entitled "**Enhancing the Solar Still Performance Using Nanofluid-Based Volumetric Absorption Solar Collector and Solar Pond: An Experimental Investigation**" in partial fulfillment of the requirement for the award of the degree of **Doctor of Philosophy** and submitted in Mechanical Engineering department of Thapar Institute of Engineering & Technology, Patiala, is an authentic record of my own research work carried out during a period from July 2017 to February 2023 under the supervision of **Dr. Madhup Kumar Mittal,** Associate Professor and **Dr. Vikrant Khullar**, Associate Professor, Mechanical Engineering Department of Thapar Institute of Engineering & Technology, Patiala. The matter presented in this thesis has not been submitted by me for the award of any other degree of this or any other Institute.

Jagteshwar Singh

(Registration no. 951708003)

This is to certify that the above statement made by the candidate is correct to the best of our knowledge and belief.

Dr. Madhup Kumar Mittal

(Supervisor)

Associate Professor, Mechanical Engineering Department Thapar Institute of Engineering & Technology, Patiala

Dr. Vikrant Khullar

(Supervisor)

Associate Professor, Mechanical Engineering Department Thapar Institute of Engineering & Technology, Patiala

Acknowledgements

I would like to express my sincere gratitude to my supervisors Dr. Madhup Kumar Mittal, Associate Professor and Dr. Vikrant Khullar, Associate Professor, Department of Mechanical Engineering, Thapar Institute of Engineering & Technology, Patiala, for introducing the present topic and for their inspiring guidance, constructive criticism, essential support, valuable suggestions and constant encouragement during the entire research work. I really feel privileged to have worked under their supervision. I express my sincere thanks to the members of my doctoral research committee Dr. T.K. Bera, Professor and Head, Department of Mechanical Engineering, Thapar Institute of Engineering & Technology; Dr. R.K. Gupta, Professor and Head, Department of Chemical Engineering, Thapar Institute of Engineering & Technology; Dr. Amandeep Singh Oberoi, Assistant Professor, Department of Mechanical Engineering, Thapar Institute of Engineering & Technology and Dr. Rohit Kumar Singla, Assistant Professor, Department of Mechanical Engineering, Thapar Institute of Engineering & Technology for providing necessary facilities and valuable suggestions throughout this research work and in the submission of this manuscript. I am very thankful to Head of Central Workshop, Department of Mechanical Engineering, Thapar Institute of Engineering & Technology, for providing the necessary facilities in the workshop to fabricate the experimental set-up. I am also thankful to all workshop staff, specially Mr. Rakęsh Kumar, Sheet Metal Shop Instructor, Department of Mechanical Engineering, Thapar Institute of Engineering & Technology for all their help provided during the fabrication stage of the experimental set-up. I extend my warm thanks to all teaching and non-teaching staff, Department of Mechanical Engineering, Thapar Institute of Engineering & Technology for their day-to-day co-operation. I am thankful to M.E. students Mr. Shubham, Mr.

Sudhir Singh and Mr. Vijay for their support in fabrication work of experimental setup, and experimental work.

Special regards to my wife, Surinder Kaur and friends whose blessings and wishes helped me to reach this end.

Finally, I owe deeply to my parents, Kamaljit Kaur (Mother) and Harkewal Singh (Father), who, despite their sufferings and sacrifices, continued to extend their moral support, encouragement, and financial support, helped me reach the target for which I shall ever remain indebted.

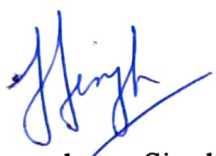

(Jagteshwar Singh)

Abstract

The aim of the present research work is not only to enhance the diurnal distillate output but also to generate nocturnal distillate and, in turn, enhance the performance of the solar still. In the present work, a novel nanofluid-based volumetric absorption solar collector (NBVASC) has been employed for efficiently harnessing the solar energy and supplying the same to solar still during sunshine hours for improving its diurnal production rate. A convective solar pond has also been used for supplying the stored sensible thermal energy to the basin of the solar still via heat exchangers during the non-sunshine period to produce the nocturnal distillate, which makes the system a 'round-the-clock' unit to produce potable water. The research work was done in a proper sequence and hence the complete research was done in three phases.

In the study's first phase, a novel nanofluid-based volumetric absorption solar collector (NBVASC) was fabricated to provide supplementary thermal energy to the modified solar still during sunshine hours. It was fabricated by constructing a shallow container, filling it with nanofluid and covering its top surface with two closely spaced transparent glass covers. The base and sidewalls of the solar collector have been insulated with polyurethane foam to reduce the thermal losses to the surroundings. Further, this foam was covered with a 1mm thick galvanized iron sheet to protect this insulation foam from weather conditions. A serpentine type of copper pipe heat exchanger (circulating ethylene glycol-based water-soluble heat transfer fluid, using a 12V DC pump having a rated power of 19 W) was also placed within the NBVASC to exchange the absorbed thermal energy from the solar collector to the water in the still. The NBVASC was filled with nanofluid, which was prepared by using a small amount of used engine oil acquired from a four-stroke diesel engine. After filtering the resin, sludge etc., with a cotton cloth, the filtered oil was then again refined with 0.7μm filter paper. The filtered oil was then mixed with

paraffin oil (followed by 30 minutes of ultra-sonication in a bath-type ultra-sonicator), consequently forming nanofluids of different concentrations (1.25mlL^{-1}, 2.5mlL^{-1}, and 5mlL^{-1}).

In the study's second phase, the fabricated NBVASC was coupled with the solar still to evaluate its impact on the performance of the modified solar still compared to the conventional solar still under identical outdoor conditions. The experiments were done on the modified still [MS] (CSASC- and NBVASC-coupled solar stills) and the conventional still at the same time for a number of days through the period from March to July 2020. In this phase, the optimum nanoparticle concentration that should be employed in the NBVASC for obtaining maximum distillate output was also identified. It was found that the solar still coupled with NBVASC (at optimum nanoparticle concentration of 1.25mlL^{-1}) performed better than the solar still coupled with paraffin oil-based conventional surface absorption-based solar collector (CSASC), suggesting that harvesting solar energy through volumetric absorption by nanofluids is more efficient and effective. The distillate productivity and efficiency of the modified still coupled with NBVASC (1.25 mlL^{-1}) were found to be 75.3 % and 66.9 % more than the conventional still. A significant amount of night distillate was obtained from the modified solar still (MS) coupled with NBVASC owing to the large quantity of thermal energy stored in the basin water at the end of the sunshine of the day. The night distillate produced by the modified still was found to be 33.9% higher than the conventional still.

In the third and final phase of the study, the solar still was tested for round-the-clock distillate production by integrating it with NBVASC during sunshine hours and with the solar pond during non-sunshine hours (integrated solar still). The thermal energy harnessed by the NBVASC was supplied continuously from 9:00 am to 6:00 pm, whereas the thermal energy stored in the solar

pond was supplied during night hours (1:00 am to 4:00 am). Floating wicks were also placed in the basin of the integrated still to enhance the evaporation rates and hence improving the overall distillate and efficiency of the still. Economic analysis and the payback period were also calculated, which can be used to carry out commercial feasibility studies before the installation of similar types of solar desalination units in any part of the world. The integrated solar stills performed better than conventional still in all the experiments when coupled with the solar collector (9 am to 6 pm) and solar pond (1 am to 4 am), whether with or without wicks. The integrated solar still without wicks, when coupled with a paraffin oil-based surface absorption solar collector during sunshine hours and with a solar pond during the night, showed an increase of 44.8% and 33.6% over conventional solar still in productivity and efficiency, respectively. The integrated solar still with wicks, when coupled with the paraffin oil-based solar collector during sunshine hours and with solar pond during the night, showed an increase of 74.3% and 50.2% over conventional solar still in productivity and efficiency, respectively. The integrated solar still without wicks, when coupled with nanofluid (1.25 mlL^{-1}) based volumetrically absorbing solar collector (NBVASC) during sunshine hours and with solar pond during night hours, showed an increase of 64.9% and 66.4% over conventional solar still in productivity and efficiency, respectively. The integrated solar still with wicks, when coupled with nanofluid (1.25 mlL^{-1}) based volumetric absorption solar collector (NBVASC) during sunshine hours and with solar pond during night hours, showed an increase of 111.1% and 89.4% over conventional solar still in productivity and efficiency, respectively. A considerable amount of night distillate (after 1 am) was produced by integrated solar stills (with and without wicks) due to the coupling of integrated stills with the solar pond at night; there was a maximum increase of 268.9% in productivity compared to conventional still when integrated still has wicks in its basin. Manufacturing cost has increased by 59.1%, whereas

distillate production cost decreased by 32.5% relative to conventional still. Exergy efficiency was 3.40% when wicks were used in the basin of integrated solar still coupled with NBVASC, and conventional still had the lowest with a value of 1.48%. The typical winter and summer day distillate produced by the modified stills coupled with NBVASC and the solar pond was found to be 2.05 L/m^2/day and 4.62 L/m^2/day, respectively. The diurnal and nocturnal distillate produced during summer experiments was 144.02% and 64.52% higher than in winter.

Contents

List of publications from present work

(i) Singh, J., M. K. Mittal, and V. Khullar. (2021) Experimental study of single-slope solar still coupled with nanofluid-based volumetric absorption solar collector. Journal of Solar Energy Engineering 144 (1):144. doi:10.1115/1.4052478.

Publisher: ASME

Impact factor: 2.384

(ii) Singh, J., Mittal, M. K., & Khullar, V. (2022). Nanofluid-based wick-type integrated solar still for improved diurnal and nocturnal distillate production. Energy Sources, Part A: Recovery, Utilization, and Environmental Effects, 44(4), 10094-10115.

Publisher: Taylor and Francis

Impact factor: 2.902

Nomenclature

A_b	Basin surface area, m^2
C	Specific heat of heat transfer fluid, kJ/kg/K
G_T	Overall solar radiation impinging on the still, kJ/m^2/day
h_{fg}	Latent heat of water, kJ/kg
$\dot{m}$	heat transfer fluid flow rate in heat exchanger, kg/sec
m_d	Mass of distillate, kg
P_p	Pump rating, W
Q_{sc}	Heat energy provided to modified still from the solar collector, kJ
W_p	Pump work, kJ
Δt	Average temperature difference of HTF at inlet & outlet of basin still HE, ^oC
m_i	Yield produced by integrated still, l/m^2
m_c	Yield produced by conventional still, l/m^2
Q_{sp}	Heat energy provided to integrated still from the solar pond, kJ
R_e	Reynolds number
d	Diameter of the pipe, m
v	Velocity of the fluid, m/s

f	Coefficient of friction
l	Pipe length, m
g	Acceleration due to gravity, m/s^2
h_f	Frictional head loss, m
h_h	Horizontal head loss, m
h_b	Head loss due to bends, m
h_v	Vertical head loss, m
n	Total number of bends
P	Pump power, kW
h	Total head loss, m

Greek letters

η	Efficiency, %
τ	Overall running time of the pump, sec
ρ	Fluid density, kg/m^3
μ	Dynamic viscosity of the fluid, Ns/m^2

Abbreviations

CPVC	Chlorinated polyvinyl chloride

CSASC	Conventional surface absorption based solar collector
HE	Heat exchanger
HTF	Heat transfer fluid
MS	Modified still
CS	Conventional/reference solar still
NBVASC	Nanofluid based volumetric absorption solar collector
FPC	Flat plate collector
PV/T	Photovoltaic thermal
NCSP	Non-convective solar pond
PTC	Parabolic trough collector
ETC	Evacuated tube collector
PCM	Phase change material

List of Figures

List of Tables

Chapter 1

Introduction

1.1 General background

Conventional fossil fuel energy sources are on the verge of extinction as they are being used up at a fast rate. Due to the growing population and increasing energy demands, the available conventional energy resources are under tremendous stress and are being exploited beyond restoration. The need of the hour is to cut down the dependence on conventional energy resources, and exploration of non-conventional or renewable sources is warranted. One of the renewable, clean and abundantly available sources of energy is solar energy. It can be utilized for air heating [1–3], water heating [4], refrigeration [5], solar drying [6], desalination [7–9] etc.

Drinkable water is one of the essential necessities for our existence. Earth has plenty of water, but most of it is in the oceans and is not fit for drinking purposes because of its high salt content. The availability of clean water is quite scarce, particularly in poor, underdeveloped and remote areas. The people living in these areas have to rely on contaminated water resources, which are often filled with dirt and garbage and are a potential danger to their overall health and development [10]. The non-drinkable water can be made drinkable by using thermal, mechanical and chemical desalination techniques. All these techniques use either heat energy or electricity generated from conventional fossil fuels. Given the huge potential, solar energy-based distillation systems are promising contenders to produce drinkable water. However, presently, these systems constitute only about 0.01% of the incumbent desalination units [11]. This may be attributed to the low distillate output of the incumbent solar energy-based desalination technologies. In particular, to

engineer efficient solar-driven desalination processes, efficient photo-thermal energy conversion and its subsequent transfer to the water (to be purified) to maximize evaporation is warranted. In other words, an optimized solar desalination system requires the efficient collection of solar energy [12–15] and employing efficient heat transfer methods [16].

Among the existing solar energy-driven desalination systems, single slope solar still is a very uncomplicated solar desalination platform for transforming saline/impure water into potable water, particularly in remote under-developed areas. In the past, tremendous effort has been made for the distillate output improvement from solar by supplying extra heat from extrinsic devices such as flat plate collectors (FPCs) [17,18], concentrating collectors [19,20], hybrid PVT collectors [21–23] and solar ponds [24,25].

Herein, the basic idea and constructional details of solar distillation particularly using solar stills, are presented. The emphasis of the present research is on developing methods for the improvement of the efficiency of solar stills via the use of nanofluid-based volumetric absorption solar collector (NBVASC) and solar pond; hence, the brief introduction of nanofluids (NBVASC) and solar pond is also discussed in this chapter. Objectives of the current work are detailed at the end of this chapter.

1.2 Solar distillation and solar still

The process of purifying water by utilising solar thermal energy for heating the impure water to vaporize it and separate it from contaminants; and then condensing the water vapours to obtain purified water is known as solar distillation.

The apparatus which utilises solar energy to transform impure water into pure drinkable form is known as solar still. Figure 1.1 depicts the conventional single-slope solar still using a line

diagram. Essentially, it consists of a basin-liner which absorbs solar radiation, water basin which houses the water to be distilled, and a transparent cover through which the sunlight enters; also, this cover acts as the condensing surface for the vapours in the still. For a single slope solar still, photo-thermal energy conversion results in heating of the basin water; this results in accelerated vaporization of basin water, which condenses and is then collected from the inside of the glass coverings.

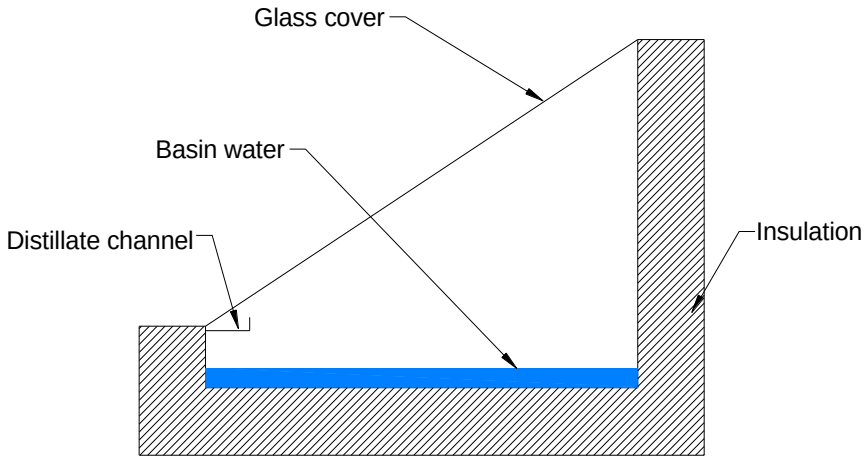

Fig. 1.1 Conventional single-slope solar still

1.3 Passive and active solar still

In a passive type solar still, the solar energy that is able to go all the way through the transparent glass covering and get to the basin-liner causes the basin water temperature to rise, and there is no additional source of heat which is supplied to this system. Therefore, its operation is restricted to sunlight hours only (with basin water temperatures not reaching very high values) and hence relatively low distillate output. To circumvent the issue of low distillate output, active solar stills have been built and investigated. Herein, basin water is supplied with heat from solar ponds, flat plate collectors, and concentrating collectors [11]. Active Solar stills could be in natural and forced circulation (without or

with pump) modes. Additionally supplied energy increases the basin water temperature (to relatively high values), which increases the vaporization rate and, hence, improves distillate output.

1.4 Nanofluids

Nanofluids are essentially stable dispersions of nanoparticles in base fluids. These exhibits improved thermophysical and optical characteristics. In light of the growing need for compact systems in today's technological landscape, nanofluids may be used as a practical alternative to conventional heat transfer fluids. Researchers were motivated to explore renewable energy sources like solar thermal power because of growing environmental and energy security issues. Thus, developing efficient solar thermal systems is crucial. Nanoparticles (being very small in size) when dispersed in the base fluid substantially increase the effective surface area where the absorption of solar energy can happen. Opposed to surface absorption, volumetric absorption via nanofluids has been shown to increase the effective absorption area by more than 300 times [15]. As a result of which a relatively high temperature can be achieved in volumetric based collectors compared to the conventional surface absorption based solar collectors.

1.5 Nanofluid-based volumetric absorption solar collector (NBVASC)

Recent years have seen the advent of solar thermal systems that directly absorb solar energy through volumetric absorption. These novel systems perform better comparative to conventional surface absorption-based equivalents.

Figure 1.2 details the design and working of a typical NBVASC. Herein, the solar energy directly interacts with the nanofluid and thus converts radiant energy to thermal energy through absorption and scattering mechanisms. Nanoparticle material, shape, volume fraction and the base-

fluid significantly impact the optical and thermophysical properties of the resulting nanofluid, thus dictating the overall efficiency of these novel nanofluid-based solar collectors.

Because of direct interaction of spectral electromagnetic energy and working fluid, no intervening solar selective surface is required. Furthermore, the aforementioned characteristic lends volumetric absorption as an effective method to circumvent the issue of high overheat temperatures at high solar concentration ratios.

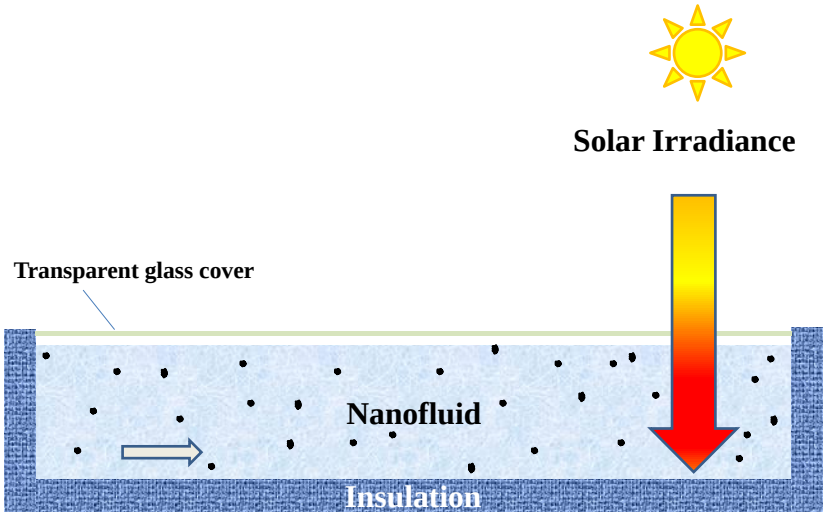

Fig. 1.2 Schematic diagram of NBVASC.

1.6 Solar pond

It is a commonly employed apparatus for storing solar energy in sunshine hours and using it during non-sunshine hours or cloudy days for a host of applications, viz., water purification, water heating, air conditioning, electricity generation etc. They are basically of two categories:

- Non-convective solar pond (NCSP)
- Convective solar pond

A NCSP houses a large quantity of water in which convection is suppressed to reduce thermal losses from top to environment. The most common NCSP is the one in which convection is suppressed by using salt water having an increasing concentration from top to bottom. Thus, allowing the energy transformation, storage, as well as transportation of the stored thermal energy from it. Figure 1.3 shows the schematic of NCSP.

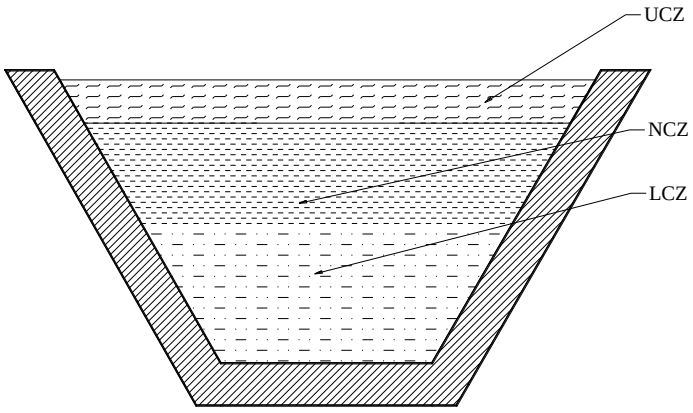

Fig. 1.3 Schematic diagram of non-convective solar pond

As against the NCSP, the convective solar pond houses a large quantity of water which does not have an increasing salt concentration gradient along the depth of the pond, and hence convection takes place within the water body, the warm water rises upwards. The heat loss from the top was minimised by installing two transparent shields at close intervals as shown in Fig. 1.4. The aforementioned shields also keep it contamination free from the atmosphere. The inside surfaces are painted black, and the outer surfaces are insulated to ensure minimum thermal losses.

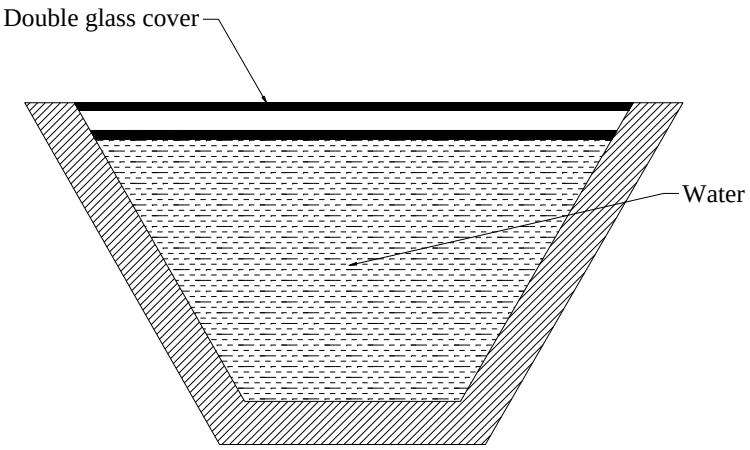

Fig. 1.4 Schematic diagram of convective solar pond

1.7 Motivation for present research work

At present, there is a scarcity of clean drinkable water in various parts of the globe. In many regions in India, the groundwater level has decreased significantly due to excessive and arbitrary usage of water for irrigation and industrial purpose. The situation in these regions becomes even worse during the summer season as the surface water bodies such as ponds and lakes also start drying up. As a result, there is a serious shortage of clean, drinkable water in various Indian regions during the summer. The incumbent desalination techniques use fossil fuels based energy for the desalination of water. With growing energy needs and rapidly depleting fossil fuels, the utilisation of non-conventional energy like solar energy for desalination has become a necessity. Despite being a necessary alternative for the future, the most common single-slope solar still has not yet been able to compete well with other water purification devices due to its low productivity and efficiency. Solar stills must be highly productive and efficient for producing pure water in order for them to be widely used and popularised. Thus, in order to make solar desalination technology an acceptable, alluring, and

practical choice for obtaining pure drinkable water, an effort needs to be made to improve the efficiency by incorporating appropriate modifications into the existing single-slope solar still.

1.8 Novelty of present research work

The majority of the efforts made in the past are focused on enhancing the diurnal distillate output. However, the aim of the current work is not only enhancing the diurnal distillate output, but it also aims at generating nocturnal distillate from the still and improving the total distillate. Being in the sun-belt, India has a good potential to benefit from the advantages of solar energy and utilisation of its related technologies. However, to the best of our knowledge, NBVASC, as an upcoming solar energy harnessing and collection system, is not properly investigated and utilised for solar distillation systems in this region and hence requires special attention. Furthermore, it has been observed from the literature survey that researchers have used conventional surface absorption-based solar collectors like flat plate collectors [26], parabolic trough concentrators [27], hybrid PV/T [22] etc., to transfer external thermal energy for enhancing the diurnal distillate production rate. Whereas in the present work, a novel NBVASC has been employed for efficiently harnessing the solar energy and supplying the same to solar still during sunshine hours for improving its diurnal production rate. During the non-sunshine time, a convective solar pond has also been employed to deliver the stored sensible thermal energy to the basin of the solar still using heat exchangers to produce the nocturnal distillate and makes the system a 'round-the-clock' unit to produce potable water.

1.9 Significance of present research work

In the current endeavour, we have engineered a highly stable nanofluid which allows efficient volumetric photo-thermal conversion and storage in useful sensible heat. Thereafter, this energy is transported to the basin of the solar still via heat exchanger continuously during sunshine hours. Moreover, the stored sensible heat in trapezoidal solar pond is also supplied to the basin of integrated solar still via heat exchangers during the non-sunshine period to increase the production rates and makes the system a 'round-the-clock' unit to produce potable water. This modified solar still is anticipated to be a boon to those living in desert, semi-arid, and coastal locations throughout the globe who face a severe scarcity of drinking water. Moreover, for the first time in the literature, the current investigation (experimental) of a single slope basin type solar still integrated with NBVASC during the day and a solar pond during the night for transferring thermal energy to the still's basin water has been reported. Therefore, the current effort has bridged the technological and knowledge gap that existed in this emerging and important field of solar energy.

1.10 Research Objectives

The on-Sun testing of the developed novel solar stills was done to achieve the following specific objectives:

1. To investigate the performance of single slope solar still coupled with nanofluid-based solar collector and compare with the performance of conventional single slope solar still.

2. To investigate the performance of single slope solar still coupled with nanofluid-based solar collector and solar pond and compare with the performance of conventional single slope solar still.

3. To investigate and compare summer and winter performance of single slope solar still coupled with nanofluid-based solar collector and solar pond.

4. To examine 24 h distillate production pattern of single slope solar still coupled with a nanofluid-based solar collector and solar pond with the help of 24 h temperature distribution of various components of solar still, solar collector and solar pond.

1.11 Organisation of thesis

Chapter 1 describes solar desalination, the categorization of solar stills, nanofluids and the concept of NBVASC. The motivation, novelty, significance, and the objectives of the current research have been detailed. Chapter 2 reviews the existing literature pertinent to solar desalination technologies. The single effect stills, particularly the solar stills integrated with solar collectors, have been covered. The literature related to nanofluids based volumetrically absorbing solar collectors has also been discussed. Finally, the research gaps identified from the literature review are clearly delineated, and the methodology to achieve the objectives of the present work has been listed. In chapter 3, the details of experimental test rig components and various instruments used for the measurement of data have been provided along with the experimental procedure. Chapter 4 presents the results of experimentation testing on the NBVASC and solar pond integrated solar still. The on-sun testing results are presented in graphical form, and are analysed and discussed in detail. Chapter 5 covers the summary and the important conclusions of the present research work.

1.12 Concluding remarks

The general background of solar desalination and basic construction of single slope solar still have been provided. The concept of a nanofluid and NBVASC have been discussed.

Together with the significance of the current study and its particular goals, the motivation for the current research endeavour and its novelty have also been mentioned.

Chapter 2

Literature review

Herein, a survey of the published literature on different desalination technologies and solar stills has been presented. In particular, "solar stills" of various types developed and investigated by researchers in the past have been critically reviewed. The literature review is compiled and presented according to the flowchart given below in Fig. 2.1.

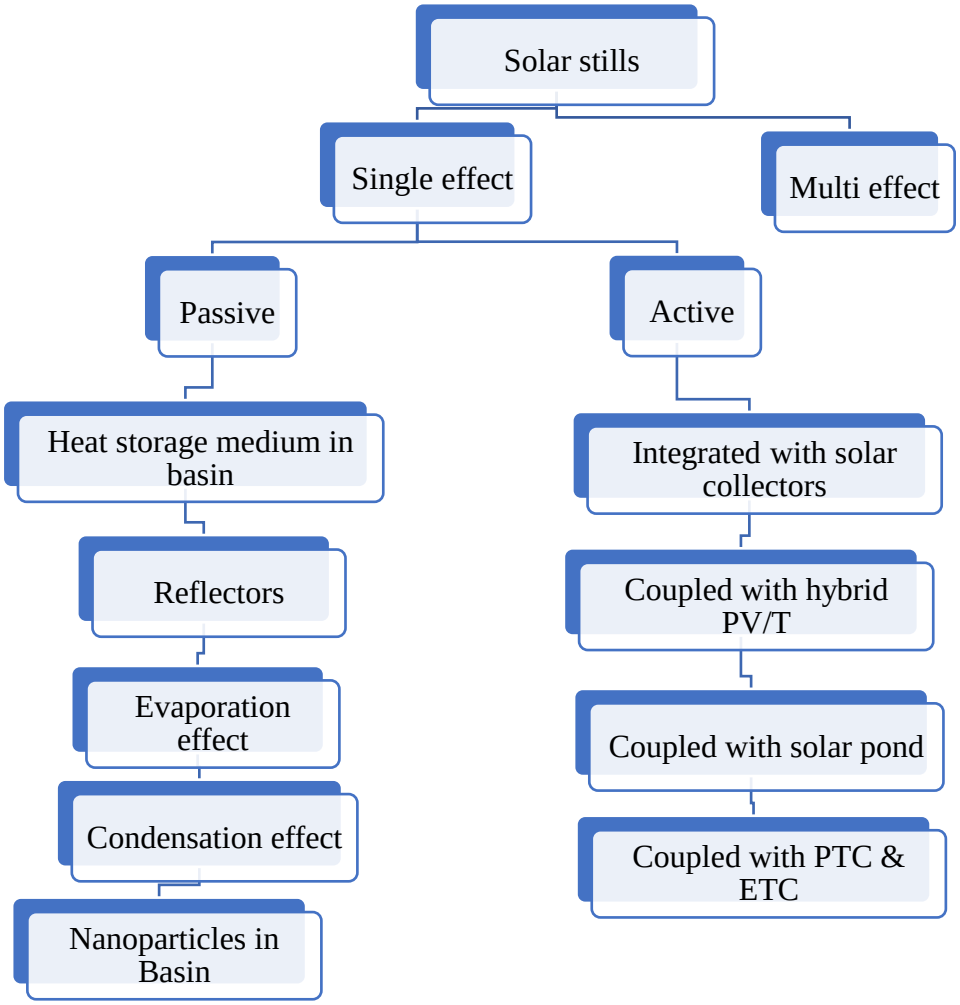

Fig. 2.1 Organization of literature review

2.1 Solar stills

Single-effect and multi-effect solar stills are the two categories into which solar stills can be divided. Depending on how thermal energy is provided to the basin water, they may also be divided into active and passive systems. With active systems, in addition to solar energy directly interacting with the water in the basin, thermal energy is also supplied through extrinsic solar thermal systems viz., concentrating and non-concentrating solar collectors and storage units.

2.1.1 Single effect solar stills

This sort of still uses input energy just once to make distillate output. Nonetheless, a conventional still is the most typical single-effect solar still. It has a straightforward design but has low productivity. There are two basic kinds of solar stills used for a single effect: passive and active. Although passive stills are powered only by the solar radiation, active stills also make use of supplementary heat from a variety of other sources. Literature on single-effect solar stills may be broken down into two categories: passive and active. Also, several strategies for enhancing the efficiency of single-effect passive solar stills are discussed independently.

2.1.1.1 Single effect passive solar still

Increased distillate output from a single-effect passive solar still is possible via the use of a heat storage medium in the basin, reflectors, higher condensation and evaporation rates, and the addition of nanoparticles to the basin water.

2.1.1.1.1 Using heat storage medium in the basin

Surplus heat from basin water can be stored using various heat storage mediums such as black coated surfaces, inks, sand, pebbles, and phase change materials to produce night-time distillate

from still, thus improving the overall efficiency of still. Omara et al. [28] employed various types of sands within the basin water. They reported that sand bed and water heights and the type of sand (black or yellow) impact the distillate output most significantly. Employing black and yellow sands @ 0.01m bed height result in enhancements (relative to conventional solar still) on the order of 42% and 17%, respectively. Murugavel et al. [29] employed various refractory and metallic materials in basin water. The best option was found to be quartzite rock with a size of 19 mm. Tabrizi et al. [30] constructed and evaluated a solar still that was combined with sand heat storage beneath the basin liner; they decided for this combination owing to its straightforward construction and low cost, since the cost to make the alteration was just 10% of the entire cost.. No pumping system or operator was required, and the sandy reservoir provided heat energy during non-sunshine and low solar intensity periods. It was the reason that the nocturnal production of distillate was 12 % of the total daily yield.

Kabeel and Abdelgaied [31] employed paraffin wax in the basin to store energy through a phase change. Distillate output was found to be enhanced by 67.18% relative to conventional still. The cost of the distillate comes out to be 0.03$/L for the conventional still and 0.032$/L for the still with PCM; the increase in cost is insignificant as compared to the rise in distillate production. Panchal and Shah [32] constructed solar still with double basin. They modified the higher basin by incorporating refractory material to enhance the surface area in order to increase evaporation rates. They concluded that owing to higher heat capacity, the nocturnal distillate with calcium stone was much better than other materials.

Rajaseenivasan et al. [34] built and tested both single- and double-basin solar stills with a double slope and a basin area that was statistically indistinguishable from one another.

Experiments were conducted using wicks, porous materials, and a range of energy storage materials at varied basin water depths. Maximum distillate output found to be 3.58 L/m^2/day when using the double slope double basin solar still. In order to maintain constant production rates of distillate, regular cleaning of both the basins and absorber surfaces was recommended.

2.1.1.1.2 Employing internal and external reflectors

Internal and external reflectors can be employed for augmenting the solar still productivity. The primary function of reflectors is to direct the solar radiations towards the basin area to increase evaporation rates for improving distillate production. Al-Hayek and Badran [33] conducted a study on symmetrical and asymmetrical greenhouse types of solar stills. Distillate production has been found to be proportional to water depth and to have improved by adding dye in the basin, also, as deduced from the research, internal mirror reflectors helped reduce radiation loss. The findings indicate that the asymmetrical type solar still had 20% more distillate output relative to the symmetrical still when operating in the arid areas of Jordan and can significantly reduce drinking water problems of the region.

Karimi et al. [34] conducted study on single-effect solar stills, it was found from their research that using a reflector on both the front and sidewalls concurrently enhanced productivity by 18%. The productivity increased by 22% on average when the reflectors were employed at the back walls. The productivity enhancement of stills that has reflectors on all inside walls during summer, winter and the whole year was noted to be 22%, 65%, and 34%, respectively. The developed mathematical model was found to be consistent with the experimentally measured values, and it predicted the values by considering the effects of reflectors on all walls. Furthermore, due to low capital cost and almost no operating cost, the internal reflectors were recommended by the researchers, especially for high latitude regions with clear skies. Tanaka and Nakatake [35] studied

a basin solar still that had hinged exterior reflectors in addition to a fixed interior reflector. They discovered that the output of the modified still was 2.3 times more than the conventional still. El-Swify and Metias [36] investigated double-exposure solar still (employing internal reflectors); the analysis was done theoretically as well as experimentally. They concluded that the overall percentage increase in distillate production due to the incorporated modifications was calculated to be 82.6% in winter and 22% in summer. Using a variety of operational settings, Abdullah et al. [39] studied many variants of a rotating wick-type solar still (RWSS). A DC motor was employed for the rotation of the wicks (made of jute). Analysis was also done for different belt sliding speeds and with the installation of internal and external reflectors as well. Enhancements (in terms of distillate output) on the order of 260% and 300%, respectively were reported for RWSS relative to the conventional solar still. In terms of the overall efficiency RWSS was found to have 47% higher value @ $0.05m^{-1}$sliding speed.

2.1.1.1.3 Enhancing evaporation rate

A number of researchers worked towards the goal of increasing the output of the stills by lowering the basin water's thermal inertia using fins, wicks, and sponges in the still's basin. Mahdi et al. [37] developed a tilted wick-type solar still (employing charcoal cloth to build the wicks). Both indoor and outdoor testing revealed that the maximum efficiency obtained on a clear sunny day was 53%. The increase of water salinity from 0% to 10% by weight decreased the efficiency from 37.7% to 20%. Srivastava and Agrawal [38] employed floating wicks fabricated from black jute fabric as floating porous absorbers to augment basin water evaporation and discovered that productivity of still rose by 68% and 35% over conventional still. After conducting research on capillary rise phenomena and thermal parameters, Wang and Torng [39] came to the conclusion that the porosity, absorptivity, and thermal conductivity of the wick material are the most important

factors in determining the wick's effectiveness (and, consequently, the distillate output). Haddad et al. [40] reported the influence of a vertical spinning wick on the distillate output. During the winter months, the daily distillate output was recorded to be 5.03 kg/m^2, whereas during the summer, it increased to 7.17 kg/m^2. In the winter and summer seasons, the distillate output improved by 51.1% and 14.72%, respectively, relative to the traditional still. The proposed modified still's distillate cost and thermal efficacy were 0.011 $/kg and 65%, respectively, compared to the traditional still's 0.009 $/kg distillate cost and 46% thermal efficacy.

The effect of placing varying sized cube shaped sponge pieces in the basin of the solar still was examined by Hijley et al. [41]. They concluded that sponge cubes enlarged the surface area across which water evaporates, which resulted in an 18% to 273% increase in solar still yield. Srivastava et al. [42] studied the impacts of employing extended porous fins (black-dyed cotton cloths hung from bamboo rods) in the basin. Relative to the conventional still, for the months of February and May, productivity was enhanced by 48% and 15%, respectively. Omara et al. [43] investigated what would happen if a significant number of changes were made all at once, such as making use of a corrugated basin liner, adding wicks into the design, and installing internal reflectors. They recorded a 145% increase in daily production as compared to the traditional still. Naggar et al. [44] implied from their research that adding fins to basin enhances the convective heat transfer coefficient by 3.6 times, resulting in a 13% improvement in efficiency relative to the conventional still. Rajasenivasan et al. [45] performed theoretical study on single-effect basins with square and circular fins, as well as trials with both types of fins covered with the wick. They discovered that using square fins in the basin boosted output by 26% when compared to traditional stills and that using square fins covered with wicks enhanced productivity by 36%. Productivities for circular fins (with and without wicks) were observed to be 36.7% and 45.8% higher than for conventional

stills, respectively. Alaian et al. [46] recorded a 23% increase in distillate output while evaluating the impacts of pin-fin extended wick surfaces in the basin of the modified still relative to the conventional still.

2.1.1.1.4 Enhancing condensation rate

Several efforts have been made for enhancing the condensation rate of water vapours by utilizing condensers, glass cover cooling, and other methods. Kabeel et al. [47] thoroughly examined the impact of employing condensers in solar stills. Ahmed [48] reported that installing an internal condenser in the basin improved distillate output by 10%. Tiwari and Rao [49] examined the influence of flowing water on the glass cover of the solar still and found that distillate production approximately doubled as a result of the presence of the flowing water. El-bahi and Inan [50] explored a basin still fitted with an outside passive condenser and an external reflector that forms a shadow over the condenser. The vapours that were produced in the basin condensed simultaneously on the glass of the basin as well as the outer condenser, producing a total of 7 $kg/m^2/day$. Nijegorodov et al. [51] conducted research to determine how the use of an exhaust fan and an external condenser impacted the effectiveness of a solar still as well as the amount of distillate it produced. It was stated that the modified still's distillate production was 2.5 times that of the conventional still at noon, compared to the traditional still. Abu-Hijleh [52] investigated the effect of glass cover cooling on the performance of a still by passing a water layer on the coverings of glass. He found that the efficiency of the still could be boosted by up to 6% if cooling factors were used well.

2.1.1.1.5 Using nanoparticles in the basin

Seeding nanoparticles (1-100 nm) into the basin water is a simple technology that improve its thermophysical properties, therefore, enhancing the productivity of the passive still. Elango et al. [53] conducted research to determine the impact of using varying quantities of a variety of nanoparticles (such as Al_2O_3, ZnO, Fe_2O_3, SnO_2). They observed that Aluminum Oxide (Al_2O_3) nanoparticles outperform others in terms of productivity. Sahota et al. [54] found that in the case of passive double slope solar still, adding small amounts of Al_2O_3 nanoparticles (0.12%) into the basin water enhanced the distillate output by 8.4% - 12.2%. Gupta et al. [54] investigated solar stills employing CuO nanoparticles at different depths (namely 5 cm and 10 cm). They reported that relative to the conventional still, distillate output improved by 30.1% (@ 5 cm) and 22.42% (@ 10 cm). Modi et al. [55] performed a host of experiments for various basin water depths with Al_2O_3 and CuO nanoparticles having 0.1% mass concentration. The glass cover's orientation was also varied from East-West and North-South directions for different experiments. An increase of 28.53% and 26.59% along with 58.25% and 56.31% in distillate production with aluminium oxide and copper oxide (at 2 cm and 1 cm), respectively, was recorded. It was observed that the CuO nanoparticles outperforms the aluminium oxide nanoparticles and showed promising results for future studies. Satyamurthy et. al [56] studied a stepped solar still with TiO_2 and MgO nanoparticles in the basin, they revealed that the potable water production was 4.5 kg/m^2/day and 2.7 kg/m^2/day for TiO_2 and MgO nanoparticles, correspondingly. In comparison to conventional still, the yield observed an increase of 40% and 60% while using TiO_2 and MgO nanoparticles.

Balachandran et al. [57] loaded the basin layer of solar still with nano and micro-coated Fe_2O_3 particles. The addition of both particles with a weight proportion of 10% in the absorbent layer improved the performance of the still. The cumulative yield for micro-coated and nano coated

layer was measured to be 3.23 kg/m^2/day and 4.39 kg/m^2/day. The results revealed highest efficiency of 66% in the case of nano absorbent layer solar still, which was more than the micro-coated layer and of still without any layer. The rise of distillate with the addition of particles also reduced the payback period by 51 days.

Kumar et al. [58] performed experiments on the effects of the nano-doped black colour painted absorber layer (CS-NDBP), and evaluated the results along with the normal black paint-coated absorber layer in conventional solar still (CS-BP). SiO_2 with 0.5% mass concentration was used as nano-dope in the black paint, and results showed an enhancement of 7.83 % and 8.78 % in yield with nano paint and had 25 mm and 15 mm water depths, correspondingly.

Arani et al. [59] had done a study on tubular solar still (TSS) with SiO_2 nanoparticle (10-40% mass concentration) based absorber plate and fins in the basin section of the TSS. They concluded that the nanoparticle-based paint performs better than the ordinary paint, and the fins further augment the distillate output. The results showed a 55.18% increase in yield with a 20% mass concentration of SiO_2 nanoparticles than ordinary TSS.

Panchal et al. [60] experimentally explored the effects of coating the solar still walls with manganese oxide (MnO_2) based black chrome paint comparing it with conventional still. The MnO_2 concentration was kept between 20-50% mass concentration with a depth of 2 cm (water) for experiments. They concluded that nanoparticle-based still performed better, with 19.2% more yield. Because of higher yield produced, the payback period was reduced by 16 days than conventional still.

2.1.1.2 Single effect active solar still

Active solar stills have an extra source of heat that is supplied to the basin water from the outside. This helps to increase the still's overall productivity and effectiveness. The additional heat can be supplied by connecting the still to various types of external heat-supplying devices, for example, hybrid photovoltaic panels, solar collectors, solar ponds, parabolic trough collectors, evacuated tube collectors, and so on.

2.1.1.2.1 Solar still integrated with solar collectors

In their study, Lawrence and Tiwari [61] conducted an in-depth analysis of the performance of a single basin solar still that was connected to a flat plate collector (FPC) by means of a heat exchanger. Their research showed that while operating in the active mode, the amount of distillate produced is proportional to the amount of water depth in the system. In contrast, it diminishes in passive mode. Rajesh et al. [62] investigated FPC integrated solar still, performance was evaluated with and without FPC coupling. The distillate output from both the stills was determined hourly from 8 am till 5 pm; the modified system with FPC showed a 25-40% increase over still without FPC. An asymmetrical, large greenhouse-type single-effect solar still was studied by Voropoulos et al. [63] in the lab in combination with a heated water supply and flat plate collectors. They used a heat exchanger to transport heat from an external flat plate solar collector to the still's thermal storage, and found that output was double that of a system without external heating. Nighttime distillate production was found to be greater than diurnal distillate output due to larger potential difference. Basin-type single-stage solar still with an FPC was analysed by Badran et al. [64] the first mode had the still attached to the collector from 8 a.m. to 5 p.m.; the second had the still running independently. Distillate from the still was found to be produced at a daily rate of 2 L/m^2, with an efficiency of 27%. Collector integrated still showed an increase of 231% in distillate

production, but the integrated system's efficiency was reduced by 2.5% in comparison with the alone still.

Badran and Al-Tahainesh [65] analysed solar still integrated with FPC and an internal reflector. It was inferred that the performance of the combined solar still rose by 36% when it was connected to a solar collector. Yadav [66] analysed the thermosyphon, and the forced circulation form performance of the FPC-integrated solar still. In comparison with thermosyphon still, the author found a 5-10% increase in yield when employing the forced circulation type still.

Chaudhari et al. [67] experimented with a parabolic trough collector and observed that the thermal efficiency of PTC increases by 7% when 0.1% Al_2O_3-Water nanofluid by volume was used as HTF in comparison to the base fluid. It means collection and transfer of energy are more efficient if nanofluid is used as an HTF in solar collectors. That is why researchers have also made efforts with nanofluid being used as an HTF for transferring of thermal energy from collector to solar still. Subhedar [68] conducted experiments on water and Al_2O_3/Water nanofluid as HTF in collector integrated solar still. Significant enhancements, both in distillate output (66%) and efficiency (70%), were reported for a 0.1% volume fraction of Al_2O_3 nanoparticles. Gholamabbas et al. [69] reported that adding $AgFe_3O_4$ nanoparticles into the basin water of the solar still integrated with concentrating solar collector significantly improved the distillate output (by 218%) and efficiency (by 117%) relative to the solar still.

Mahian et al. [70] evaluated the coupled system of solar collector and solar still linked via heat exchangers employing nanofluid as the HTF. They found that usage of nanofluids in heat exchangers improved the performance characteristics by 1 - 10%.

2.1.1.2.2 Solar still with hybrid photovoltaic thermal (PV/T) hybrid system.

PVT collectors are photovoltaic-thermal modules coupled to flat plate collectors that gather direct sun thermal energy beneficial for heating basin water and providing direct current to drive pumps and other electrical equipment. PVT collectors are beneficial for solar still systems and integrated standalone solar systems. Gaur et al. [71] computed that two PV/T collectors are optimum for PV/T coupled solar stills. The maximum daily yield is 7.9 kg with daily efficiency of 28%. Dev et al. [72] studied the active solar still integrated with an FPC and PV module. At a water level of 5 cm the daily production was found to be 7.223 kg/m^2. They also concluded that due to the existence of unsteady state parameters in actual climatic conditions, the non-linear equations were best suitable for analysing active solar stills integrated with PVT modules. Al-Nimer et al. [73] conducted experiments by putting photovoltaic cells at the base of the basin of the solar still having mirror reflectors (interior) and separate finned condenser carefully placed in the shadow zone of the modified still. A steady-state mathematical model was also developed. Daily distillate production grew from 5.8 kg/m^2 to 7.8 kg/m^2 when ambient temperature rose from 10^{o}C to 30^{o}C. Yari et al. [74] proposed a mathematical model in which they integrated ETC and semitransparent PVT to the solar still, the model was created to forecast the distillate production rate and electricity produced. The results indicate a decrease in yield with increase in water depth. The distillate produced was 2.3 kg/m^2/day with 10 collector tubes and it boosted to 4.76 kg/m^2/day with the help of 30 tubes thus indicating a linear relation between number of collector tubes and distillate produced. The maximum electrical energy produced was 70.47 w/m^2 at the noon.

2.1.1.2.3 Solar still integrated with solar pond

A solar pond is a device that is capable of collecting and storing solar energy in order to feed it to thermal uses later on. It may be used for water desalination, drying, space heating, refrigeration, and even power production during overcast or otherwise non-sunny hours of the day. It has a broad variety of possible applications. It is possible to improve both the nighttime distillate and the overall performance of the system by integrating solar ponds and solar stills.

Velmurugan et al. [75] carried out experimentation on modified solar still (having industrial effluent as raw water) coupled with mini solar pond. The distillate production of the modified still enhanced by 53% with fins; it was increased by 63% when fins in combination with pebbles were used, and the highest productivity rise was recorded when fins and pebbles were used with the sponge in the basin of stills. In addition to this, they mentioned that there was a linear correlation between solar intensity and distillate production. El-Sabaii et al. [25] integrated the solar still and shallow solar pond (SSP) found that distillate output per day improved by approximately 26.3%. The daily efficiency of the integrated still was 54.98% greater than the conventional still. Dhindsa and Mittal [75] conducted an experiment to investigate the effectiveness of a vertical multiple-effect diffusion solar still that was connected to a mini solar pond and had floating wicks in the basin. The study showed a rise of 71.21% in the yield of integrated solar still over the conventional still, and an increase of 49.87% was recorded when only floating wicks were employed. The cumulative daily efficiency for the four effects modified still was 80.29%, whereas the efficiency of conventional still was 59.6% with a feed rate of 0.13 $g/m^2/s$.

2.1.1.2.4 Solar still integrated with PTC & ETC

Using a tracking mechanism that follows the path of the sun, parabolic trough collectors (PTC) are able to concentrate the incident radiation on the absorber tube or receiver tube. This is accomplished by positioning the tubes such that they are parallel to the focal line of the PTC. Various researchers have integrated PTC with solar stills to improve the yield of still. Energy and Exergy were studied by Amiri et al. [76] for a novel PTC standalone collector that has a solar still built-in analysis was done for fixed PTC and PTC with a tracking system. There was a 55% increase in distillate yield using the fixed parabolic trough collector and a 70% increase using the collector with a tracking system in summer than in winter. Experiments were conducted by Kumar et al. [77] to test the performance of a single slope solar still connected with a parabolic trough collector for three different brine depths of 5, 10, and 15 centimetres, respectively. They found that the productivity and brine depth were inversely proportional to each other. The maximum efficiency achieved was 16.6% with 5 cm brine depth.

Kumar et al. [76] analysed the ETC integrated solar still, they achieved a production of 3.9 $kg/m^2/day$ with efficiency of 33.8%. The annual production that was acquired using an ETC-connected solar still was 567.3 kg, which was higher than the annual productivity that was attained using active hybrid solar still or an ETC-coupled solar still operating in the natural mode. Mohammad Behshad Shafii et al. [77] examined integrated solar still with ETC. Two evacuated tubes were used as a collector in the experimental arrangement. The highest water productivity every hour and efficiency were 1.11 kg per metre square and 68%. The yield rose by 27% when ETC was used. Omara et al. [78] carried out research on a hybrid desalination system consisting of solar still integrated with evacuated solar water heater having twenty vacuum tubes. They compared the effectiveness of conventional solar still (CSS) to that of SLWSS and DLWSS

(single- and double-layer wick solar stills). Fresh water production was increased by 107% using double-layer lined wick (DLLW).

2.2 Direct Volumetric absorption of solar energy by nanofluids

Solar thermal systems that capture solar energy directly by volumetric absorption have evolved in recent years. In terms of performance, these unique solar thermal systems outperform their typical surface absorption equivalents. The solar irradiance directly interacts with the working fluid (nanofluid) after passing across the glass covering, and via a combination of absorption and scattering processes, the radiant energy is converted into the thermal energy of the fluid. The nanoparticle material, size, shape, volume fraction, and base fluid all play a role in determining the thermophysical and optical properties of the resulting nanofluid. These properties, in turn, have an impact on the overall performance characteristics of these novel solar thermal collectors. Some of the work done by various researchers has been mentioned below.

Using the volumetric absorption concept Gupta et al. [79] conducted experiments on a solar collector coated with a thin layer of aluminium oxide-based nanofluid with water as the base fluid for direct absorption. In each of the four scenarios (four different concentrations of the nanofluid), when nanofluids were used in place of water, the efficiency recorded as 22.1%, 39.6%, 24.6%, and 18.75% for nanofluid concentrations of 0.001%, 0.005%, 0.01%, and 0.05%, respectively. Experiments also showed that collector efficiency was maximum at a particular volume fraction and declined for both smaller and larger values of this parameter. Khullar et al. [80] investigated a number of nanofluids for their optical and thermophysical properties in order to assess their suitability for solar thermal applications. They discovered that weighted absorptivity is the primary property that allows the respective nanofluids to be suitable for solar thermal applications. They also figured that amorphous carbon nanoparticles were most appropriate for direct volumetric

absorption from the selected lot, and these nanofluids reached significantly high temperatures and weighted absorptivity values during on-sun testing with a parabolic trough collector. Otanicar et al. [15] did a study on a mini solar thermal collector with three different nanofluids based on silver, graphite and carbon nanoparticles. Silver nanoparticle (20nm) based nanofluid showed an increase of efficiency up to 5% over the conventional surface absorption collectors, whereas the graphite nanoparticles (30nm) showed an increase of 3% in efficiency. They also determined that using nanofluids can significantly enhance surface area; in their study, using 30 nm particles at 1% volume fraction observed a 300 times greater surface area than the bottom surface area. Vakili et al. [81] tested graphene-based nanoplatelets for optical characteristics and thermal conductivity at weight percentages of 0.00025, 0.0005, 0.001, and 0.005. They discovered that the nanofluid is stable over long periods of time and has good dispersion quality. Absorption was directly proportional to weight percentage, but transmittance was inversely proportional to weight percentage. They concluded that with an increase of from 0.00025 to 0.005 (nanofluid concentration) by weight reduced the solar energy absorption height for direct absorption solar collectors from 10 cm to 2 cm. Karami et al. [82] performed experiments on a direct absorption solar collector prototype utilizing CuO-based nanofluid as a working fluid, promoting its use as a solar water heater in domestic applications. They conducted experiments to determine the optimal volume percent of CuO nanoparticles, and the optimal internal surface area of the collector's bottom wall. The maximum collector efficiency achieved during the study was at 100 ppm volume fraction.

2.3 Concluding Remarks

The literature study led us to the overall conclusion that the productivity of active solar stills is greater than that of passive solar stills. However, a critical and thorough review of the literature revealed that there still exist few research gaps/limitations in the presently available solar desalination technology; hence there is enough room for modification in the existing active solar still to improve its productivity. These limitations noticed from the study of literature are listed pointwise here, and the alterations that were made to the current study endeavour in order to circumvent these restrictions are discussed below:

1) It has been found from the literature survey that researchers have used conventional surface absorption-based solar collectors like flat plate collectors, parabolic trough concentrators, hybrid PV/T and evacuated tube collectors to transfer external thermal energy to the basin water of solar still during sunshine hours to enhance diurnal distillate production rate. Whereas in the present work a novel NBVASC has been employed for efficiently harnessing the solar energy and supplying the same to solar still during sunshine hours for improving its diurnal production rate.
2) Literature review on the solar stills revealed that most of the studies have been devoted to enhancing the daytime distillate output of the stills. However, the aim of the present work is not only the enhancement of day-time distillate output of the stills, but it also aims at utilizing the solar still even during night for the production of distillate.
3) All the studies on solar still have mentioned the hourly distillate output during sunshine hours; however, none has reported the hourly distillate output obtained beyond sunshine hours. In the present work, the hourly performance of still even during night-time was investigated.

4) The 24-hour performance of solar still has been reported by very few researchers. Very few studies have reported the day and night distillates separately. Very few researchers have reported instantaneous and hourly variation of still efficiency.

To overcome all these shortfalls in information existing in the literature, the current research work incorporated all of them to fill the existing gaps in the literature.

Chapter 3

Experimental setup and data acquisition

The experimental equipment for the present investigation was constructed in Thapar Institute's central workshop and then installed at the testing location. The literature review served as the basis for the adjustments made to the original basin-type solar still to address the noted gaps and shortcomings to create the modified still. NBVASC was employed to supply thermal energy during sunshine hours to the basin water via the heat exchangers placed both in NBVASC and the solar still to improve the diurnal distillate. A mini solar pond was used to collect and store solar energy during the sunshine hours and the same is supplied to the solar still during non-sunshine hours to generate nocturnal distillate. A closed-loop system of heat exchangers to transport heat from the NBVASC, and the solar pond to the solar still's water during the day and at night was employed. The modified/integrated solar still's productivity was boosted using several floating wicks, which aided the evaporation process. All the pipe connections of the NBVASC, solar pond, and solar still were done using chlorinated polyvinyl chloride (CPVC) pipes and valve connections. This chapter describes the key components of the NBVASC, solar pond, and solar still. Key specifications of several measuring instruments used for measuring and collecting data during experiments are provided. The experimental procedure for all experiments has been explained.

3.1 Single slope solar still integrated with nanofluid-based volumetric absorption solar collector (NBVASC) and solar pond.

For achieving the aims of the proposed study, two conventional single-slope solar stills were built. Both the stills were made with the same materials and dimensions. For improving the solar

still's performance, an NBVASC and a convective solar pond were connected in one of these two conventional stills to provide supplemental heat energy. For the sake of comparison, the research was conducted on both stills at the same time, side by side, and under identical operating circumstances. The constructional details and dimensions of the key components are provided in Table 3.1.

Table 3.1: Construction details and dimensions of solar still and solar collector

SOLAR STILL	
DESCRIPTION	**DETAILS**
Overall dimensions	1.5m × 0.77m × 0.3m
Construction material	Glass cover, stainless steel and galvanised iron sheets and black butyl rubber liner
Glass cover thickness	5 mm
Angle between basin and glass cover	40^{o}
Insulation	Rockwool @ 100mm thick
Working fluid and its volume/mass or mass flow rate	Tap water@ 34.65L
Transport phenomena involved	Radiation, conduction convection, evaporation, and condensation
SOLAR COLLECTOR	
Overall dimensions	1.20m × 1.07m × 0.10m
Construction material	Glass cover, stainless and galvanised iron sheets
Insulation	Polyurethane foam@100mm thick
Thickness of glass coverings	5 mm

Glass coverings gap	10 mm
Working fluid and its volume/mass or mass flow rate	Paraffin oil @ 47L (surface absorption mode) Nanofluid @47L (volumetric absorption mode)
Transport phenomena involved	Radiation, conduction, and convection

The constructional details and dimensions of the convective solar pond along with the incorporated heat exchangers of NBVASC, the convective solar pond, and solar still, along with floating wick details that were also used in the experiment, are described in Table 3.2.

Table 3.2 Construction details and dimensions of the solar pond, heat exchangers and wicks

SOLAR POND	
Overall dimensions	Top surface: 1.62 m × 1.62 m Bottom surface: 0.71 m × 0.71 m Depth: 0.90 m
Construction material	Glass cover, stainless steel, mild steel, and galvanised iron sheets
Insulation	Rockwool @ 150 mm thick
Thickness of glass coverings	5 mm
Glass coverings gap	10 mm
Working fluid and its volume/mass or mass flow rate	Tap water @ 640 L
Transport phenomena involved	Radiation, conduction, and convection
HEAT EXCHANGERS	
SOLAR STILL HEAT EXCHANGER	

Overall dimensions	Diameter: 15 mm Length: 9.144 m
Construction material	Copper
Working fluid and its volume/mass or mass flow rate	Ethylene glycol-based water-soluble heat transfer fluid @3lpm
NBVASC HEAT EXCHANGER	
Overall dimensions	Diameter: 15 mm Length: 10.66 m
Construction material	Copper
Working fluid and its volume/mass or mass flow rate	Ethylene glycol-based water-soluble heat transfer fluid @3lpm
SOLAR POND HEAT EXCHANGER	
Overall dimensions	Diameter: 12 mm Length: 10.98 m
Construction material	Copper and GI
Working fluid and its volume/mass or mass flow rate	Ethylene glycol-based water-soluble heat transfer fluid @ 3lpm
FLOATING WICKS	
Overall dimensions	Thickness: 20 mm Width: 50 mm Length: 600 mm
Construction material	Polyurethane foam, black cotton cloth and cotton threads
Transport phenomena involved	Capillary action, radiation, and evaporation

Fig. 3.1 and Fig. 3.2 provide a schematic and a pictorial representation, respectively, of the modified still.

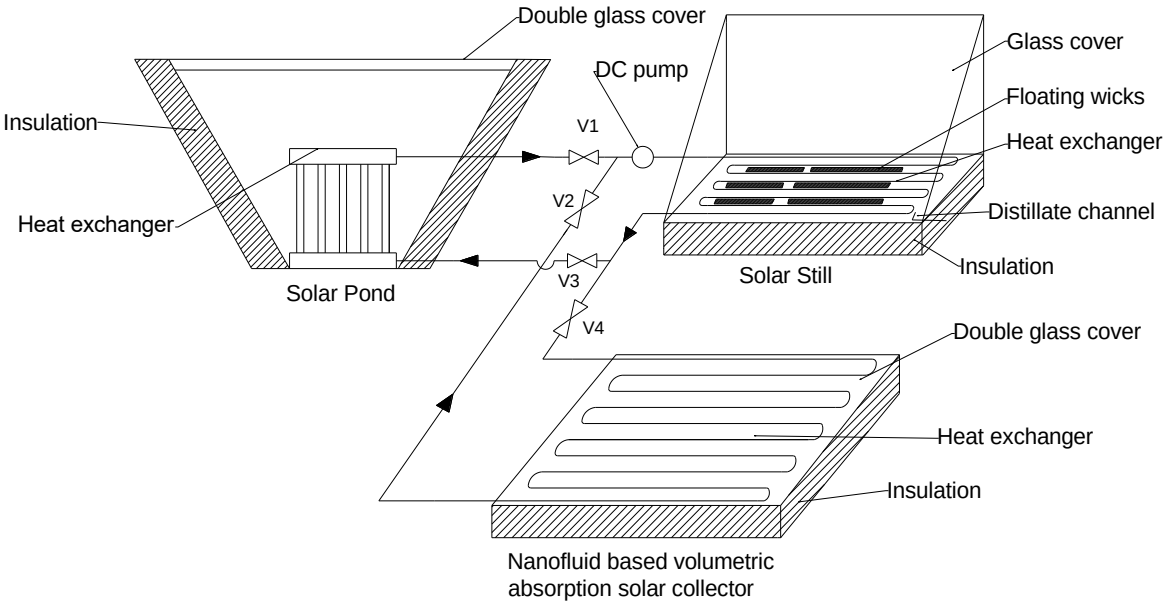

Fig. 3.1 Schematic diagram of modified solar still

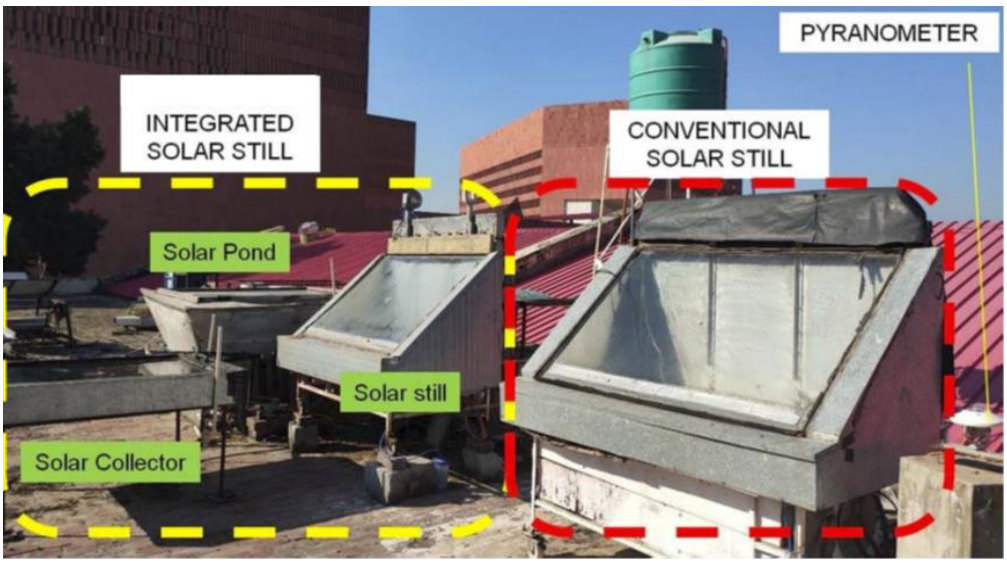

Fig. 3.2 Pictorial view of modified solar still integrated with NBVASC and solar pond

The combination of NBVASC-Solar pond-Solar still comprises the integrated solar still. The following is a description of the constructional details of the integrated solar still's essential components:

3.1.1 solar still

As shown in Fig. 3.3, the solar still comprises a flat basin tray of size 1.50 m × 0.70 m, a sloping single glass cover, a rectangular back wall and mirror polished triangular side walls were made up of stainless-steel sheets. For the purpose of absorbing solar radiation, the basin tray is covered with black butyl rubber. The reason for using black butyl rubber is its ability to withstand high temperatures and it has a relatively long life. For heat loss reduction, 100 mm of glass wool insulation was used to cover its outside surfaces. Supplementary, glass wool insulation was also shielded with galvanised iron (GI) sheet of 1mm thickness to protect the insulation from weather conditions. The potential leakage sections where one component of the solar still meets the other were sealed with high-temperature silicone sealant to ensure waterproofing of the assembled system. The whole system was mounted on a framed stand with wheels to facilitate the movement of the still according to the situation. A heat exchanger of the serpentine form (employing copper tubes; diameter, 15 mm with 2 mm wall thickness) was positioned in the basin of the still, and an HTF was passed through it in a closed loop to transmit the heat energy from NBVASC to the solar still.

Fig. 3.3 Single slope solar still

3.1.2 Nanofluid-based volumetric absorption solar collector (NBVASC)

A nanofluid-based volumetric absorption solar collector (NBVASC), as shown in Fig. 3.4, was fabricated to provide solar still with supplementary thermal energy during the daytime. It was manufactured by constructing a shallow container, filling it with nanofluid and covering its top surface with two closely spaced transparent glass covers. A 3 mm thick sheet of mild steel was used to construct the shallow container with a bottom and top surface size of 1.07 m × 1.20 m and a depth of 0.1 m. A frame was constructed to house the two coverings of glass having a 10 mm gap. An adjustable support system was made on the inner walls of the shallow container to support

and fix the double glass cover frame at any height from the bottom surface of the container to provide an option for height adjustment for varying the depth of nanofluid in the volumetric absorption solar collector. This adjustable support system ensured that the bottom glass was in continuous contact with the nanofluid to suppress the evaporation of the nanofluid. An air gap between the nanofluid and the bottom glass could have led to the potential cooling of the nanofluid owing to evaporation and subsequent rejection of the 'heat of condensation' onto the inside surface of the bottom glass. Moreover, the thermal losses were reduced by having a second glass placed at a distance of 10 mm from the bottom glass cover. The transfer of heat from the bottom glass covering is restricted through this air gap along with second glass covering. Overall, two glass covering configuration helps in reducing the thermal losses from the collector. For this specific experiment, the depth of nanofluid in the solar collector was kept at 0.04 m. Polyurethane foam has been used to insulate the solar collector's bottom and walls, lowering the heat loss rate to the environment. Further, this foam was covered with a 1 mm thick galvanised iron sheet to protect this insulation foam from weather conditions. Black enamel was used as coating on the inner portions (surfaces) of the NBVASC to maximize solar energy absorption. A serpentine type of copper pipe heat exchanger (circulating ethylene glycol-based water-soluble heat transfer fluid, using a 12V DC pump having a rated power of 19 W) was also placed within the NBVASC. The external surface of the copper tube was also coated with black enamel to maximise solar energy absorption and heat transfer from the nanofluid to the copper tube.

Fig. 3.4 Nanofluid-based volumetric absorption solar collector.

3.1.3 Nanofluid

For the present work, nanofluid was prepared by using a small amount of used engine oil acquired from a 15,000 km run four-stroke diesel engine. After filtering the resin, sludge etc., with a cotton cloth, the filtered oil was then again refined with 0.7 µm filter paper. Nanofluids of different concentrations were produced by mixing filtered oil and paraffin oil (then ultra-sonicating

the mixture for 30 minutes in a bath-type ultra-sonicator) forming concentrations ($1.25mlL^{-1}$, $2.5mlL^{-1}$, and $5mlL^{-1}$). Fig. 3.5 illustrates the graphical representation of the nanofluid preparation process. The pictures of the nanofluids after eight months of synthesis are shown in Fig. 3.6(a). Figures 3.6(b) and 3.6(c) reveal the particle size distribution of the carbon soot particles (TEM image) and in the as-prepared nanofluid (hydrodynamic particle size distribution measured through DLS), respectively.

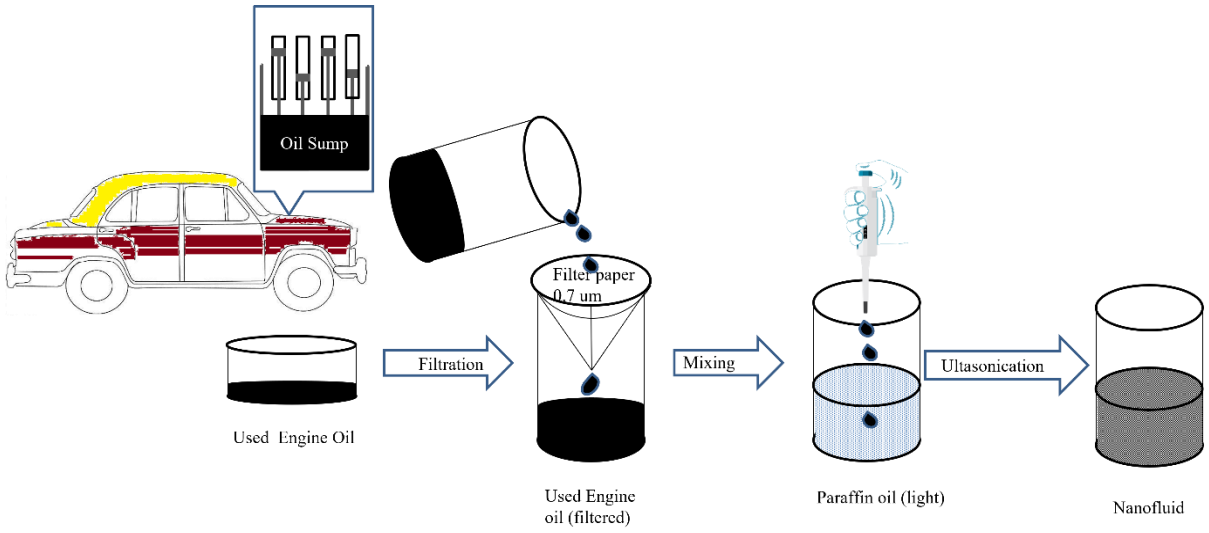

Fig. 3.5 Nanofluid preparation process

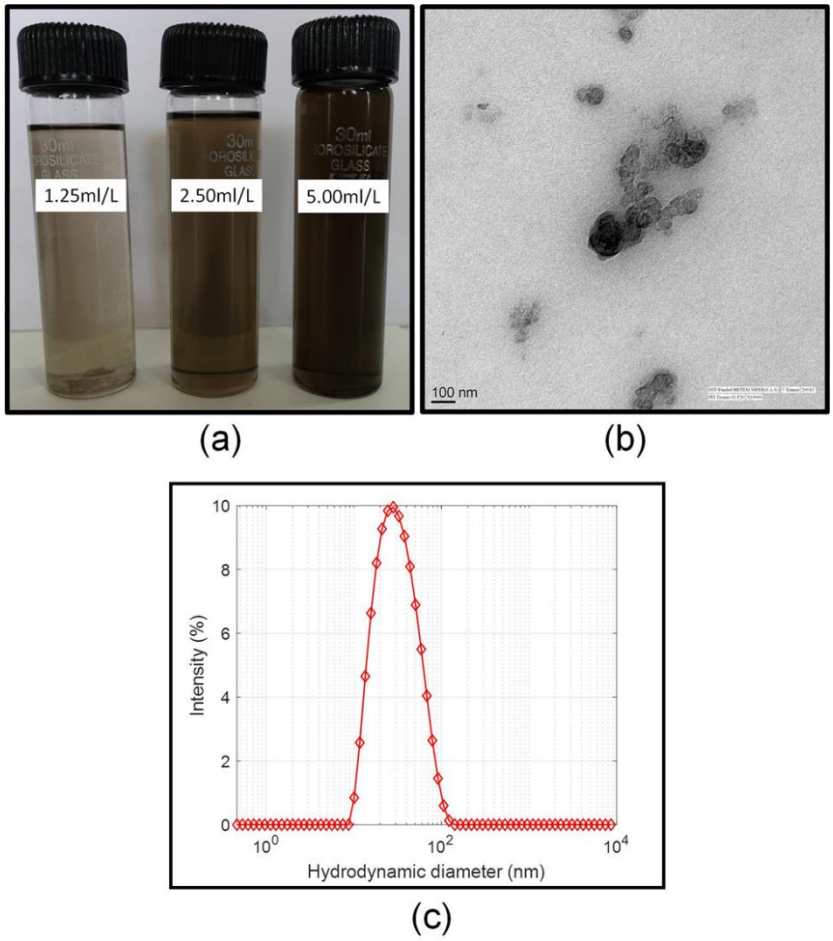

Fig. 3.6 (a) Pictures of the as-prepared nanofluids after eight months of synthesis, (b) TEM image, and (c) hydrodynamic particle size distribution (1.25mlL^{-1} nanoparticle concentration).

3.1.4 Solar Pond

The trapezoidal-shaped solar pond was built using a mild steel sheet (3 mm thick) with a top surface of 1.62 m x 1.62 m, a bottom surface of 0.71 m x 0.71 m, and a depth of 0.90 m, as illustrated in Fig. 3.7, to minimise heat loss from the solar pond, rock-wool insulation (150 mm thick) was employed. The insulation layer was then wrapped by 1 mm thick polycarbonate panels. To maximise solar energy absorption the inner walls of the solar pond were painted with corrosion resistant black paint. Two transparent toughened glass coverings were used at top of solar pond,

reducing the potential thermal losses. (each 5 mm thick, and spaced 10 mm apart by employing spacers in between).

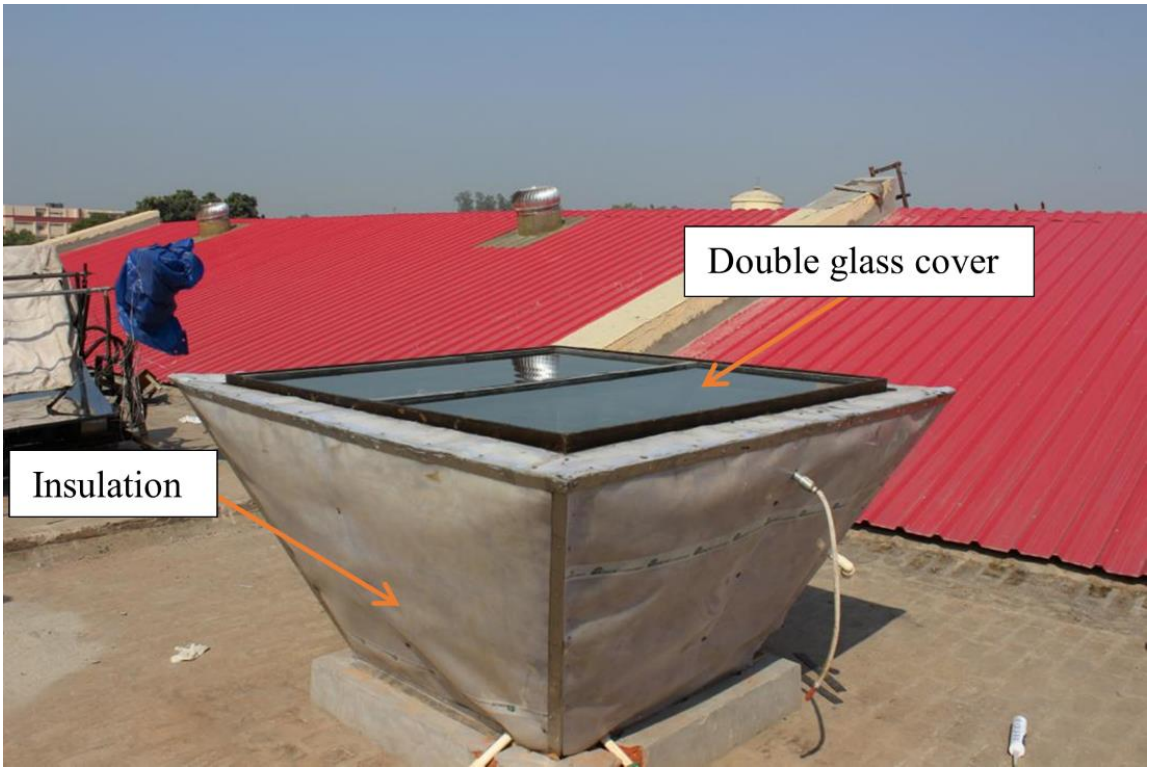

Fig. 3.7 Solar Pond

A heat exchanger, as shown in Fig. 3.8, was constructed to transfer heat from the solar pond into the still's water basin. Eight copper tubes (12 mm diameter, 2 mm thick, and 915 mm in length) were used to build the heat exchanger, with galvanised iron tube acting as the headers at the top and bottom (25 mm diameter, 610 mm in length). To transmit heat by circulating heat transfer fluid (HTF) using a 19 W rated liquid pump, the top and bottom headers of the solar pond heat exchanger were connected to the intake and exit pipes of the solar still heat exchanger through CPVC (Chlorinated polyvinyl chloride) pipes.

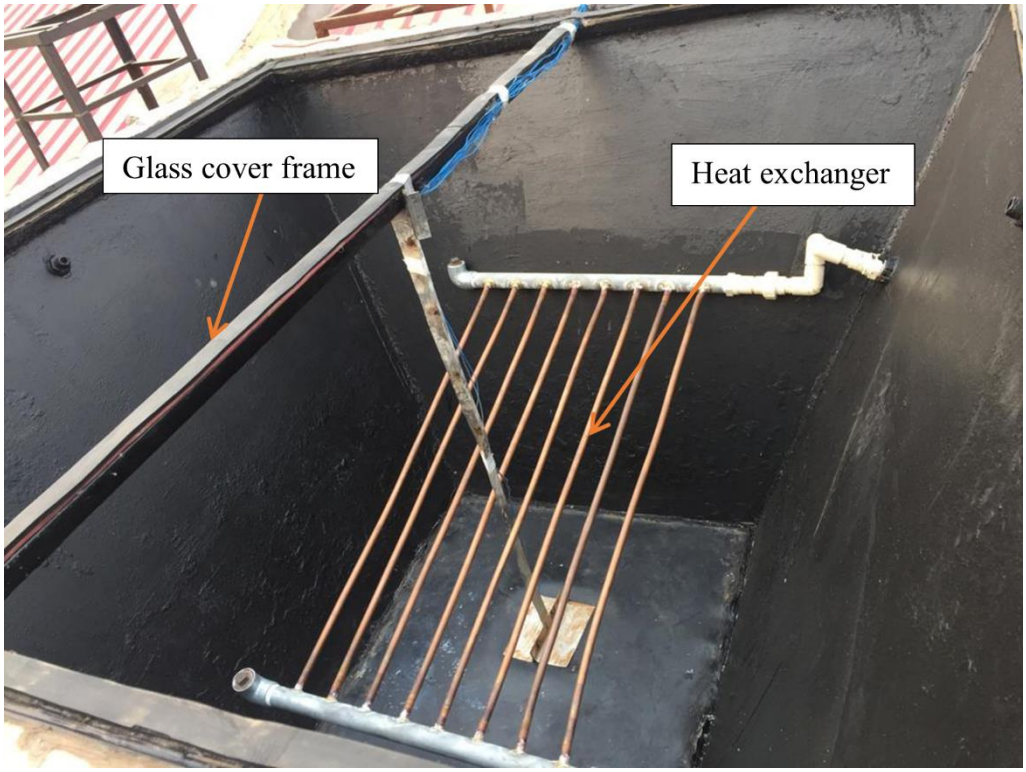

Fig. 3.8 Pictorial view of solar pond heat exchanger

3.1.5 DC pump

As illustrated in Fig. 3.9, a DC pump was employed to transfer heat from the NBVASC (via heat exchanger) to the solar still (via heat exchanger) throughout the sunshine hours. The pump employed for the circulation of fluid in the serpentine heat exchanger was chosen after calculating the various factors regarding pump work. Firstly, the flow type was determined, i.e., whether it's laminar or a turbulent flow (from Reynolds number, $Re = \rho vd/\mu$; where ρ (fluid density, kg/m^3)**,** v (velocity of the fluid, m/s)**,** d (diameter of the pipe, m)**,** and μ (dynamic viscosity of the fluid, Ns/m^2)

The Reynolds number (Re = 4243) being in the turbulent regime, the Darcy-Weisbach equation ($h_f = 4flv^2/2gd$; where f (coefficient of friction), and l (pipe length) was invoked for calculating the frictional pipe losses. Furthermore, the head losses due to bends have been found through h_b =

$nKv^2/2g$ (K = loss coefficient/resistance coefficient of bend, 0.2 and 0.45 for 180^o and 90^o bends, and n (total number of bends, for present work, n = 18 @180^o bends and n = 20 @ 90^o bends)

To calculate the pump's power requirement for the above flow rates and dimensions, power has been calculated using the relation $P = \rho ghQ$. (where $h = h_h + h_v$: $h_h = h_f + h_b$ is the horizontal head loss and h_v is the vertical head loss.

Accounting for both the minor and major losses in the pipe and bends, the power rating comes out to be 1.653 watts; this is the minimum requirement for the pump to make the fluid flow in the system. However, to compensate for any fluctuations and other unaccounted losses, we have employed a 19 W-rated pump.

The pump was switched on at 9 am and off at 6 pm. The 'integrated solar still' was constantly supplied with solar energy throughout the day by NBVASC in order to raise the basin water temperature resulting an increased distillate production rate due to increase in evaporation rate.

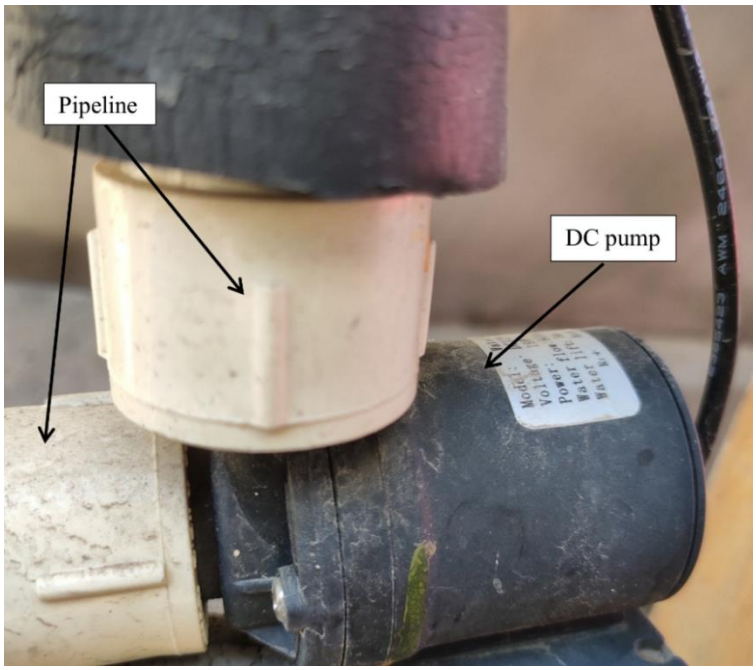

Fig. 3.9 DC pump fitted in the pipeline

3.1.6 Floating wicks

Several floating wicks of solar were put in the basin of the modified solar still to maximise the amount of distillate that could be generated both during the day and at night. The wicks, as shown in Fig. 3.10, were made from thermocol and polyurethane foam, which were then wrapped in a black cotton cloth and tied with cotton threads. Because of the wicks, the water in the basin had a greater surface area, which resulted in lower thermal inertia. Due to this, the rates of evaporation increased, thus increasing the diurnal distillate. During the hours of the day when the sun was not shining, the wicks acted as a thermal storage medium, releasing the heat that they had gathered during the hours of the day when the sun was shining. As a consequence of this, there was a considerable increase in the total quantity of the nocturnal distillate.

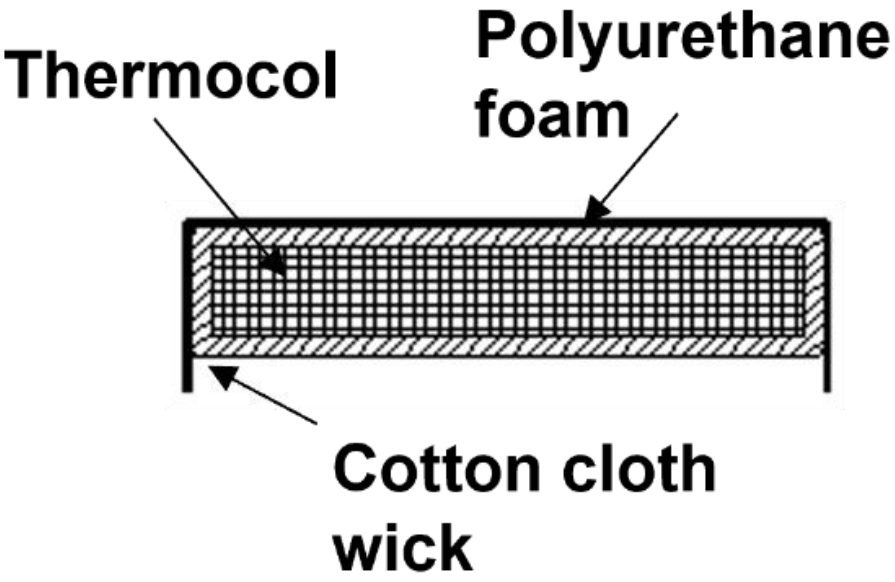

Fig. 3.10 Schematic diagram of floating wicks

3.2 INSTRUMENTATION AND MEASUREMENT

3.2.1 Solar radiation measurement

Using a Kipp and Zonen pyranometer, measurements of the global solar radiation on the integrated solar still's glass cover surface was recorded as illustrated in Fig. 3.11; the equipment can measure from 0 to 4000 W/m^2 with 1 W/m^2 of accuracy. The pyranometer was stationed next to the integrated solar still and reference still arrangement. The pyranometer was installed on a pedestal and was firmly screwed using a nut and bolt arrangement fixed to a levelled metallic plate. The global solar radiation was recorded at 10-minute intervals using a Log box SD data logger.

Fig. 3.11 Pyranometer

3.2.2 TDS measurement

The TDS (total dissolved solvents) of the input water and the distillate produced were measured using a TDS metre (Fig. 3.12) (make: Spectralab; model: COT-2). That has a microprocessor and an LCD display, it is a TDS measurement tool. The equipment can detect concentrations from 1 ppm to 200 ppm. The instrument's accuracy is 2% of the reading. At regular intervals, the TDS content of the input water and the distillate produced by the solar still were monitored.

Fig. 3.12 TDS meter

3.2.3 Programmable timer electric switch

The pump was set to run automatically at night through a programmable electric switch (Fig. 3.13) with a programmable timer. One can schedule the switch's on and off times by selecting the day of the week and a specific time slot within that day. The switch allows for several time settings

to accommodate odd working hours. The pump was turned on at 1:00 am and turned off at 4:00 am for the current study.

Fig. 3.13 Programmable timer electric switch

3.2.4 Temperature measurement

Type K thermocouples (range: -150 °C to 300 °C, accuracy 1 °C) were used to measure the temperatures of the integrated solar still and a conventional still. Temperature data logger (Fig. 3.14; Make: HPG systems) automatically recorded all temperature observations. The temperatures at all key locations of both integrated and conventional solar stills were measured. In addition to this, the temperatures of the inlet and exit sections of the solar pond, integrated solar still, and NBVASC collector heat exchangers were also measured. The glass coverings of the solar pond and the NBVASC were both monitored for temperature. The placement of thermocouples at the bottom, 2 cm and 4 cm in height, allows spatial temperature distribution calculation within the NBVASC. The average solar pond temperature was measured using three thermocouples: one at the bottom, one in the middle, and one ten centimetres below the top of the solar pond. For all temperature measurements, the logging frequency was set to 10 minutes. To attach the

thermocouple to the glass surfaces of both the stills and the solar pond, a bead of thermocouple was placed in contact with the glass surface using aluminium foil tape, and then silicon glue was applied over it. The aluminium foil acts as a barrier, preventing direct solar radiation from falling on the glass surface thermocouple bead.

Fig. 3.14 Temperature data logger

3.3 EXPERIMENTAL PROCEDURE

The experimentation was done at Patiala, India, located at 30.35 °N latitudes and 76.36 °E longitudes. For the current study two identical conventional solar stills (having single basin and single-slope) with glass covers were constructed and analyzed. Same material, size and shapes were employed for constructing both the stills. One of the two conventional stills was modified by connecting it with the solar pond and the NBVASC to provide supplementary heat energy to the basin water. For comparison purposes, experiments were done on both the stills at the same time, placed adjacent to each other, under identical weather and solar surroundings. Before connecting

the NBVASC and solar pond with any one of the still, it was ensured that the performance of both the conventional stills was the same under the same outdoor and operational conditions. For this, the performance of both the conventional stills was checked by running them simultaneously for 24 h on three different days. In each of the three calibration tests, it was discovered that the difference in production between the two types of stills was within $\pm$1% of the difference. All the pipeline connections were tested for any leakages during operation.

Experimental duration was from 8 am to 6 pm to compare the modified still's performance with the conventional solar still. The reason for performing tests from 8 am to 6 pm is that the experiment location is surrounded by multistory buildings, which prevent direct solar radiation from reaching the experiment site before 8 am and after 6 pm. Studies were carried out with 3 cm water depth in both stills. The flowing rate of the HTF in the pipeline connecting the heat exchangers of NBVASC and solar still was maintained at 3 litres per minute by using a 12 V DC pump. It was turned on one hour after the beginning of the experiment (i.e., at 9 am) to give some time to the nanofluid of NBVASC to absorb solar radiation and reach a temperature higher than the solar still, and it was switched off at 6 pm. The experiments were performed with different nanofluid concentrations in the solar collector (viz. $0mlL^{-1}$, $1.25mlL^{-1}$, $2.5mlL^{-1}$, and $5mlL^{-1}$), which is coupled to the solar still. The first category being $0mlL^{-1}$ concentration nanofluid, i.e., pure paraffin oil (simulating a conventional surface absorption-based collector (CSASC)) and the second category constitutes volumetric absorption-based solar collectors with nanofluid concentrations as $1.25mlL^{-1}$, $2.5mlL^{-1}$, and $5mlL^{-1}$. Distillates formed in both cases, viz., modified solar still coupled with paraffin oil-based solar collector (CSASC) and modified solar still coupled with NBVASC, were calculated every hour between 8 am to 6 pm to examine the stills' performance for every hour during the sunshine hours. The distillate generated throughout non-

sunny times was gathered only once, at 8:00 am the following morning (it may be noted that the distillate was measured every hour while performing 24-hrs experiments for both the stills), and it is referred to as the nocturnal distillate of the still.

A trapezoidal shape solar pond was constructed to provide thermal energy to the solar still during non-sunshine hours (particularly during nighttime, 1:00 am – 4:00 am) with the help of a pump (controlled through a programmable electric switch).

The solar radiation impinging on the glass cover of the solar still was recorded using a pyranometer (Kipp and Zonen), and the data was continuously logged within the LOG BOX data logger. K-type thermocouples were employed for temperature measurement at several key positions in the solar still and in the NBVASC, and in the pipeline system. The spatial temperature distribution in the NBVASC was measured by fixing the thermocouples at the bottom, at 2 cm height and 4 cm height of the NBVASC. The temperature data was logged continuously in a separate microprocessor-based multi-channel data logger. The temperatures of the internal and external glazing of the NBVASC were also measured. The logging frequency was fixed at 10 minutes for all the measuring instruments. The quality of impure water and distillate produced was measured at regular intervals by checking the TDS levels of the distillate.

The following three stages comprised the current experimental work:

3.3.1 Fabrication and performance investigation of nanofluid-based volumetric absorption solar collector (NBVASC)

At the preliminary phase of the study, a NBVASC was constructed to continuously deliver additional heat to the solar still during daylight hours. It was built by manufacturing a shallow container fixed on a stand and covering its top surface with two transparent glass coverings; the

container has a hole in the bottom surface which is fitted with chlorinated polyvinyl chloride pipe (CPVC), and two valves in such a manner that this hole is used as both as charging and discharging point for the fluid. The collector's top and bottom surfaces measure 1.20 m x1.07 m, and its depth is 0.10 m. It was constructed from a 3 mm-thick sheet of mild steel. The side walls of the NBVASC were insulated with polyurethane measuring 100 millimetres thick for reducing the heat that would have been lost from the solar collector. In addition, in order for this rock-wool insulation to endure the extremes of the outdoor weather, it was covered with galvanised iron sheets that were one millimetre thick. Two transparent toughened glass covers, 5 mm thick and 10 mm apart, were placed over the top of the nanofluid-based solar collector to cut down on convective losses. The glass covers were mounted to an internal frame, allowing the container's fluid level to be modified as needed. The fluid was to be in touch with the lower glass cover to minimise convective heat transfer losses. To prevent fluid and thermal energy leakages, high-temperature silicone sealant was used to seal all the connection points of the solar collector container, including the glass cover with the frame, the glass cover with the collector container, inlet, and outlet connections of the heat exchanger and the CPVC pipes with the container. In the testing phase the fabricated solar collector was filled with pure paraffin oil and then with nanofluids of various concentrations (1.25 mlL^{-1}, 2.5 mlL^{-1} and 5 mlL^{-1}). During extensive on-sun testing of the solar collector, the spatial temperature distribution was determined by measuring the temperatures at the bottom, at 2 cm height and 4 cm height of the solar collector. It was concluded that temperature was uniform in the pure paraffin oil-based collector throughout the fluid depth. In the next phase, the collector was filled with different nanofluid concentrations. The maximum temperatures were recorded in the middle and top layers of the nanofluid for all the concentrations. The final thickness of the nanofluid layer was decided to be 4 cm as, at this thickness, the chosen nanofluids absorb more

than 80% of the solar radiation impinged on it [83]. Further, a serpentine-type heat exchanger (filled with ethylene glycol-based heat transfer fluid to transport the collected thermal energy to the integrated solar still) was fitted in the region of 2 cm and 4 cm from the bottom of the basin of the collector. From the abovementioned testing of the fabricated solar collector, it was concluded that the nanofluids reach higher temperatures and they harness solar energy more efficiently than the base fluid (Paraffin oil); the solar energy was absorbed by volumetric absorption and scattering mechanism by nanofluids.

3.3.2 Performance investigation of solar still integrated with nanofluid-based volumetric absorption solar collector (NBVASC).

In the study's second phase, in order to assess the effectiveness of the modified solar still in relation to that of a conventional solar still under same environmental circumstances, the fabricated and tested NBVASC was connected to the solar still. The experiments were done on the modified still (CSASC- and NBVASC-coupled solar stills) and the conventional still at the same time for a number of days through the period from March to July 2020. In this phase, the optimum nanoparticle concentration that should be employed in the NBVASC for obtaining maximum distillate output was also identified.

3.3.3 Performance investigation of solar still integrated with NBVASC and solar pond

In the third and final phase of the study, the integrated solar still was studied for its round-the-clock performance by coupling it with a NBVASC during sunshine hours and with a solar pond during non-sunshine hours. The collected thermal energy by the NBVASC during the daytime was continuously supplied (9 am to 6 pm) to the integrated still. During the non-sunshine hours when there was no direct sunlight, the integrated solar still received the thermal energy that had been accumulated by the convective solar pond during the day. Different timings and durations were tested for supplying thermal energy during the night, but the timings between 1:00 am – 4:00 am

were found to impact the distillate production and efficiency of the still significantly. Heat exchanger was installed in the convective solar pond to transfer the accumulated thermal energy to the still. The solar still and solar pond heat exchangers were then filled with HTF and connected to each other by a series of valves and a pipeline system. The flow rate was maintained at 3 litres per minute with the help of a DC pump, and a programmable electric switch controlled the timings. To enhance the performance of the modified solar still, floating wicks were also utilised in the present set of experiments. Table 3.3 lists the range of parameters utilised in current experimentation.

Table 3.3 Range of parameters for performance testing of solar still integrated with NBVASC and solar pond.

Design and operational parameters	
Nanofluid concentration	Pristine paraffin oil,1.25mlL^{-1}, 2.5mlL^{-1}, and 5mlL^{-1}
HTF flow rate	3 LPM
Basin water depth	3 cm, 4 cm, 5 cm
Nanofluid depth (All concentrations)	4 cm
Floating wicks	Thickness:20mm Width: 50mm Length: 600mm
Convective solar pond	Tap water
Heat transfer fluid (HTF)	Ethylene glycol and water solution

3.4 Concluding remarks

All components of the NBVASC, solar still, and solar pond utilised for the experiment have been described in terms of their dimensions, construction materials, working fluids, and phenomena. The range and accuracy of the measurement instruments are provided. Each experiment's procedure has been discussed in detail. The experimental investigation of the solar still combined with NBVASC and a solar pond has documented the design and operating range of parameters employed in the study.

Chapter 4

Experimental results and data analysis

Present chapter summarises the results of each set of experiments discussed in Chapter 3. To identify the optimal depth and concentration of the nanofluid to be utilised in the solar collector and to determine if the nanofluid had advantages over the pure paraffin oil (base fluid), a host of experiments were conducted on NBVASC. The prediction of the thickness of the nanofluid (in the solar collector) where the maximum temperature will exist was crucial as it decided the placement of the heat exchanger. The analysis of solar still integrated with a paraffin oil-based surface absorption solar collector (CSASC) is presented here in comparison with the conventional solar still. The conventional still was placed adjacent to the integrated still under similar conditions to determine the effects of the paraffin oil-based solar collector on the production and efficiency of the modified still. Further, the experiments were conducted on the NBVASC with concentrations of $1.25 mlL^{-1}$ and $2.5 mlL^{-1}$ of nanofluid. In these experiments, the effect of nanoparticle concentration (in NBVASC) on production and efficiency of the NBVASC-integrated still was determined. Finally, the integrated solar still was analysed for round-the-clock performance when integrated with NBVASC during the sunshine hours (9 am to 6 pm) (here, the thermal energy was supplied continuously) and with the solar pond (thermal energy was supplied from 1:00 am to 4:00 am). Thermal energy transfer was done by circulating heat transfer fluid (HTF) through the heat exchangers. There was no direct contact of the nanofluids with the HTF or the water in the integrated system.

Moreover, the performance of a modified solar still was compared with that of a conventional solar still, and the impact of floating wicks and varying basin water depth (BWD) was also

assessed. Economic analysis was performed to determine the system's viability for commercialization and on-site use to aid communities and regions having little or no access to potable water, and finally, uncertainty analysis was done to ascertain the uncertainties involved in the research. The experimental results obtained from each set of experiments and their analysis are presented in the following sections.

4.1 Performance investigation of nanofluid-based volumetric absorption solar collector (NBVASC)

The experiment was performed to find out the variation in the temperature at different nanofluid heights to finalize the height at which the heat must be efficiently and effectively extracted by the heat exchanger.

Figure 4.1 illustrates the spatial temperature distribution concerning NBVASC - temperatures at the bottom, middle (2 cm height) and top (4 cm height) layers of the solar collector. During this experiment, no heat was extracted from the NBVASC. This experiment was performed to find out the variation in the temperature at different nanofluid heights to finalize the position at which the heat exchanger must be placed to extract heat effectively and efficiently. Several trial experiments were performed for this, and the reported one was performed a day before (8th June 2020) the actual experiment, as the solar conditions were almost similar on both days. Herein, 'actual experiment' refers to the experiment in which NBVASC was used to supply heat to solar still. Fig. 4.1 depicts that the top and mid-layer temperatures follow trends like solar irradiation, i.e., temperatures increase during forenoon hours and decrease during afternoon hours. On the other hand, the bottom layer temperature increases during the first two hours only, after which the bottom layer temperature stagnates, i.e., remains almost constant throughout the remaining part of the day. The temperatures in both the top and middle layers are almost the same throughout the day (except in forenoon hours, where the top layer has a slightly higher temperature). The observed

pronounced spatial temperature variation in the vertical direction could be understood from the fact that the incident irradiation attenuates exponentially along this direction. This causes the highest temperatures to be found at the top, while the lowest temperatures may be found at the bottom. Moreover, in the absence of natural convection effects, the absorbed energy in the layers is stratified - heat transfer among the layers being limited to conduction mode only. The maximum temperatures recorded at 4 cm height, 2 cm height and at the bottom of the NBVASC were 84°C, 82°C and 46.5°C, respectively. It could be interpreted from Fig. 4.1 that the highest temperatures in the NBVASC occur in the region of 2 cm to 4 cm in height in the nanofluid. The heat exchanger should be located here so that it can absorb the highest amount of thermal energy.

In the backdrop of the aforementioned fact, the heat exchanger in the NBVASC was fitted such that it was just submerged in the nanofluid. As the heat exchanger tube is 1.5 cm in diameter, it is always at the hottest part of the NBVASC, which ranges in height from 2 cm to 4 cm.

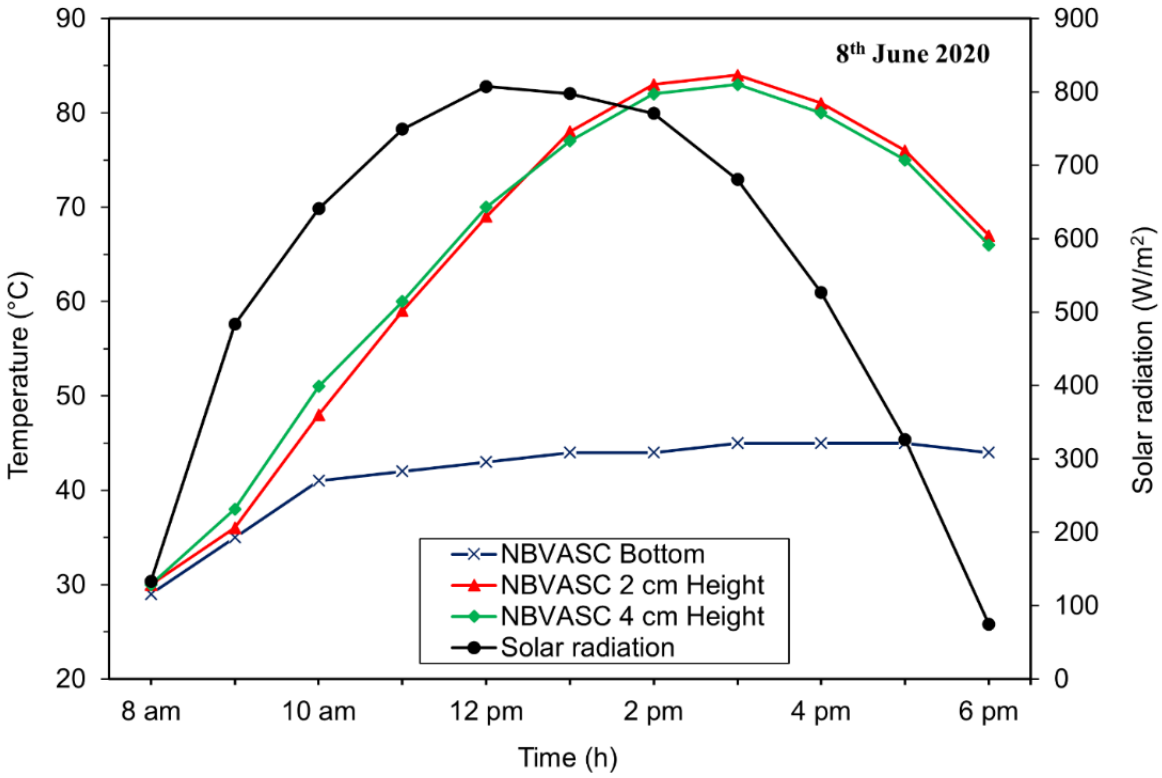

Fig. 4.1 Variation of temperature in the NBVASC without heat extraction. Nanoparticle concentration is 1.25mlL^{-1}

Figure 4.2 indicates the distribution of temperature in the NBVASC at the bottom, 2 cm, and 4 cm heights on the day of the 'actual experiment' (9th June 2020). It can be seen that the upper layers remain at higher temperatures than the bottom layers, as expected and as seen in the previous experiment where there was no heat extraction. The top region at 4 cm height remains the hottest, maintaining a slight edge over the 2 cm region temperature during the course of the experimentation. Highest temperature of 82°C was noted at the top layer at 2:30 pm and 81.5°C at the middle layer at 2:50 pm, whereas the bottom layer recorded highest of 47°C at 3:10 pm, which is very low in comparison to the middle and upper layers.

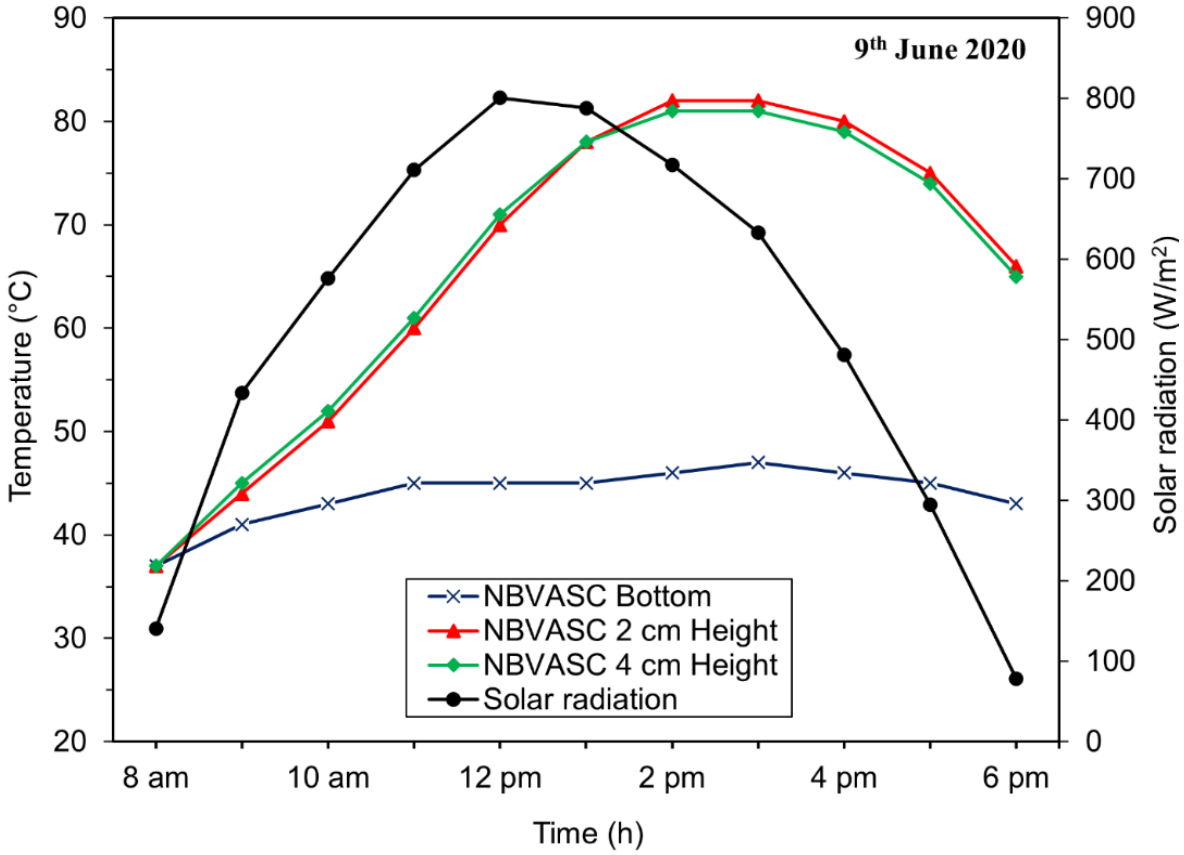

Fig. 4.2 Temperature variation in NBVASC with heat extraction. Nanoparticle concentration is 1.25mlL^{-1}.

4.2 Performance investigation of solar still integrated with nanofluid-based volumetric absorption solar collector (NBVASC)

All the experiments were done on the modified still (MS) [CSASC and NBVASC coupled solar stills] and the conventional still at the same time for a number of days through the period from May to July 2020. In order to identify the optimum nanoparticle concentration that should be employed in the NBVASC coupled solar still, initial experiments were carried out at all the nanoparticle concentrations (1.25mlL^{-1}, 2.5mlL^{-1}, and 5mlL^{-1}). Extensive on-sun testing reveals that NBVASC coupled solar still has distillate productivity values (from 8:00 am to 6:00 pm) of

$3.69Lm^{-2}$, $3.20Lm^{-2}$, and $2.37Lm^{-2}$ at nanoparticle concentrations of $1.25mlL^{-1}$, $2.5mlL^{-1}$, and $5mlL^{-1}$. This clearly establishes that for the given depth, $1.25mlL^{-1}$ is the optimum nanoparticle concentration at which distillate output is at a maximum. At nanoparticle concentrations higher than the optimum value, the incoming solar radiation gets absorbed on the surface (within a few layers at the top) - thus resulting in an escalation of thermal losses and hence reduction in distillate output.

Now that we have identified the optimum nanoparticle concentration to be employed in NBVASC coupled solar still, it is imperative to carefully investigate the performance characteristics of NBVASC coupled solar still (at optimum nanoparticles concentration) and the CSASC (pure paraffin oil-based solar collector, i.e. nanofluid concentration is $0mlL^{-1}$) coupled solar still. It may be noted that the on-sun experiments have been performed for a number of days, and the fact that the environmental conditions do not remain exactly the same on any two consecutive days of the year, it is imperative to carefully define the performance characteristics to correctly compare various solar still configurations. At any given time, two solar stills are in operation - one being the modified still (coupled with CSASC or NBVASC) and the other being the conventional still. Therefore, conventional solar still is the common configuration in each of the experiments - representing the reference configuration. Hence, in order to compare the modified stills among themselves, the performance characteristics have been normalized with the corresponding performance characteristic of the reference still.

The findings of the experiment that was carried out on 25th May 2020, with solar still coupled with the pure paraffin oil-based solar collector and the experiment conducted on 9th June 2020 with solar still coupled with the nanofluid ($1.25\ mlL^{-1}$) based solar collector are reported here. As noted earlier, these two experiments were conducted on different days; therefore, comparison of the two

aforementioned variants of modified solar stills necessitates non-dimensionalization of the performance parameters. All the performance parameters/characteristics of modified stills are compared and discussed here in terms of the ratio of the values of modified still to that of the corresponding conventional still (which is used as a reference still in the present work). For example, the modified still's basin water temperature is represented and discussed in terms of the ratio of the modified still's basin water temperature to that of the conventional still. As the variation in basin water temperature during the daytime for the conventional still is representative of the variations in solar and ambient conditions on a particular day, this basin water temperature ratio facilitates the comparison between the experiments conducted on different days. Similarly, the hourly distillate production of the modified still is presented in terms of the hourly productivity ratio, i.e., the ratio of the hourly distillate productivity of the modified still to the hourly distillate productivity of the conventional still. Figure 4.3 details the solar radiation distribution and ambient temperatures on 25th May 2020 and 9th June 2020, respectively. The smooth variation of solar radiation throughout the day on these two days shows that they are clear sunny days. Solar radiation intensity on these two days, i.e., 25th May 2020 and 9th June 2020, attained its maximum value at 12:20 pm and 12:30 pm, respectively, whereas ambient temperature achieved its maximum value at 1:00 pm and 1:10 pm, correspondingly.

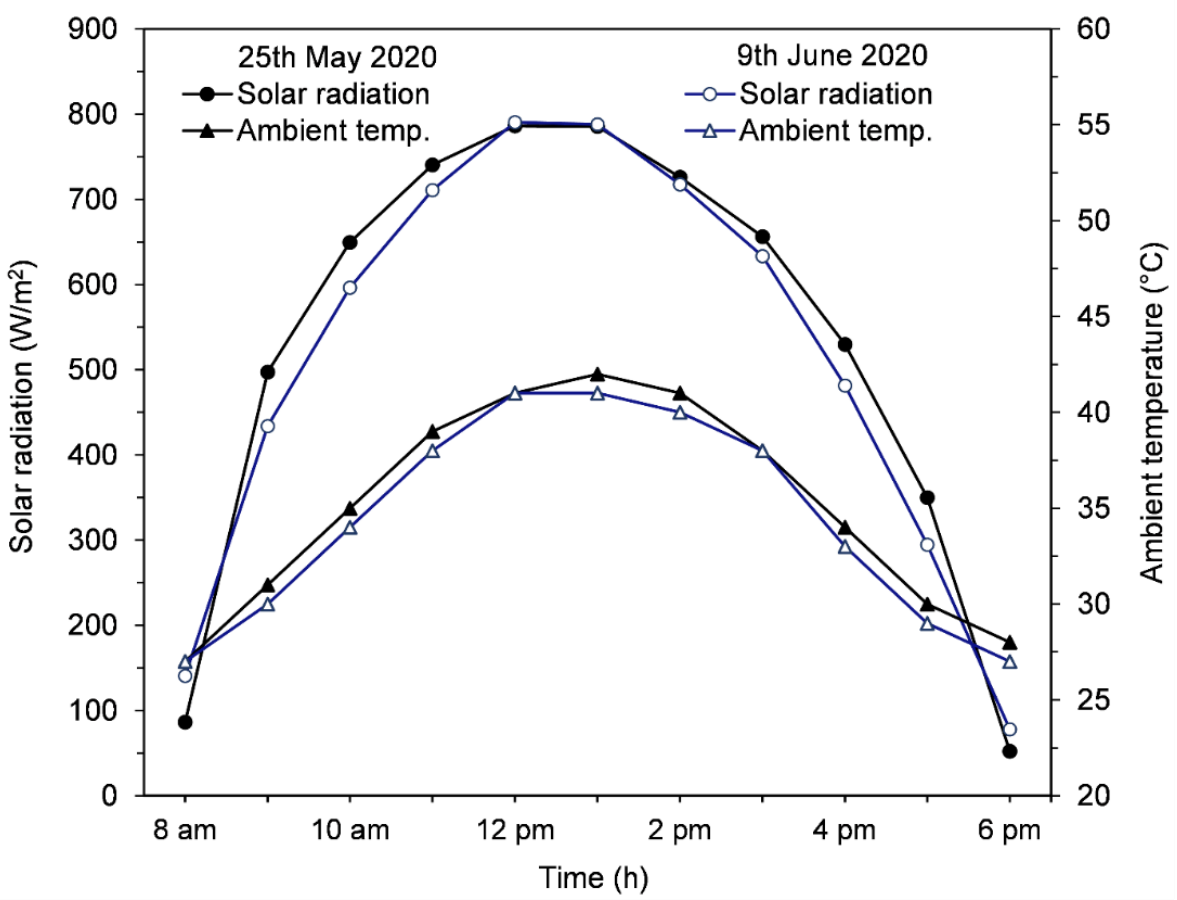

Fig. 4.3 Variation of solar radiation and ambient temperature at Patiala (30.35°N latitude and 76.36°E longitude), India

4.2.1 Comparison of basin water temperature of conventional and modified still (MS)

Figure 4.4 illustrates the average spatial basin water temperature distribution of reference still along with modified still coupled with nanofluid (1.25mlL^{-1}) based solar collector along with the temperature variation of NBVASC at 4 cm height. It can be observed that the temperature in the upper region (at 4 cm height) remains substantially higher. No extra heat was applied to the modified still during the first hour of the experiment (8-9 am), therefore water temperatures in both the conventional and modified stills were identical. From 9:00 am to 12:00 noon, the water temperature in the modified still increases at a higher rate as compared to that in the conventional

still because of continuous additional heat transport from NBVASC to the solar still. From 12 pm, till evening, with an average difference of 5.8°C, the modified still's basin water temperature maintains a nearly continuous advantage over conventional still's basin water temperature. Afternoon solar radiation raises the modified still's basin water temperature, which enhances the water's evaporation rate and improves the modified still's performance (relative to the conventional still).

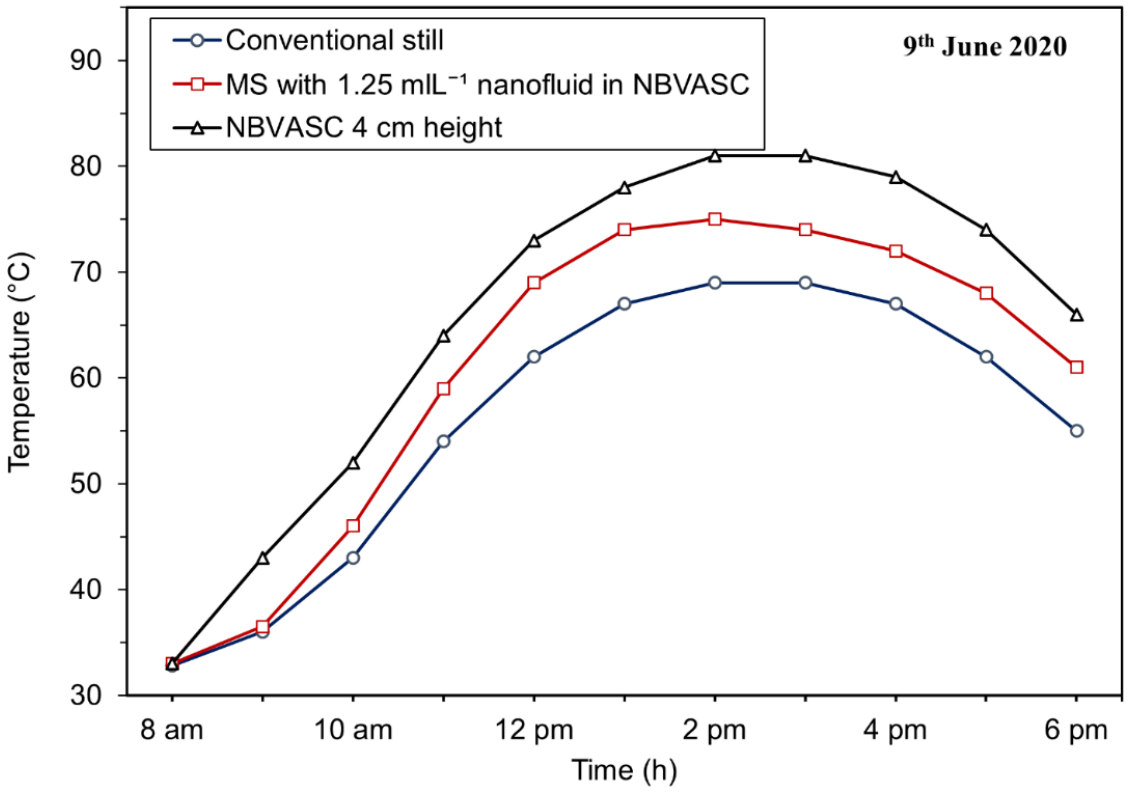

Fig. 4.4 Temperature variation of basin water in conventional and modified solar stills

Figure 4.5 illustrates the comparison of temperature of basin water in both modified solar stills, i.e., solar still coupled with CSASC and solar still coupled with nanofluid (1.25 mlL^{-1}) based

volumetric absorption solar collector. Since the experiments on these two modified stills were conducted on different days, the comparison of basin water temperatures of these two stills is plotted and discussed in terms of basin water temperature ratio, i.e., the ratio of modified still's to that of conventional still's basin water temperature. The basin water temperature ratio curve for solar still with nanofluid (1.25 mlL^{-1}) based solar collector stays above the corresponding curve for solar still with paraffin oil-based solar collector throughout the day, which suggests that the performance of solar still with NBVASC (1.25 mlL^{-1}) is better than the CSASC coupled still.

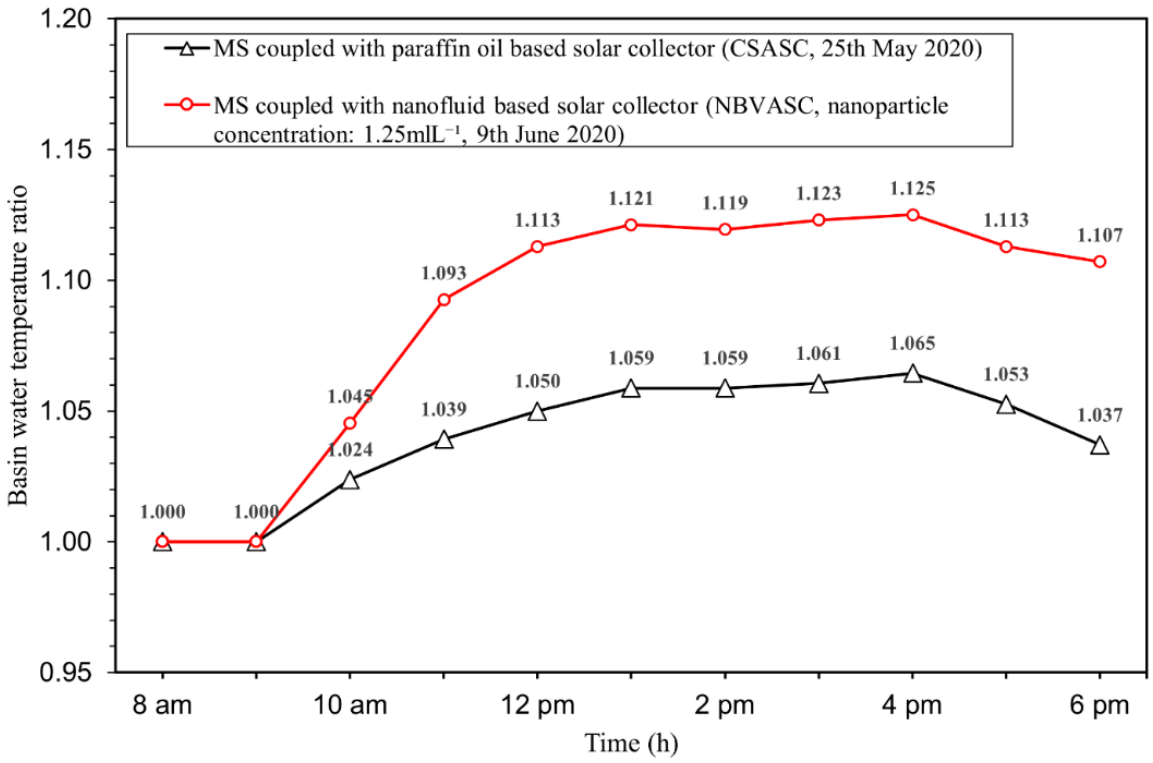

Fig. 4.5 Comparison of basin water temperature in modified stills

4.2.2 Hourly performance and cumulative distillate productivity of solar stills

Hourly performance of modified solar stills coupled with paraffin oil based solar collector and nanofluid (1.25 mlL^{-1}) based solar collector respectively, is compared in terms of their hourly productivity ratio in Fig. 4.6. The rapid rise in hourly productivity after 9 am is attributable to the supply of external heat from the solar collector, which increases the evaporation rate by increasing the temperature of the basin water. After 10 am, when the solar still stabilises, the rate of increase in hourly productivity relatively decreases. After 11 am, when solar radiations increase, the temperature of the basin water increases and reaches its maximum value around 1 pm. With a drop in solar radiation in the afternoon, the hourly production steadily declines. It can be inferred from the graph that the hourly distillate obtained from solar still with nanofluid (1.25 mlL^{-1}) based solar collector, during each hourly time interval from 9 am to 6 pm was higher than the corresponding hourly distillate obtained from solar still coupled with paraffin oil based solar collector.

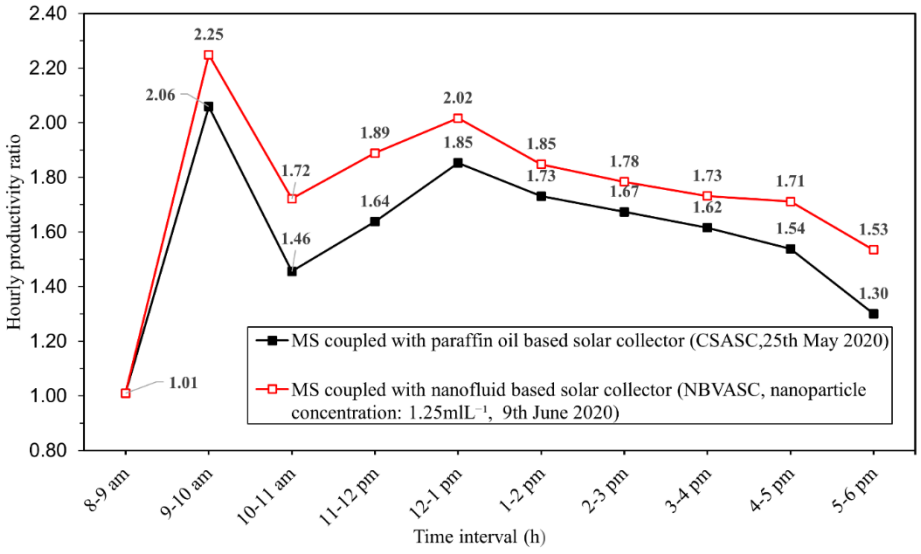

Fig. 4.6 Hourly "distillate productivity ratio" comparison for modified stills

Figure 4.7 depicts the variance in cumulative distillate of a conventional still and a modified still coupled with a nanofluid (1.25 mlL^{-1}) based solar collector. Since the amount of distillate produced is dependent on the solar insolation, the cumulative distillate production curves for both conventional and modified stills rise as the day passes from morning to midday and fall in the afternoon. Figure 4.7 also shows the amount of night distillate produced from these two stills. The distillate that had been generated over the previous night was measured the next morning before dawn. There was a significant temperature disparity of about 30ºC between the temperature of the water in the modified still's basin and the temperature of the surrounding air, which resulted in the production of a sizeable quantity of nocturnal distillate from the modified still. The night distillate generated by the modified still was 33.9% greater than that produced by the conventional still. Total amount of distillate generated by the reference still and the modified still was 2.57 L/m^2 and 4.48 L/m^2, correspondingly. 75.3% more distillate was generated by modified still than the conventional still, which is a considerable improvement.

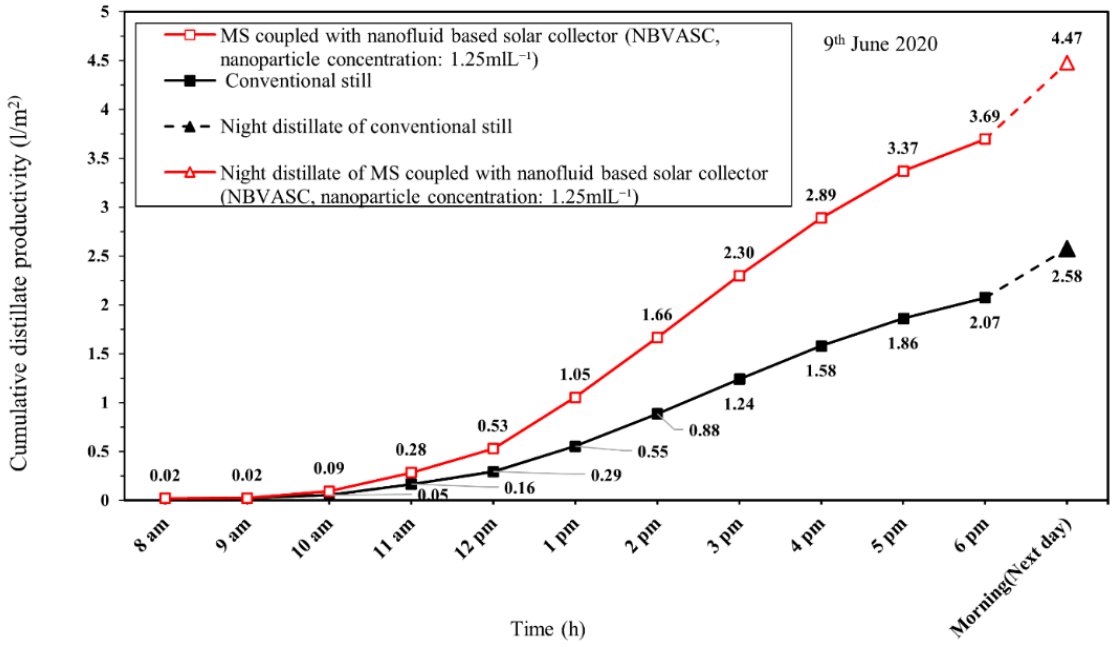

Fig. 4.7 Variation of cumulative distillate productivity of conventional and modified stills

4.3 Performance investigation of NBVASC and solar pond coupled solar still (integrated solar still)

Round-the-clock (24-hour duration) experiments were done on "integrated solar still" (with and without floating wicks) for several days from March to June 2020. The findings of the experiments carried out on March 15th and 19th, 2020, when an integrated solar still was coupled with a pure paraffin oil-based surface absorption solar collector, and the experiments performed on June 16th and 23rd, 2020, when an integrated solar still was coupled with a nanofluid (1.25mlL^{-1}) based volumetrically absorbing solar collector (NBVASC) are discussed here. Among the operational parameters, the incident sunlight and ambient temperatures are the significant parameters affecting solar still distillate and its performance. The variations on the days of experiments are presented here.

Figure 4.8 illustrates the solar irradiation and variation in the ambient temperature for the experiments when wick-type solar still was coupled with nanofluid (1.25 mlL^{-1}) based

volumetrically absorbing solar collector data for 16th and 23rd June 2020 is presented in the figure. Both were sunny days with smooth variations of solar radiations; the solar intensity on the days of experiments, i.e., on 16th and 23rd June, was maximum at 12:20 pm and 12:30 pm, respectively, with ambient temperature attaining its maximum value around 1:20 pm and 1:40 pm, correspondingly.

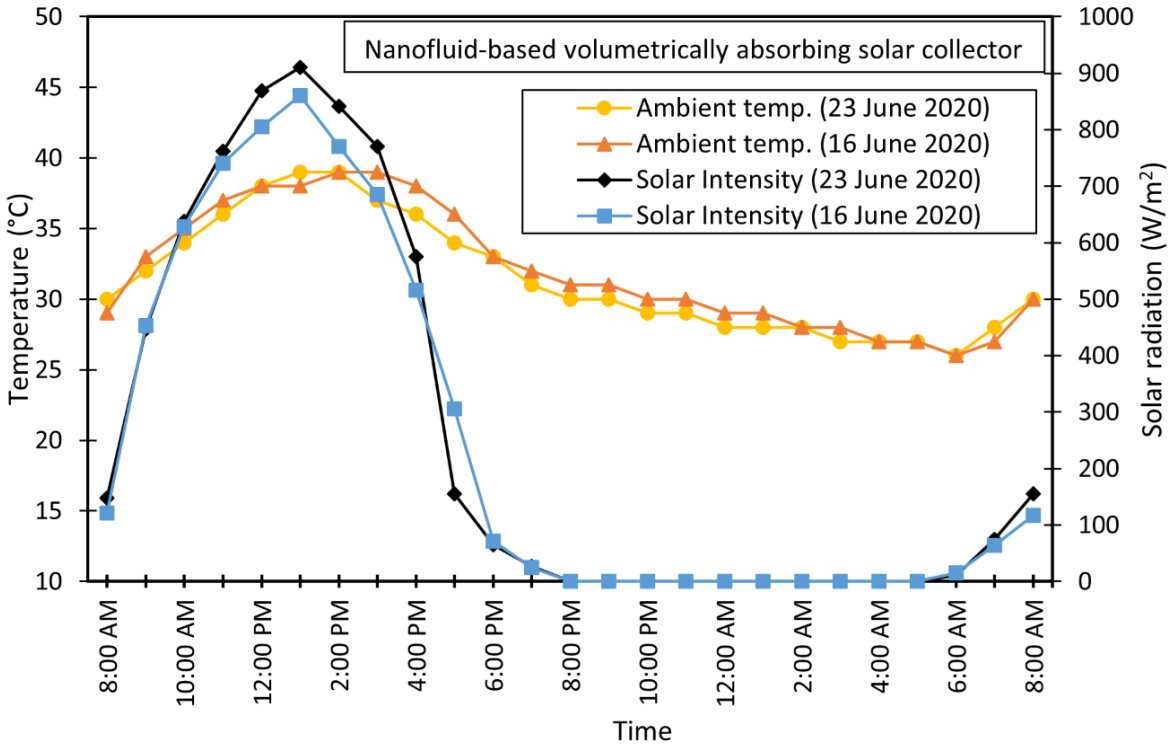

Fig. 4.8 Variation of solar radiation and ambient temperature on 16th and 23rd June 2020

Figure 4.9 represents the fluctuation in ambient temperature and solar radiation during the experiments done using a wick-type integrated solar still with a paraffin oil-based surface absorption solar collector, and a solar pond, data for 15th and 19th March 2020 is presented in the figure. Both were clear and sunny days with a smooth variation of solar radiations; the solar

intensity on the days of experiments, i.e., on 15th and 19th March, was maximum at 12:30 pm and 12:40 pm respectively, with ambient temperature attaining its maximum value around 1:40 pm and 1:50 pm.

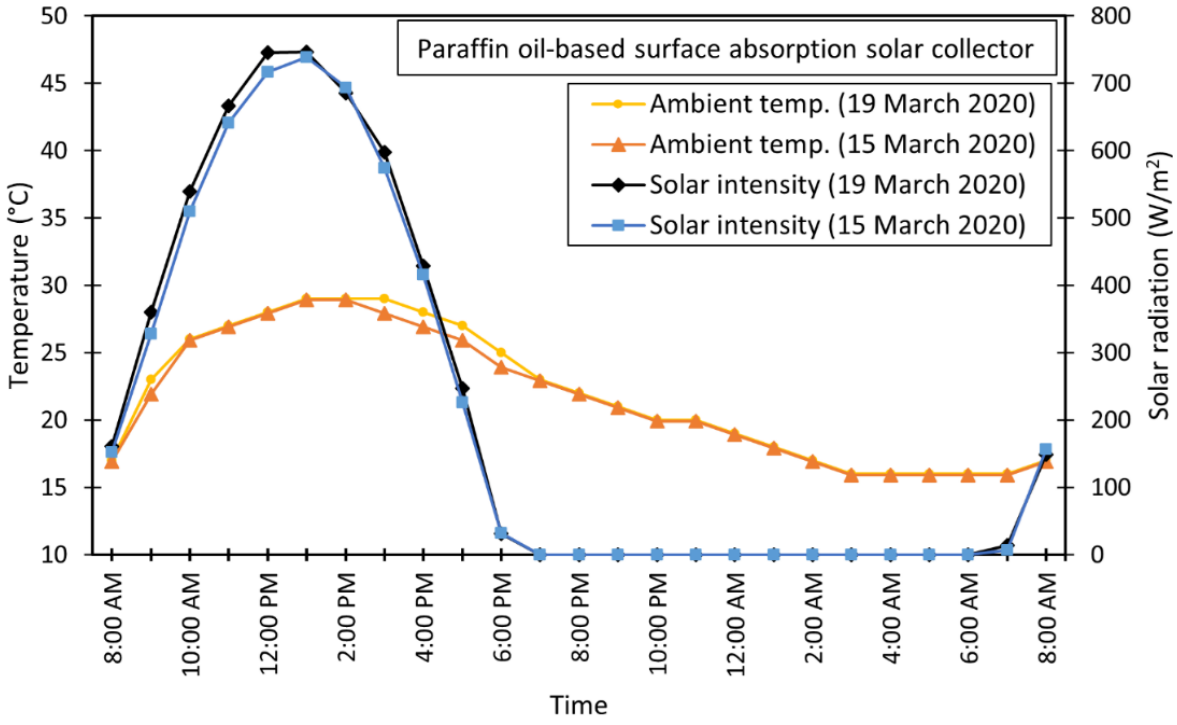

Fig. 4.9 Variation of solar radiation and ambient temperature on 15th and 19th March 2020.

The solar collector provides continuous thermal energy during sunshine hours to the integrated still. The experimentation has been carried out with two fluid variants in the solar collector, firstly with pure paraffin oil and secondly with nanofluid (1.25 mlL^{-1}). The heat exchanger in the solar collector is mounted such that it is just submerged in the fluid, and the average height of the heat exchanger is 35 - 40 mm. The temperature in the solar collector was measured at different heights, and it has been noted that the temperature in the region of 40 mm (where the heat exchanger is

placed) affects the heat transfer rate the most. Therefore, the comparison of temperature at 40 mm in the solar collector for the performed experiments is reported here.

4.3.1 Temperature variation in Pure paraffin oil-based solar collector (CSASC)

Figure 4.10 indicates the temperature variation in the paraffin oil-based surface absorption solar collector on the days of experiments (15th and 19th March 2020). On 15th March 2020, the collector temperature was slightly higher in the forenoon and afternoon, but it remained in the vicinity of the temperature on the 19th March 2020 experiment. The maximum temperature attained in the solar collector for experiments on the aforementioned dates was 72°C and 73°C, respectively.

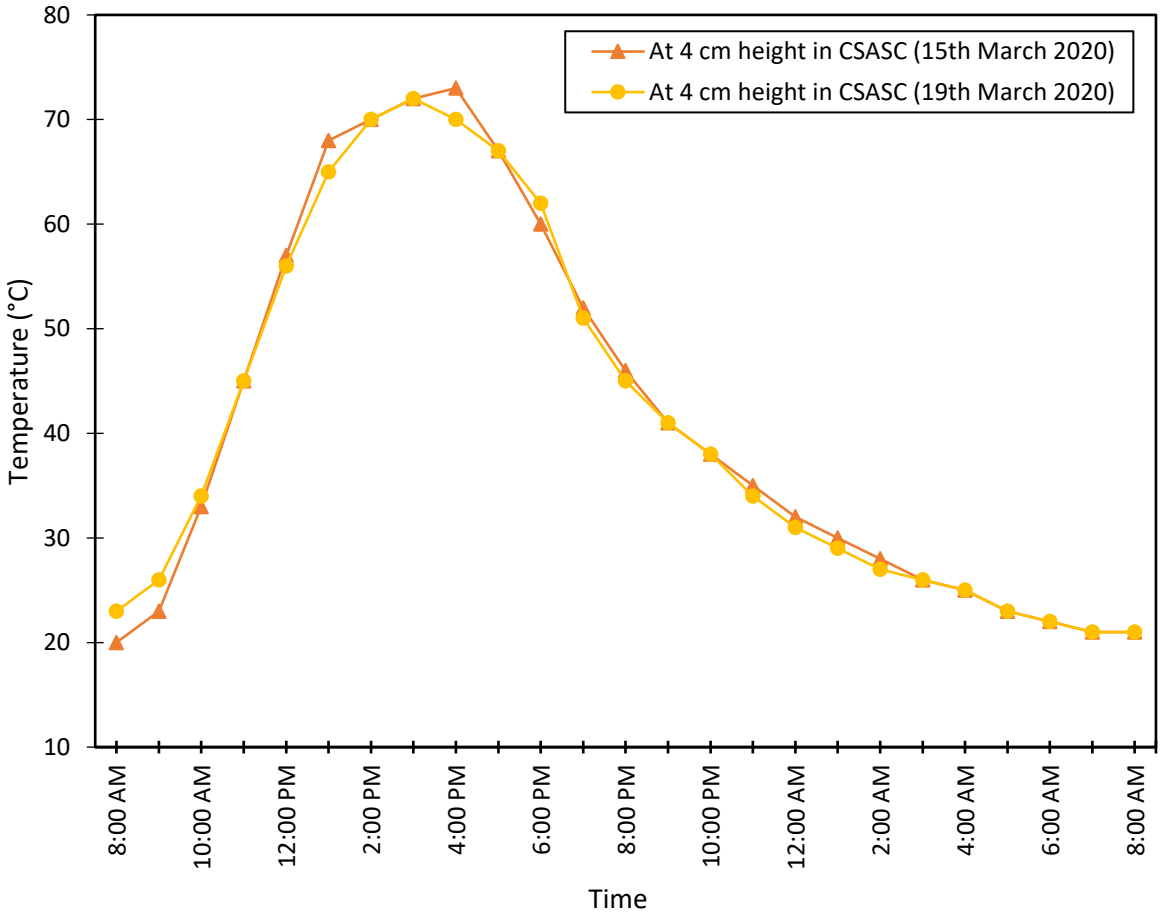

Fig. 4.10 Variation of temperature in paraffin oil-based surface absorption solar collector.

4.3.2 Temperature variation in Nanofluid-based volumetric absorption solar collector (NBVASC)

Figure 4.11 illustrates the variation of the temperature in a NBVASC with ambient temperature for the experiments on integrated still (with and without wicks). The temperature in the solar collector increases as time passes, achieves its highest value and then starts decreasing. The nature of the curve remains the same as in the case of solar collectors with paraffin oil, and the temperature has a highest value of 82°C and 83°C for the experiments with and without wick integrated solar still. The ambient temperature follows the typical pattern of rising in the morning, peaking in the afternoon, and falling in the evening.

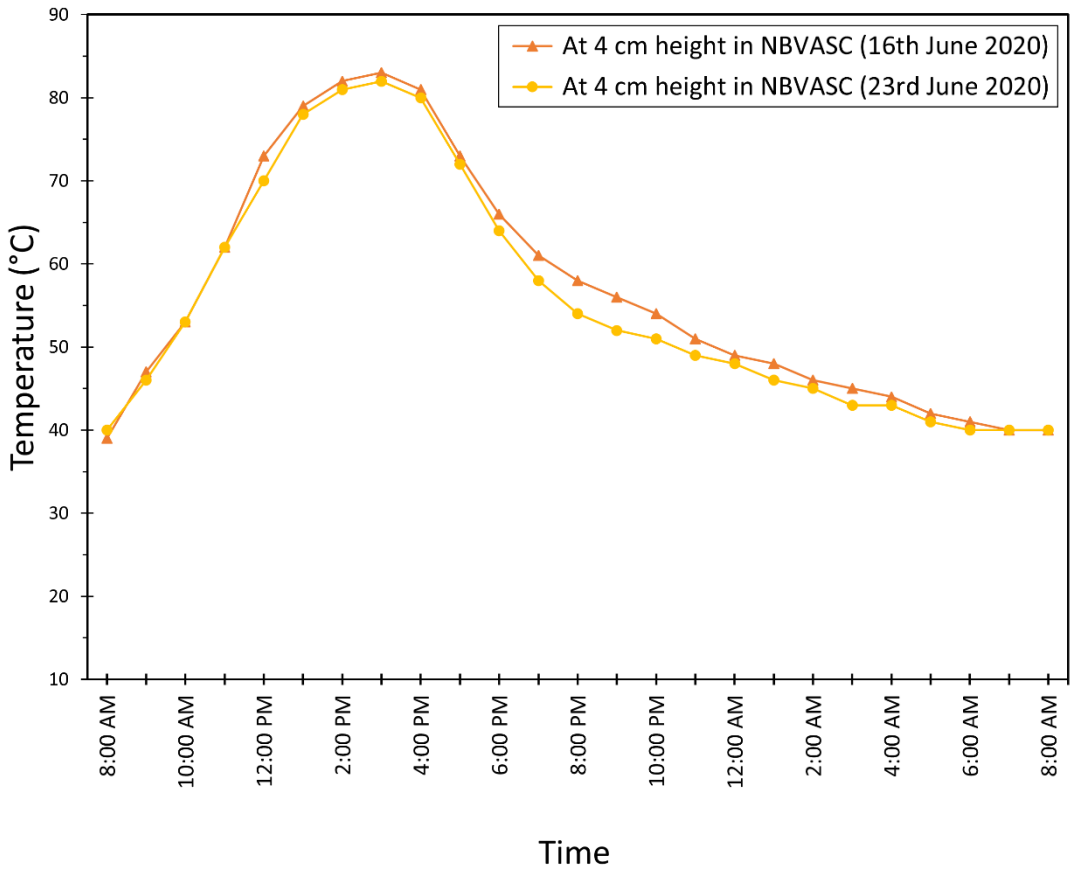

Fig. 4.11 Variation of temperature in NBVASC.

4.3.3 Comparison of basin water temperature of conventional and integrated solar stills (solar still integrated with NBVASC and solar pond)

Figure 4.12 represents the variations in basin water temperature ratio of "integrated solar stills". The graph represents the temperature ratio for the experiments done on integrated stills with floating wicks (19th March 2020) and without floating wicks (15th March 2020). It can be noticed from the graphs that the nature of the curve remains similar for both cases, as the solar conditions are identical on the days of the experiments. There is a slight increase in the temperature ratio when there are wicks (offering low thermal inertia [84]) in the basin of the integrated still during the sunshine period when thermal energy is supplied from the paraffin oil-based surface absorption solar collector to the integrated solar stills, and after that both temperature ratios become identical. A sudden increase can be observed after 1 am when the solar pond supplies the stored sensible thermal energy.

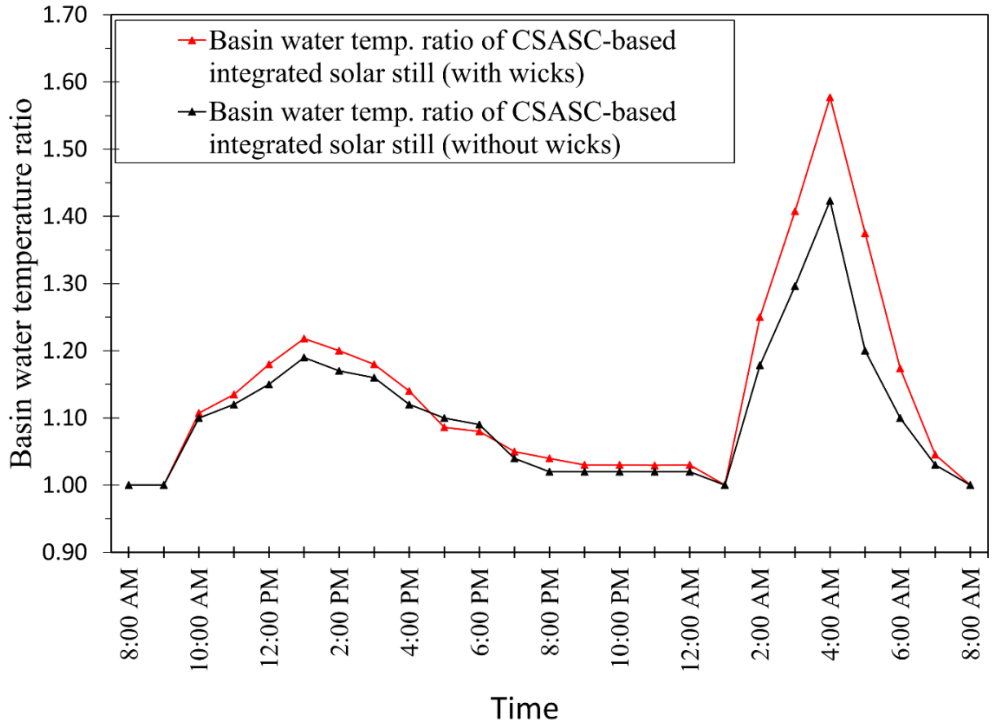

Fig. 4.12 Basin water temperature comparison in “wick-type and non-wick type CSASC-based integrated solar stills”

Figure 4.13 illustrates the temperature ratio of an "integrated solar still" with and without wicks when attached to NBVASC; temperature ratio of an "integrated solar still" with wicks remains greater than the temperature ratio of an "integrated solar still" without wicks when external thermal energy is supplied from NBVASC between 9 am and 6 pm and when the solar pond is connected between 1 am and 4 am.

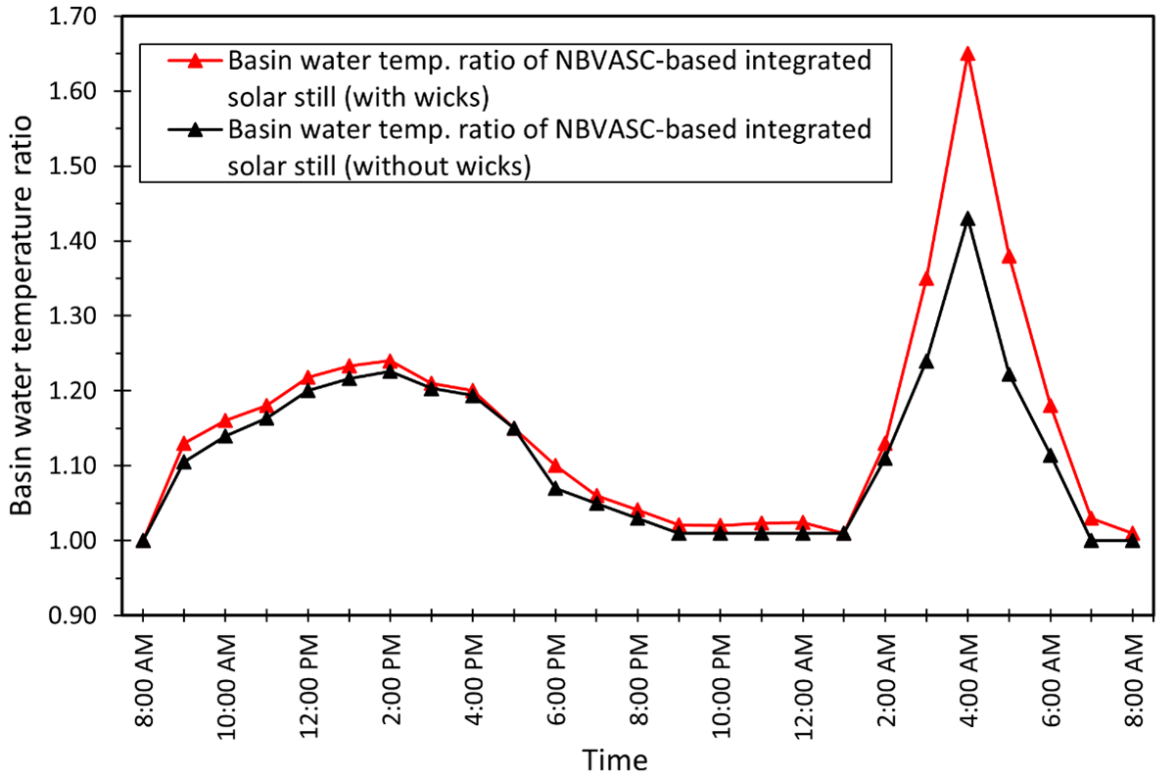

Fig. 4.13 Basin water temperature comparison in “wick-type and non-wick type NBVASC-based integrated solar still”.

4.3.4 Productivity ratio and cumulative distillate of integrated solar stills (solar still integrated with NBVASC and solar pond).

Figure 4.14 represents the hourly performance comparison of integrated stills without (15th March 2020) and with floating wicks (19th March 2020) coupled with paraffin oil-based surface

absorption solar collectors in terms of their hourly productivity ratio. It can be observed from the graph that during the hours when the solar collector supplies the thermal energy from 9 am to 6 pm, and from 1 am to 4 am from the solar pond, the integrated still with wicks showed higher productivity during that period. It can be attributed to the higher evaporation rates and higher temperatures gained from the same solar insolation by the floating wicks.

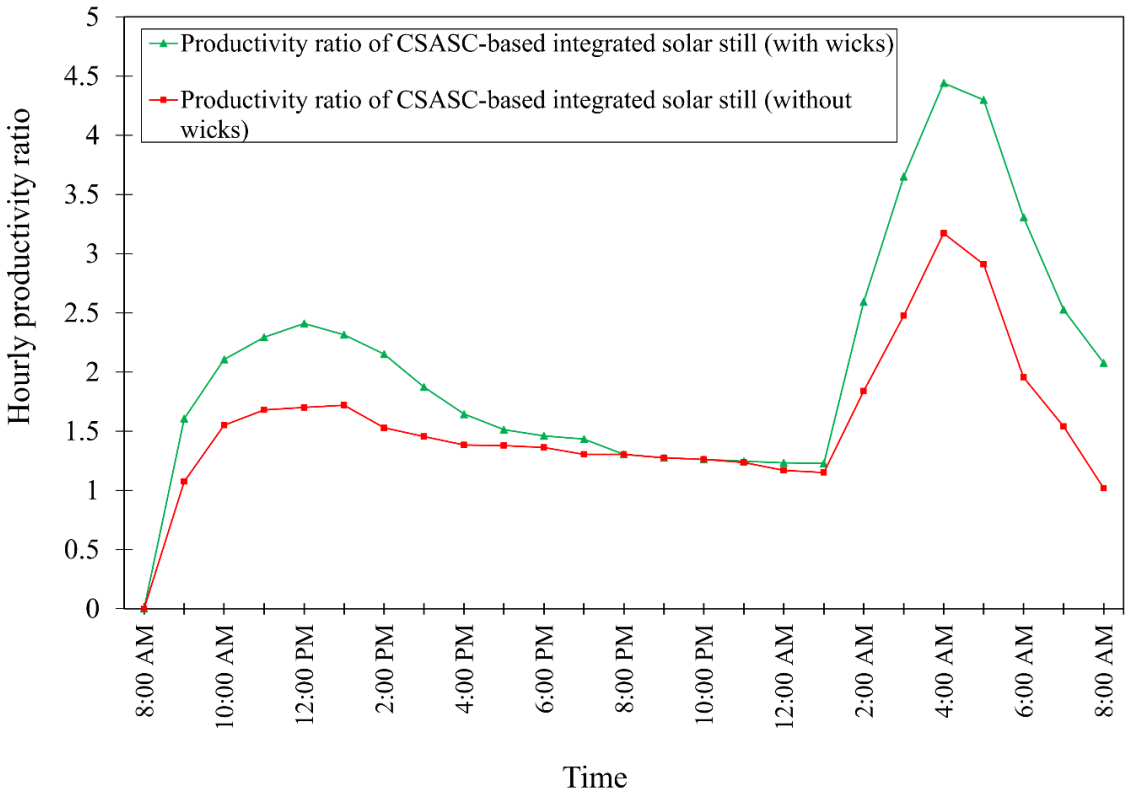

Fig. 4.14 Hourly performance comparison of "wick-type and non-wick type CSASC-based integrated solar stills"

Figure 4.15 presents the hourly productivity ratio of "integrated solar stills" with and without wicks when they are coupled with a nanofluid (1.25 mlL^{-1}) based volumetrically absorbing solar collector. A sudden surge in distillate production when the solar collector supplies the thermal energy at 9 am; a substantial increase in productivity can be seen till 6 pm when the DC pump is

switched off. After the solar collector's disengagement, the integrated still's productivity becomes almost equal to conventional solar still after 8 pm; it increases at night when heat energy from the solar pond is supplied from 1 am to 4 am.

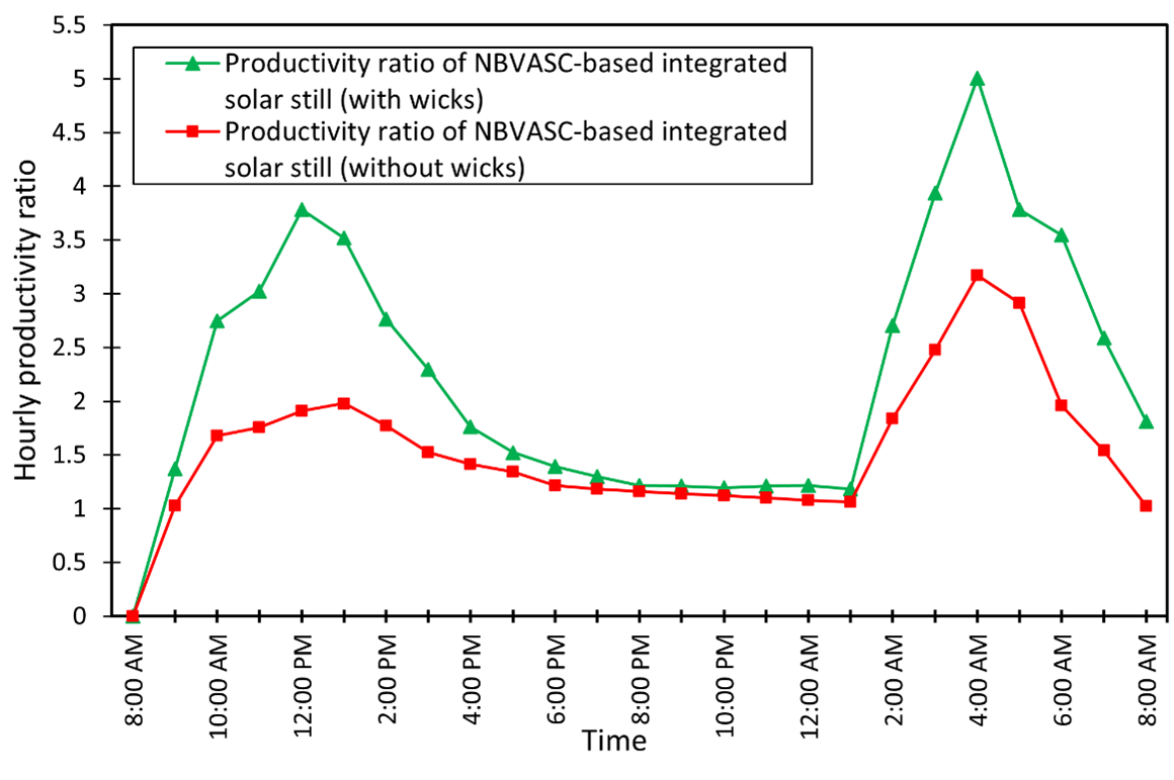

Fig. 4.15 Hourly performance comparison of wick-type and non-wick type NBVASC-based integrated solar stills.

Figure 4.16 shows the comparison among the cumulative productivity distillate of "integrated solar stills" (wick-type and non-wick type) coupled with paraffin oil-based surface absorption solar collectors and conventional still. It can be inferred from the graph that the cumulative distillate of conventional stills is lower as compared to the cumulative distillate of CSASC-based integrated stills with floating wicks is more than the cumulative distillate ratio of "integrated solar still" without wicks. There is a steep increase in distillate when the CSASC is coupled with an "integrated solar still" from 9 am to 6 pm and from 1 am to 4 am when the water-based solar pond

is connected to the "integrated solar still". Though the nature of the curves remains similar for integrated stills with and without wicks, the amount and magnitude are more for "integrated solar still" with floating wicks. The cumulative distillate output for conventional non-wick and "CSASC-based integrated solar still" measured to be 2.88 L/m^2 and 4.17 L/m^2, there was an increase of 44.8% of distillate production from "integrated solar still" in comparison to the reference still. The distillate for wick-type "CSASC-based integrated solar stills" was 5.02 L/m^2, and there was an increase of 76.1% of distillate production from "integrated solar still" in comparison to reference still.

Percentage rise in yield was calculated using the formula:

Percentage increase in yield $=[(m_i - m_c)/m_c] \times 100$ (1)

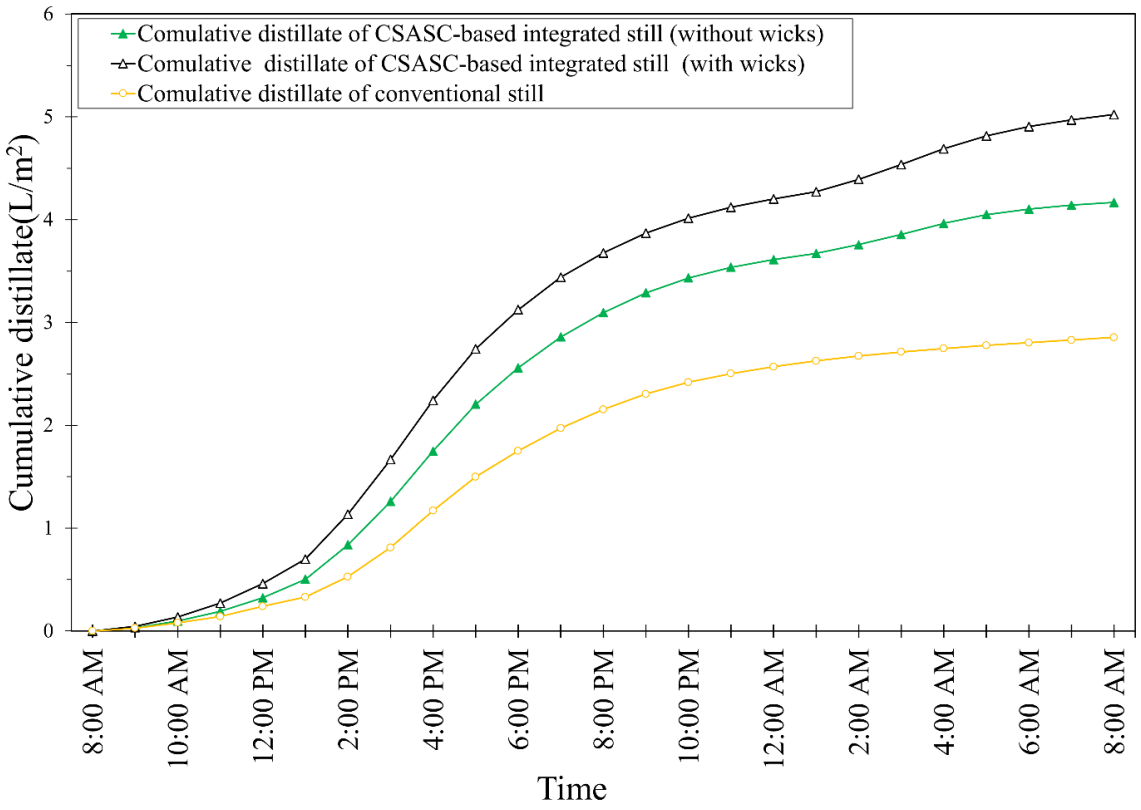

Fig. 4.16 Cumulative distillate productivity of wick-type and non-wick type CSASC-based integrated solar stills and conventional still.

Figure 4.17 compares the cumulative productivity distillate of "integrated solar stills" (with and without wicks) coupled with NBVASC and conventional still. The distillate increases when NBVASC is coupled with integrated still in both (with and without wicks) cases, from 9 am to 6 pm. The enhancement is more in the case of "integrated solar still" with wicks than without wicks. A significant increase can also be observed from 1 am to 4 am in the morning when solar is connected with the "integrated solar still"; afterwards, the distillate becomes almost comparable to reference still. The cumulative distillate production of reference and "integrated solar still" without wicks was measured to be 3.09 L/m^2 and 4.75 L/m^2, respectively. There was an increase of 56.8% of the distillate production of "integrated solar still" compared to the reference still. Distillate production of "integrated solar stills" with wicks was 6.08 L/m^2, and there was an increase of 98.04% in the distillate of integrated still with wicks in comparison to conventional solar still.

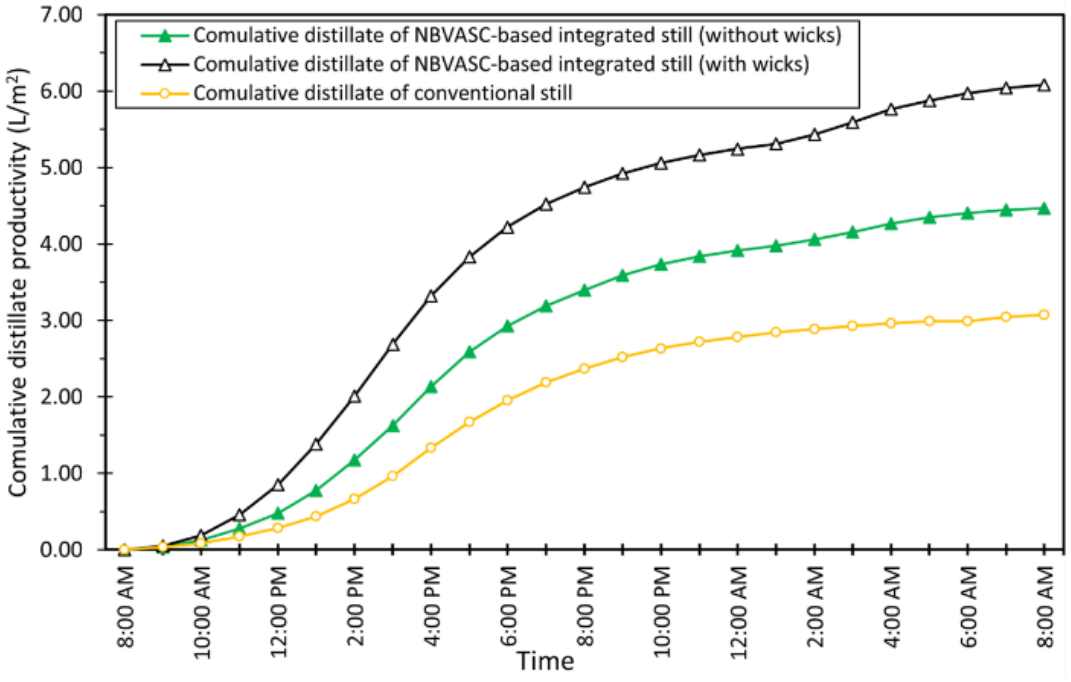

Fig. 4.17 Cumulative distillate productivity of wick-type and non-wick type NBVASC-based integrated solar and conventional still

4.4 Winter and summer performance comparison of solar still integrated with NBVASC and solar pond

Experiments done on several days throughout the summer season revealed that solar productivity is still greatly dependent on the quantity and availability of solar radiation. Therefore, the productivity of solar still degrades in the winter when the intensity and duration of solar radiation are significantly lower than in summer. Hence an attempt has been made in the present research work to determine the typical winter day distillate of the modified solar still coupled with NBVASC (with 1.25 mlL^{-1} nanofluid concentration, from 8 am to 6 pm) and solar pond (from 1 am to 4 am) and compare it to the performance of the experiments conducted on the modified solar still coupled with NBVASC and solar pond, on a typical summer day. Fig. 4.18 illustrates the variation of solar radiation and the temperature of the basin water of the modified stills over 24 hours on a typical summer (the 16^{th} of June) and winter (the 18^{th} of December) day. It can be seen from the graph that the slope of the solar radiation curve for summer day remains higher than the winter day as of 8 am to 7 pm. The winter day solar radiation almost becomes zero after 5 pm, whereas summer radiation diminishes after 7 pm, remains zero until 6 am the next morning, and gains some value at 7 am after sunrise. The solar radiation on summer day peaks at 1 pm (813.87 W/m^2) and forms a bell-shaped curve resembling a normal distribution curve, whereas the solar radiation on the winter day reaches a maximum value at 2 pm (560.34 W/m^2), and its curve is tilted towards the right side of the graph. The basin water temperature of the modified stills increases with the increase in solar intensity during forenoon and achieves a maximum value of 76^oC around 2 pm for the summer day and a value of 56^oC around 3 pm for the winter day experiment. The time lag between the highest basin water temperature and the maximum solar intensity is primarily due to the thermal capacity of the basin water; however, other elements such as air density, humidity, and other factors also play a role. The basin water temperature decreases in the afternoon

in both cases, but the slope is steeper in the case of winter than in summer. The basin water temperature curve observes a sudden spike in both experiments after 1:00 am when the supplementary thermal energy was supplied via heat exchangers till 4:00 am. A pump (controlled through a programmable electric switch) was fitted in the pipeline system connecting the NBVASC-Solar still and solar pond. The basin water temperature gradually declines after the pump is turned off; the summer day curve remains higher and maintains a greater temperature than the winter day curve, which decreases at a sharper pace. The overall curve (temperature) of the summer experiment is smoother than the curve (temperature) of the winter experiment, observing a gradual rise and fall in the temperature with the solar intensity.

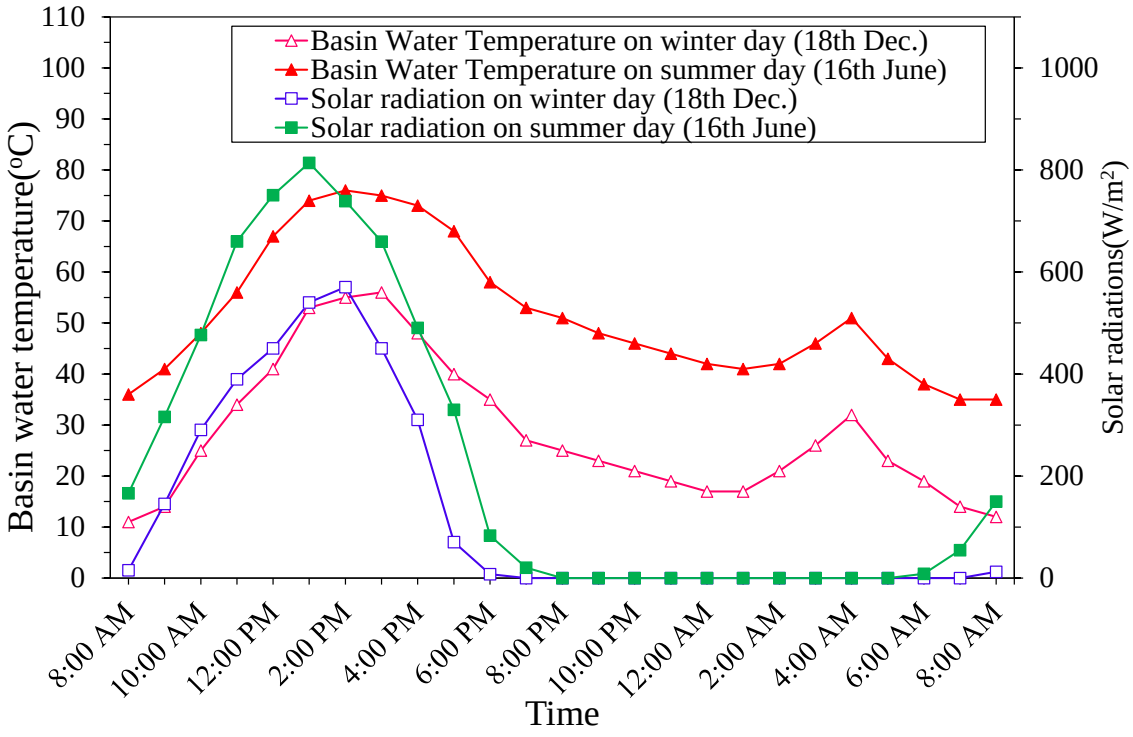

Fig. 4.18 Variation of solar radiation and basin water temperature of modified still on winter and summer day

Furthermore, the cumulative distillate produced by modified stills is shown in Fig. 4.19, indicating that the distillate curve for the summer experiment remains higher than the winter throughout the experiment duration. The cumulative curve in the winter experiment becomes almost flat after 5 pm, suggesting a decrease in distillate production with diminishing solar radiation. The cumulative distillate curve in summer rises steeply away from the winter curve in the afternoon. The total value of the solar radiation during the experiment on the summer day (the 16th of June) was 19.77 MJ/m^2/day and 12.8 MJ/m^2/day during the winter day (the 18th of December), respectively. The total distillate produced during the summer experiment was 4.62 L/m^2/day, corresponding to the 2.05 L/m^2/day during the winter. In both cases, a significant amount of nocturnal distillate was collected; however, on expected terms, the nocturnal distillate in the summer experiment was much higher than in the winter experiment due to the more elevated basin water temperatures after the non-sunshine hours, creating a significant difference with the ambient temperature and enhancing the evaporation rates, thus increasing the nighttime productivity. Overall, the typical summer day experiment produced 144.02% more diurnal and 64.52% more nocturnal distillate than the typical winter day experiment.

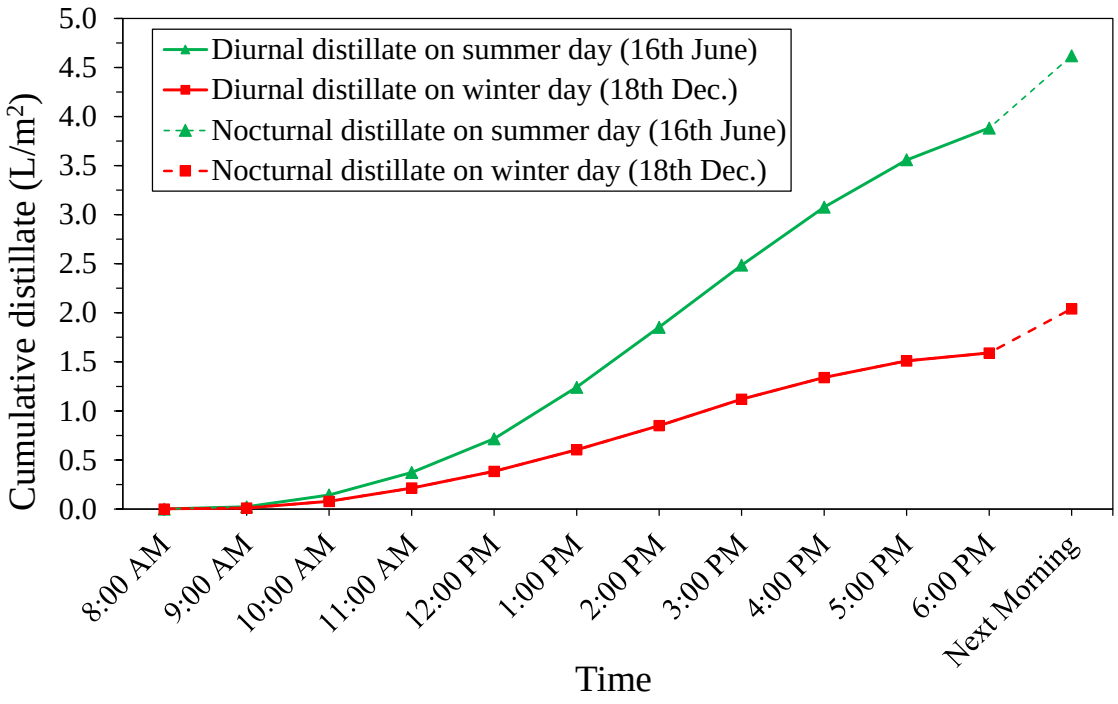

Fig. 4.19 Comparison of Cumulative distillate productivity of modified still on winter and summer day

4.5 Efficiency of conventional and modified stills

The efficiency of conventional solar still is computed as given below:

$$\eta = \frac{m_d \times h_{fg}}{G_T \times A_b} \quad (2)$$

where m_d is the total distillate output of the still, h_{fg} represents water latent heat (2300 kJ/kg) [85], the total incident solar energy during the experiment period is denoted by G_T, i.e., from 8 am to 6 pm, and A_b is the basin surface area of still.

Modified solar still's efficiency when coupled with the nanofluid-based solar collector is calculated as given below:

$$\eta = \frac{m_d \times h_{fg}}{(G_T \times A_b) + Q_{sc} + W_p} \quad (3)$$

Where Q_{sc} is the quantity of heat provided from the NBVASC to the modified solar still from 9 am to 6 pm, and it is computed as:

$$Q_{sc} = (\dot{m} \times c \times \Delta t) \times \tau \quad (4)$$

Where $\dot{m}$ is the mass flow rate of heat transfer fluid (HTF) flowing in the heat exchanger of modified solar still, specific heat of heat transfer fluid is represented by *c*, difference of average temperature of heat transfer fluid at the inlet section and exit of the heat exchanger during the experiment is denoted by Δt.

The work done by the pump (W_p) as illustrated in Eq. (3) is determined the same as given below:

$$W_p = P_p \times \tau \quad (5)$$

where, P_p is the power of the pump (19 W rating), and τ represents the entire operating time of the pump in seconds.

Modified solar still's efficiency when coupled with NBVASC (or CSASC), and the solar pond is calculated as [86]:

$$\eta = \frac{m_d \times h_{fg}}{(G_T \times A_b) + Q_{sc} + Q_{sp} + W_p} \quad (6)$$

where Q_{sc} and Q_{sp} are the amounts of thermal energy supplied to the integrated solar still by the collector and the solar pond, respectively, these are computed as:

$$Q_{sc} = (\dot{m} \times c \times \Delta t) \times \tau_{sc} \quad (7)$$

$$Q_{sp} = (\dot{m} \times c \times \Delta t) \times \tau_{sp} \quad (8)$$

Where $\dot{m}$ is the mass flow rate of heat transfer fluid (HTF) flowing in the heat exchanger of "integrated solar still", the specific heat of heat transfer fluid is represented by *c*, the difference in

the average temperature of heat transfer fluid at the inlet section and exit of the heat exchanger during the experiment is denoted by Δt, the total operating time of pump connecting the solar collector to "integrated solar still" is denoted as τ_{sc} And the time during which the solar pond is connected with the "integrated solar still" is denoted as τ_{sp} in seconds. The work done by the pump (W_p) in equation (6) was calculated as illustrated in equation (5).

The presented energy efficiencies in Fig. 4.20 were calculated for conventional still, modified still (MS) coupled with CSASC and modified still (MS) coupled with NBVASC to be 23.17%, 30.40% and 38.67%, respectively. The energy efficiency was 31.43% and 35.36% for "integrated solar still" still without and with floating wicks when coupled with CSASC and solar pond. The energy efficiency was 39.18% and 44.55% for "integrated solar still" without and with floating wicks, respectively, when coupled with NBVASC and solar pond.

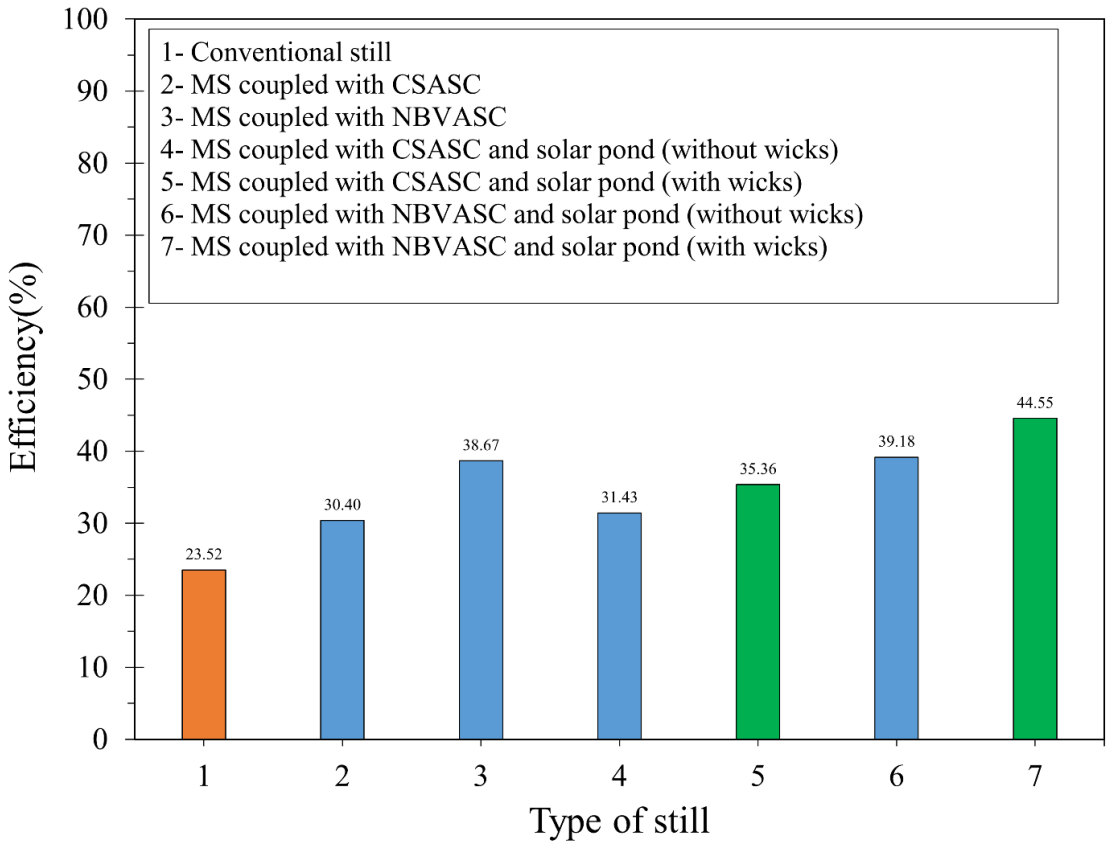

Fig. 4.20 Conventional and modified stills efficiencies

4.6 Exergy efficiency

The thermodynamics "second law" forms the basis for exergy analysis; herein, the system's total exergy influx and exergy efflux are considered. The exergy analysis for integrated solar stills can be worked as [87]:

The exergy efficiency for conventional and integrated stills can be calculated as follows:

$$\eta_{exe} = \frac{Ex_{eff}}{Ex_{in}} = \frac{Ex_{evap}}{Ex_{in}} \quad (9)$$

where $\sum E_{x_{in}}$ and $\sum Ex_{eff}$, are the exergy influx and exergy efflux, respectively.

The equation calculates the exergy output of conventional and integrated stills.

$$Ex_{eff} = Ex_{evap} = \frac{(m_{evap} \times h_{fg})}{3600} \times \left(1 - \frac{T_a + 273}{T_w + 273}\right) \quad (10)$$

where T_a and T_w are ambient and basin water temperatures, respectively.

Exergy influx for solar stills is taken as the total amount of solar radiations collected by solar stills during the experiment time. Therefore, the exergy input is calculated as:

$$E_x(solar\ still) = Ex_{in} = A_b \times I(t) \times \left[1 - \frac{4}{3} \times \left[\frac{T_a}{T_{sun}}\right] + \frac{1}{3} \times \left[\frac{T_a}{T_{sun}}\right]^4\right] + Q_{sc}\left(1 - \frac{T_a}{T_{sc}}\right) + Q_{sp}\left(1 - \frac{T_a}{T_{sp}}\right) \quad (11)$$

where T_{sun} is 'Sun's assumed blackbody surface temperature (6000 K) [87].

Figure 4.21 shows the exergy efficiencies of conventional and integrated solar stills with and without wicks when coupled with paraffin oil-based solar collector and NBVASC respectively. It can be inferred from the graph that the exergy efficiency had the highest value of 3.40% when wicks were used in the basin of "integrated solar still" coupled with NBVASC, and conventional still had the lowest with a value of 1.48%. The integrated solar stills without wicks have a comparatively low exergy efficiency.

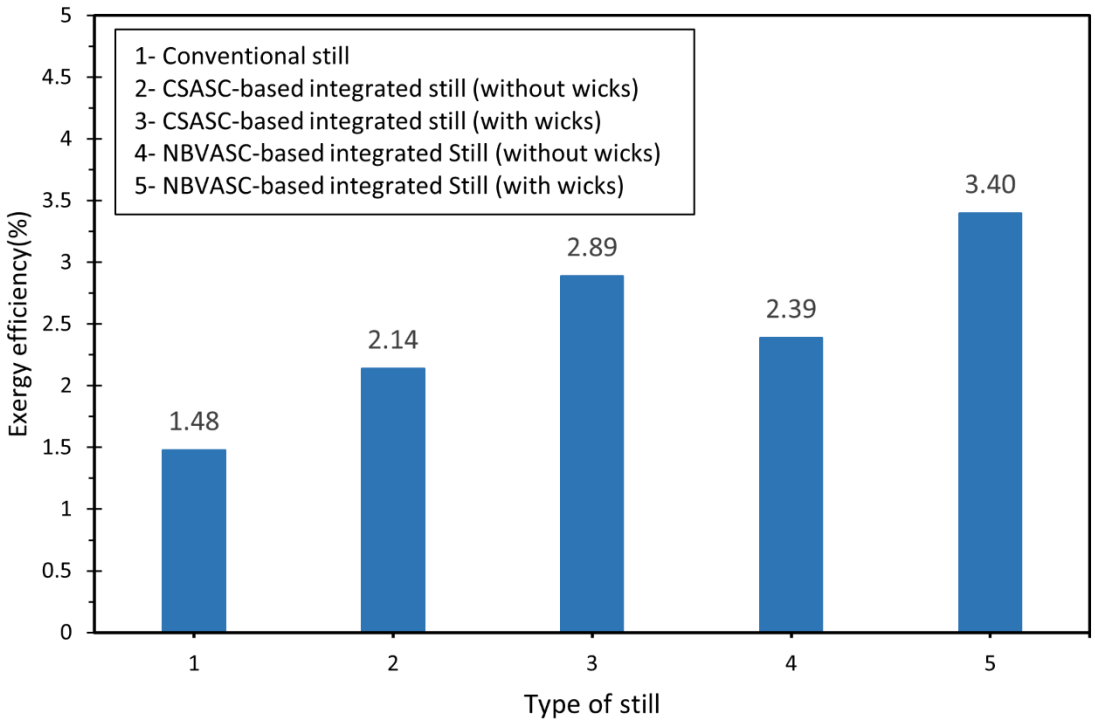

Fig. 4.21 Conventional and integrated solar stills' exergy efficiencies.

4.7 Cost estimation

The evaluation of the cost of the distillate formed by conventional still and modified stills is done by using the method detailed in Dhindsa and Mittal [86]. The cost estimation is shown in Table 4.1. The cost estimation has been done by assuming the anticipated life cycle of still as 10 years and yearly maintenance expense as 30% of the fabrication cost.

Due to the inclusion of components such as the solar collector, heat exchangers, and other various equipments in the modified still coupled with NBVASC, the manufacturing expenses of the modified still (coupled with NBVASC) has risen by 55.5% in comparison to the conventional still. However, the cost of production of distillate is decreased by 12% due to a notable rise in the productivity (74.3% increase) of the modified still (coupled with NBVASC).

Due to the inclusion of components such the solar collector, solar pond, heat exchangers, wicks, and other miscellaneous things in the modified still coupled with NBVASC and solar pond, the manufacturing cost of the modified solar still (coupled with NBVASC and solar pond) has risen by 59.1% when compared to the conventional still. Due to a significant improvement in productivity (111.1% increase) of the modified solar still (coupled with NBVASC and solar pond) comparing to the reference solar still, the cost of distillate production is reduced by 32.5%. If the cost of the commercially available drinking water is Rs 15/litre, the payback time of modified solar still (coupled with NBVASC and solar pond) is decreased to 4 years from the conventional solar still's payback time of 6 years.

Table 4.1

Cost estimation of conventional and modified stills.

Factors	**Conventional still**	**(Still coupled with NBVASC)**	**(Still coupled with NBVASC and solar pond)**
Manufacturing expenditure	Rs 11,250	Rs 17,500	Rs 19,500
Maintenance cost yearly [88].	Rs 3375	Rs 5850	Rs 6250
The anticipated lifespan	10 years	10 years	10 years
Overall expenses	Rs 45,000	Rs 70,000	Rs 78,400
Annual usage[70].	300 days	300 days	300 days
Distillate production	2.57 L/m^2/day	4.48 L/m^2/day	6.08 L/m^2/day
Total distillate production	7710 L/m^2	13440 L/m^2	18240 L/m^2
Unit price of distillate produced	Rs 5.84/l	Rs 5.21/l	Rs 4.29/l

4.8 Error and uncertainty analysis

The variation that occurs between the calculated value and the actual value of the computed parameter is what is referred to as an error in an experiment. Errors may be defined as random or systematic. The error could be from measuring tools, procedures, calibration errors, unskilled operators, experimental conditions and environmental conditions of temperature, humidity, etc.

Uncertainty is an interval close to the expected value and can be categorized into two types. Type-A is due to unsystematic mistakes and is determined by applying computative methods, whereas type-B is due to orderly mistakes. For the assessment of uncertainty related to the still efficiency, all the calculated information in this research work was supposed to have a uniform distribution. Hence the uncertainty of all the measured data (type-B) of apparatuses may be reported the same as [86].

$$u = \frac{a}{(3)^{1/2}} \tag{12}$$

Here, '*a*' represents accuracy along with '*u*' as the standard uncertainty of the calculating apparatus. The standard uncertainty of the calculating apparatuses is provided in Table 4.2.

If 'x_i' are random number of variables having '*y*' as function and '$u(x_i)$' are the uncertainties in the calculation of variables x_i, subsequently the uncertainty of '*y*' can be found as [86].

$$u(y) = \left[\left(\frac{\partial y}{\partial x_1}\right)^2 u^2(x_1) + \left(\frac{\partial y}{\partial x_2}\right)^2 u^2(x_2) + \cdots\right]^{\mathbf{1/2}} \tag{13}$$

By using above Eq. (13) and Eq. (2) for efficiency of conventional still, the equation for estimation of uncertainty of efficiency for conventional still can be derived as:

$$u(\eta) = \eta\left[\left(\frac{u(m_d)}{m_d}\right)^2 + \left(\frac{u(G_T)}{G_T}\right)^2 + \left(\frac{u(A_b)}{A_b}\right)^2\right]^{1/2} \tag{14}$$

Likewise, by means of Eq. (13) and Eq. (3) for efficiency of modified still (solar still coupled with NBVASC), the equation for estimation of uncertainty of efficiency for modified still can be derived as:

$$u(\eta) = \eta \left[\left(\frac{u(m_d)}{m_d}\right)^2 + \left(\frac{u(G_T)}{G_T + \frac{Q_{sc}+W_p}{A_b}}\right)^2 + \left(\frac{u(A_b)}{A_b + \frac{Q_{sc}\ +\ W_p}{G_T}}\right)^2 + \left(\frac{u(Q_{sc})}{(G_T \times A_b)+Q_{sc}+W_p}\right)^2 \right]^{1/2} \quad (15)$$

The maximum uncertainty of efficiency for conventional and modified still (solar still coupled with NBVASC) was determined to be 1.2% and 1.5%, respectively, by using Eq. (14) and Eq. (15), respectively.

Table 4.2

Details relevant to the instruments employed for making measurements in the present work.

S. No	Instrument	Accuracy	Range	Standard Uncertainty
1	Pyranometer	1.0 W/m^2	0-4000 W/m^2	0.58 W/m^2
2	Thermocouple (K - Type)	1 °C	-200 °C to 1350 °C	0.58 °C
3	pH meter	0.02 pH	0-14 pH	0.01 pH
4	Weighing scale	10^{-1} g	0-5 kg	0.06 g
5	Tape measure	10^{-3} m	0 – 5 m	0.00058 m
6	TDS meter	2 % of reading	0.1ppm-200,000 ppm	1.15 % of reading

4.9 Concluding remarks

The present study's experimental investigation of conventional and modified stills revealed that NBVASC coupled solar still outperforms the solar still coupled with a paraffin oil-based conventional surface absorption-based solar collector (CSASC). This finding was based on the results of a comparison between the two types of stills. This suggests that harvesting of solar energy through volumetric absorption by nanofluids is more efficient and effective. A considerable amount of night distillate was produced by integrated solar stills (with and without wicks) due to the coupling of integrated stills with the solar pond at night; there was a maximum increase of 268.9% in productivity compared to conventional still when integrated still has wicks in its basin. Additional major conclusions that may be made from the current research are given in the next chapter, point by point.

Chapter 5

Conclusions and future scope

Overall, in the present research work, the conventional basin-type solar still was integrated with NBVASC and solar pond. On-Sun testing was done for both the integrated and conventional solar stills under similar ambient and operating conditions. Testing was also done to test its 24-hour performance; summer and winter season comparison was also done to evaluate the impacts of seasons on the performance of modified solar still. Cost analysis was also done to study the effect of NBVASC and solar pond integration on the distillate production of the modified solar still over the reference/conventional still. This chapter summarizes the key conclusions of the present research study as well discusses the potential future directions.

5.1 Conclusions

Key inferences that can be taken from the experimental evaluation of the modified solar still integrated with the CSASC and NBVASC are as follows:

- It was found that the solar still coupled with NBVASC (at optimum nanoparticle concentration of 1.25mlL^{-1}) performed better than the CSASC-coupled solar still. This suggests that harvesting solar energy through volumetric absorption by nanofluids is more efficient and effective.
- The distillate production and efficiency of the NBVASC (1.25 mlL^{-1}) coupled modified still were found to be 75.3 % and 66.9 % more than the conventional still.
- A significant amount of night distillate was obtained from the NBVASC coupled modified still owing to the substantial quantity of thermal energy accumulated in the basin water at

the end of the sunshine of the day. The night distillate produced by the modified still was found to be 33.9% greater than the reference/conventional still.

- It was found from the economic study of distillate formed from modified still (NBVASC coupled solar still) and conventional still that the distillate production price of modified still is 12% less comparing to reference/conventional still.

The important inferences drawn from the 24-hour evaluation (experimental) of the modified solar still integrated with the CSASC, NBVASC and solar pond are as follows:

- The integrated solar stills performed better than conventional still in all the experiments when coupled with the solar collector (9:00 am to 6:00 pm) and from 1 am to 4 am with solar pond, with or without wicks.
- The integrated solar still without wicks, when coupled with a paraffin oil-based surface absorption solar collector during sunshine hours and with a solar pond during the night, showed an increase of 44.8% and 33.6% over conventional solar still in productivity and efficiency, respectively.
- The integrated solar still with wicks, when coupled with the paraffin oil-based solar collector during sunshine hours and with solar pond during the night, showed an increase of 74.3% and 50.2% over conventional solar still in productivity and efficiency, respectively.
- The integrated solar still without wicks, when coupled with nanofluid (1.25 mlL^{-1}) based volumetrically absorbing solar collector (NBVASC) during sunshine hours and with solar pond during night hours, showed an increase of 64.9% and 66.4% over conventional solar still in productivity and efficiency, respectively.

- The integrated solar still with wicks, when coupled with nanofluid (1.25 mlL^{-1}) based volumetric absorption solar collector (NBVASC) during sunshine hours and with solar pond during night hours, showed an increase of 111.1% and 89.4% over conventional solar still in productivity and efficiency, respectively.
- A considerable amount of night distillate (after 1 am) was produced by integrated solar stills (with and without wicks) due to the coupling of integrated stills with the solar pond at night; there was a maximum increase of 268.9% in productivity compared to conventional still when integrated still has wicks in its basin.
- Manufacturing cost increased by 59.1%, whereas distillate production cost decreased by 32.5% relative to conventional still.
- Exergy efficiency was 3.40% when wicks were used in the basin of integrated solar still coupled with NBVASC, and conventional still had the lowest with a value of 1.48%.
- The typical winter and summer day distillate produced by the modified stills coupled with NBVASC and the solar pond was found to be 2.05 L/m^2/day and 4.62 L/m^2/day, respectively. The diurnal and nocturnal distillate produced during summer experiments was 144.02% and 64.52% higher than in winter.

5.2 Scope for future work

The suggestions for future work are mentioned below:

- Round-the-year on-sun testing shall be carried out to evaluate the long-term performance characteristics of the developed integrated solar still.
- A comprehensive theoretical modelling framework for the developed integrated solar still should be created.

- The present system could be made a “stand-alone portable system” (i.e., utilizing only solar energy for running the pump and data acquisition equipment) suitable for arid as well as coastal areas.
- For the purpose of assessing the economic and technical feasibility of large-scale plants, it is necessary to construct an upsized distillation plant based on the existing technology of 100 kg to 200 kg per day capacity.
- A concentrating type nanofluid-based volumetrically absorbing solar collector could be designed and fabricated for the supply of thermal energy to solar still at a higher temperature for further improvement of distillate productivity of solar still.

References

[1] S. Singh, P. Dhiman, Analytical and experimental investigations of packed bed solar air heaters under the collective effect of recycle ratio and fractional mass flow rate, Journal of Energy Storage. 16 (2018) 167–186. https://doi.org/10.1016/j.est.2018.01.003.

[2] R. Kumar, V. Goel, P. Singh, A. Saxena, A.S. Kashyap, A. Rai, Performance evaluation and optimization of solar assisted air heater with discrete multiple arc shaped ribs, Journal of Energy Storage. 26 (2019) 100978. https://doi.org/10.1016/j.est.2019.100978.

[3] V.S. Hans, R.P. Saini, J.S. Saini, Heat transfer and friction factor correlations for a solar air heater duct roughened artificially with multiple v-ribs, Solar Energy. 84 (2010) 898–911. https://doi.org/10.1016/j.solener.2010.02.004.

[4] M.A. Abdelghani-Idrissi, S. Khalfallaoui, D. Seguin, L. Vernières-Hassimi, S. Leveneur, Solar tracker for enhancement of the thermal efficiency of solar water heating system, Renewable Energy. 119 (2018) 79–94. https://doi.org/10.1016/j.renene.2017.11.072.

[5] Y. Wang, M. Li, W. Du, X. Ji, L. Xu, Experimental investigation of a solar-powered adsorption refrigeration system with the enhancing desorption, Energy Conversion and Management. (2018). https://doi.org/10.1016/j.enconman.2017.10.065.

[6] S. Singh, S. Kumar, Testing method for thermal performance based rating of various solar dryer designs, Solar Energy. 86 (2012) 87–98. https://doi.org/10.1016/j.solener.2011.09.009.

[7] K.S. Reddy, H. Sharon, Active multi-effect vertical solar still: Mathematical modeling, performance investigation and enviro-economic analyses, Desalination. (2016). https://doi.org/10.1016/j.desal.2016.05.027.

[8] S. Rashidi, N. Rahbar, M.S. Valipour, J.A. Esfahani, Enhancement of solar still by reticular porous media: Experimental investigation with exergy and economic analysis, Applied Thermal Engineering. 130 (2018) 1341–1348. https://doi.org/10.1016/j.applthermaleng.2017.11.089.

[9] D. Dsilva Winfred Rufuss, L. Suganthi, S. Iniyan, P.A. Davies, Effects of nanoparticle-

enhanced phase change material (NPCM) on solar still productivity, Journal of Cleaner Production. 192 (2018) 9–29. https://doi.org/10.1016/j.jclepro.2018.04.201.

[10] J. Graf, S.Z. Togouet, N. Kemka, D. Niyitegeka, R. Meierhofer, J.G. Pieboji, Health gains from solar water disinfection (SODIS): Evaluation of a water quality intervention in Yaoundé, Cameroon, Journal of Water and Health. 8 (2010) 779–796. https://doi.org/10.2166/wh.2010.003.

[11] K. Sampathkumar, T. V. Arjunan, P. Pitchandi, P. Senthilkumar, Active solar distillation-A detailed review, Renewable and Sustainable Energy Reviews. 14 (2010) 1503–1526. https://doi.org/10.1016/j.rser.2010.01.023.

[12] V. Bhalla, H. Tyagi, Solar energy harvesting by cobalt oxide nanoparticles, a nanofluid absorption based system, Sustainable Energy Technologies and Assessments. 24 (2017) 45–54. https://doi.org/10.1016/j.seta.2017.01.011.

[13] A. Zeiny, H. Jin, L. Bai, G. Lin, D. Wen, A comparative study of direct absorption nanofluids for solar thermal applications, Solar Energy. 161 (2018) 74–82. https://doi.org/10.1016/j.solener.2017.12.037.

[14] M. Chen, Y. He, J. Zhu, D. Wen, Investigating the collector efficiency of silver nanofluids based direct absorption solar collectors, Applied Energy. 181 (2016) 65–74. https://doi.org/10.1016/j.apenergy.2016.08.054.

[15] T.P. Otanicar, P.E. Phelan, R.S. Prasher, G. Rosengarten, R.A. Taylor, Nanofluid-based direct absorption solar collector, Journal of Renewable and Sustainable Energy. 2 (2010). https://doi.org/10.1063/1.3429737.

[16] G.K. Sinha, R.H. Dharmaraj, D. Haridas, A. Srivastava, International Journal of Heat and Fluid Flow Performance evaluation of compact channels with surface modifications for heat transfer enhancement : An interferometric study in developing flow regime, International Journal of Heat and Fluid Flow. 64 (2017) 55–65. https://doi.org/10.1016/j.ijheatfluidflow.2017.02.002.

[17] A.A. Badran, A.A. Al-Hallaq, I.A. Eyal Salman, M.Z. Odat, A solar still augmented with a flat-plate collector, Desalination. 172 (2005) 227–234.

https://doi.org/10.1016/j.desal.2004.06.203.

[18] N.A.R. Kumar L; M. Hasanuzzaman, Real-Time Experimental Performance Assessment of a Photovoltaic Thermal System Cascaded With Flat Plate and Heat Pipe Evacuated Tube Collector, Journal of Solar Energy Engineering, Transactions of the ASME. 144 (2021) 011004.

[19] Z.S. Abdel-Rehim, A. Lasheen, Experimental and theoretical study of a solar desalination system located in Cairo, Egypt, Desalination. 217 (2007) 52–64. https://doi.org/10.1016/j.desal.2007.01.012.

[20] F.M. Abed, Design and Fabrication of a Multistage Solar Still With Three Focal Concentric Collectors, Journal of Solar Energy Engineering. 140 (2018) 041003.

[21] A.H.A. Al-Waeli, H.A. Kazem, M.T. Chaichan, K. Sopian, Experimental investigation of using nano-PCM/nanofluid on a photovoltaic thermal system (PVT): Technical and economic study, Thermal Science and Engineering Progress. 11 (2019) 213–230. https://doi.org/10.1016/j.tsep.2019.04.002.

[22] S. Kumar, A. Tiwari, Design, fabrication and performance of a hybrid photovoltaic/thermal (PV/T) active solar still, Energy Conversion and Management. 51 (2010) 1219–1229. https://doi.org/10.1016/j.enconman.2009.12.033.

[23] S. Kumar, A. Tiwari, An experimental study of hybrid photovoltaic thermal (PV/T)-active solar still, International Journal of Energy Research. 32 (2008) 847–858. https://doi.org/10.1002/er.1388.

[24] A.A. El-Sebaii, M.R.I. Ramadan, S. Aboul-Enein, N. Salem, Thermal performance of a single-basin solar still integrated with a shallow solar pond, Energy Conversion and Management. 49 (2008) 2839–2848. https://doi.org/10.1016/j.enconman.2008.03.002.

[25] A.A. El-Sebaii, S. Aboul-Enein, M.R.I. Ramadan, A.M. Khallaf, Thermal performance of an active single basin solar still (ASBS) coupled to shallow solar pond (SSP), Desalination. 280 (2011) 183–190. https://doi.org/10.1016/j.desal.2011.07.004.

[26] S.N. Rai, G.N. Tiwari, Single basin solar still coupled with flat plate collector, Energy Conversion and Management. 23 (1983) 145–149. https://doi.org/10.1016/0196-

8904(83)90057-2.

[27] Z.S. Abdel-Rehim, A. Lasheen, Experimental and theoretical study of a solar desalination system located in Cairo, Egypt, Desalination. (2007). https://doi.org/10.1016/j.desal.2007.01.012.

[28] Z.M. Omara, A.E. Kabeel, The performance of different sand beds solar stills, International Journal of Green Energy. 11 (2014) 240–254. https://doi.org/10.1080/15435075.2013.769881.

[29] K.K. Murugavel, S. Sivakumar, J.R. Ahamed, K.K.S.K. Chockalingam, K. Srithar, Single basin double slope solar still with minimum basin depth and energy storing materials, Applied Energy. 87 (2010) 514–523. https://doi.org/10.1016/j.apenergy.2009.07.023.

[30] F.F. Tabrizi, A.Z. Sharak, Experimental study of an integrated basin solar still with a sandy heat reservoir, Desalination. 253 (2010) 195–199. https://doi.org/10.1016/j.desal.2009.10.003.

[31] A.E. Kabeel, M. Abdelgaied, Improving the performance of solar still by using PCM as a thermal storage medium under Egyptian conditions, Desalination. 383 (2016) 22–28. https://doi.org/10.1016/j.desal.2016.01.006.

[32] H.N. Panchal, P.K. Shah, Enhancement of upper basin distillate output by attachment of vacuum tubes with double-basin solar still, Desalination and Water Treatment. 55 (2015) 587–595. https://doi.org/10.1080/19443994.2014.913997.

[33] I. Al-Hayeka, O.O. Badran, The effect of using different designs of solar stills on water distillation, Desalination. 169 (2004) 121–127. https://doi.org/10.1016/j.desal.2004.08.013.

[34] M.R. Karimi Estahbanati, A. Ahsan, M. Feilizadeh, K. Jafarpur, S.S. Ashrafmansouri, M. Feilizadeh, Theoretical and experimental investigation on internal reflectors in a single-slope solar still, Applied Energy. 165 (2016) 537–547. https://doi.org/10.1016/j.apenergy.2015.12.047.

[35] H. Tanaka, Y. Nakatake, Effect of inclination of external flat plate reflector of basin type still in winter, Solar Energy. 81 (2007) 1035–1042. https://doi.org/10.1016/j.solener.2006.11.006.

[36] M.E. El-Swify, M.Z. Metias, Performance of double exposure solar still, Renewable Energy. 26 (2002) 531–547. https://doi.org/10.1016/S0960-1481(01)00160-4.

[37] J.T. Mahdi, B.E. Smith, A.O. Sharif, An experimental wick-type solar still system: Design and construction, Desalination. 267 (2011) 233–238. https://doi.org/10.1016/j.desal.2010.09.032.

[38] P.K. Srivastava, S.K. Agrawal, Experimental and theoretical analysis of single sloped basin type solar still consisting of multiple low thermal inertia floating porous absorbers, Desalination. 311 (2013) 198–205. https://doi.org/10.1016/j.desal.2012.11.035.

[39] C.N. Wang, J.H. Torng, Experimental study of the absorption characteristics of some porous fibrous materials, Applied Acoustics. 62 (2001) 447–459. https://doi.org/10.1016/S0003-682X(00)00043-8.

[40] Z. Haddad, A. Chaker, A. Rahmani, Improving the basin type solar still performances using a vertical rotating wick, Desalination. 418 (2017) 71–78. https://doi.org/10.1016/j.desal.2017.05.030.

[41] B.A. Abu-Hijleh, K, Rababah, HM, 2003, Experimental study of a solar still with sponge cubes in basin, Energy Conversion and Management. 44 (2003) 1411–1418.

[42] P.K. Srivastava, S.K. Agrawal, Winter and summer performance of single sloped basin type solar still integrated with extended porous fins, Desalination. 319 (2013) 73–78. https://doi.org/10.1016/j.desal.2013.03.030.

[43] Z.M. Omara, A.E. Kabeel, A.S. Abdullah, F.A. Essa, Experimental investigation of corrugated absorber solar still with wick and reflectors, Desalination. 381 (2016) 111–116. https://doi.org/10.1016/j.desal.2015.12.001.

[44] M. El-Naggar, A.A. El-Sebaii, M.R.I. Ramadan, S. Aboul-Enein, Experimental and theoretical performance of finned-single effect solar still, Desalination and Water Treatment. 57 (2016) 17151–17166. https://doi.org/10.1080/19443994.2015.1085451.

[45] T. Rajaseenivasan, K. Srithar, Performance investigation on solar still with circular and square fins in basin with CO2 mitigation and economic analysis, Desalination. 380 (2016) 66–74. https://doi.org/10.1016/j.desal.2015.11.025.

[46] W.M. Alaian, E.A. Elnegiry, A.M. Hamed, Experimental investigation on the performance of solar still augmented with pin-finned wick, Desalination. 379 (2016) 10–15. https://doi.org/10.1016/j.desal.2015.10.010.

[47] A.E. Kabeel, Z.M. Omara, F.A. Essa, A.S. Abdullah, Solar still with condenser - A detailed review, Renewable and Sustainable Energy Reviews. 59 (2016) 839–857. https://doi.org/10.1016/j.rser.2016.01.020.

[48] S.T. AHM~, STUDY OF SINGLE-EFFECT SOLAR STILL WITH AN INTERNAL CONDENSER, Solar & Wind Technology. 5 (1988) 637–643.

[49] G.N. Tiwari, V.S.V. Bapeshwara Rao, Transient performance of a single basin solar still with water flowing over the glass cover, Desalination. 49 (1984) 231–241. https://doi.org/10.1016/0011-9164(84)85035-3.

[50] A. El-Bahi, D. Inan, A solar still with minimum inclination, coupled to an outside condenser, Desalination. 123 (1999) 79–83. https://doi.org/10.1016/S0011-9164(99)00061-2.

[51] P.K.J. and S.C. NIKOLAI NIJEGORODOV, Thermal-electrical, high efficiency solar stills, Renewable Energy. 4 (1994) 123–127.

[52] B.A.K. Abu-Hijleh, Enhanced solar still performance using water film cooling of the glass cover, Desalination. 107 (1996) 235–244. https://doi.org/10.1016/S0011-9164(96)00165-8.

[53] T. Elango, A. Kannan, K. Kalidasa Murugavel, Performance study on single basin single slope solar still with different water nanofluids, Desalination. 360 (2015) 45–51. https://doi.org/10.1016/j.desal.2015.01.004.

[54] L. Sahota, G.N. Tiwari, Effect of Al2O3 nanoparticles on the performance of passive double slope solar still, Solar Energy. 130 (2016) 260–272. https://doi.org/10.1016/j.solener.2016.02.018.

[55] K. V. Modi, H.K. Jani, I.D. Gamit, Impact of orientation and water depth on productivity of single-basin dual-slope solar still with Al2O3 and CuO nanoparticles, Journal of Thermal Analysis and Calorimetry. 143 (2021) 899–913. https://doi.org/10.1007/s10973-020-09351-1.

[56] R. Sathyamurthy, A.E. Kabeel, E.S. El-Agouz, Ds. Rufus, H. Panchal, T. Arunkumar, A.M. Manokar, D.G.P. Winston, Experimental investigation on the effect of MgO and TiO2 nanoparticles in stepped solar still, International Journal of Energy Research. 43 (2019) 3295–3305. https://doi.org/10.1002/er.4460.

[57] G.B. Balachandran, P.W. David, R.K. Mariappan, A.E. Kabeel, M.M. Athikesavan, R. Sathyamurthy, Improvising the efficiency of single-sloped solar still using thermally conductive nano-ferric oxide, Environmental Science and Pollution Research. 27 (2020) 32191–32204. https://doi.org/10.1007/s11356-019-06661-2.

[58] P. Manoj Kumar, C. Senthil Kumar, K. Muralidharan, Y. Muniratnam, K. Abraham, V. Manikandan, P. Michael Joseph Stalin, S. Jeevan Prasanth, Augmenting the performance of conventional solar still through the nano-doped black paint (NDBP) coating on absorber, Materials Today: Proceedings. 47 (2021) 4929–4933. https://doi.org/10.1016/j.matpr.2021.03.721.

[59] R.P. Arani, R. Sathyamurthy, A. Chamkha, A.E. Kabeel, M. Deverajan, K. Kamalakannan, M. Balasubramanian, A.M. Manokar, F. Essa, A. Saravanan, Effect of fins and silicon dioxide nanoparticle black paint on the absorber plate for augmenting yield from tubular solar still, Environmental Science and Pollution Research. 28 (2021) 35102–35112. https://doi.org/10.1007/s11356-021-13126-y.

[60] H. Panchal, H. Nurdiyanto, K.K. Sadasivuni, S.S. Hishan, F.A. Essa, M. Khalid, S. Dharaskar, S. Shanmugan, Experimental investigation on the yield of solar still using manganese oxide nanoparticles coated absorber, Case Studies in Thermal Engineering. 25 (2021) 100905. https://doi.org/10.1016/j.csite.2021.100905.

[61] S.A. Lawrence, G.N. Tiwari, Theoretical evaluation of solar distillation under natural circulation with heat exchanger, Energy Conversion and Management. 30 (1990) 205–213. https://doi.org/10.1016/0196-8904(90)90001-F.

[62] K.N.B. and B.R.B.K. A. M. Rajesh, Design and performance evaluation of hybrid solar still, International Conference on Control, Automation, Communication and Energy Conservation. 1 (2009) 1–6.

[63] K. Voropoulos, E. Mathioulakis, V. Belessiotis, Experimental investigation of a solar still coupled with solar collectors, Desalination. (2001). https://doi.org/10.1016/S0011-9164(01)00251-X.

[64] A.A. Badran, A.A. Al-Hallaq, I.A. Eyal Salman, M.Z. Odat, A solar still augmented with a flat-plate collector, Desalination. (2005). https://doi.org/10.1016/j.desal.2004.06.203.

[65] O.O. Badran, H.A. Al-Tahaineh, The effect of coupling a flat-plate collector on the solar still productivity, Desalination. 183 (2005) 137–142. https://doi.org/10.1016/j.desal.2005.02.046.

[66] Y.P. Yadav, Analytical performance of a solar still integrated with a flat plate solar collector: Thermosiphon mode, Energy Conversion and Management. (1991). https://doi.org/10.1016/0196-8904(91)90079-X.

[67] R.S. Chaudhari, K. S., Walke, P. V., Wankhede, U. S., & Shelke, An experimental investigation of a nanofluid (Al2O3+ H2O) based parabolic trough solar collectors., Br. J. Appl. Sci. Technol,. 9 (2015) 551-557.

[68] D.G. Subhedar, K. V. Chauhan, K. Patel, B.M. Ramani, Performance improvement of a conventional single slope single basin passive solar still by integrating with nanofluid-based parabolic trough collector: An experimental study, Materials Today: Proceedings. 26 (2019) 1478–1481. https://doi.org/10.1016/j.matpr.2020.02.304.

[69] S.N. Gholamabbas Sadeghi, Retrofitting a thermoelectric-based solar still integrated with an evacuated tube collector utilizing an antibacterial-magnetic hybrid nanofluid, Desalination. 500 (2021) 114871. https://doi.org/https://doi.org/10.1016/j.desal.2020.114871.

[70] O. Mahian, A. Kianifar, S.Z. Heris, D. Wen, A.Z. Sahin, S. Wongwises, Nanofluids effects on the evaporation rate in a solar still equipped with a heat exchanger, Nano Energy. 36 (2017) 134–155. https://doi.org/10.1016/j.nanoen.2017.04.025.

[71] M.K. Gaur, G.N. Tiwari, Optimization of number of collectors for integrated PV/T hybrid active solar still, Applied Energy. 87 (2010) 1763–1772. https://doi.org/10.1016/j.apenergy.2009.10.019.

[72] R. Dev, G.N. Tiwari, Characteristic equation of a hybrid (PV-T) active solar still, Desalination. 254 (2010) 126–137. https://doi.org/10.1016/j.desal.2009.12.004.

[73] M.A. Al-Nimr, W.A. Al-Ammari, A novel hybrid PV-distillation system, Solar Energy. 135 (2016) 874–883. https://doi.org/10.1016/j.solener.2016.06.061.

[74] M. Yari, A.E. Mazareh, A.S. Mehr, A novel cogeneration system for sustainable water and power production by integration of a solar still and PV module, Desalination. 398 (2016) 1–11. https://doi.org/10.1016/j.desal.2016.07.004.

[75] V. Velmurugan, J. Mandlin, B. Stalin, K. Srithar, Augmentation of saline streams in solar stills integrating with a mini solar pond, Desalination. 249 (2009) 143–149. https://doi.org/10.1016/j.desal.2009.06.016.

[76] S. Kumar, A. Dubey, G.N. Tiwari, A solar still augmented with an evacuated tube collector in forced mode, Desalination. 347 (2014) 15–24. https://doi.org/10.1016/j.desal.2014.05.019.

[77] M.B. Shafii, M. Shahmohamadi, M. Faegh, H. Sadrhosseini, Examination of a novel solar still equipped with evacuated tube collectors and thermoelectric modules, Desalination. 382 (2016) 21–27. https://doi.org/10.1016/j.desal.2015.12.019.

[78] Z.M. Omara, M.A. Eltawil, E.A. ElNashar, A new hybrid desalination system using wicks/solar still and evacuated solar water heater, Desalination. 325 (2013) 56–64. https://doi.org/10.1016/j.desal.2013.06.024.

[79] H.K. Gupta, G. Das Agrawal, J. Mathur, An experimental investigation of a low temperature Al2O3-H2O nanofluid based direct absorption solar collector, Solar Energy. 118 (2015) 390–396. https://doi.org/10.1016/j.solener.2015.04.041.

[80] V. Khullar, V. Bhalla, H. Tyagi, Potential heat transfer fluids (Nanofluids) for direct volumetric absorption-based solar thermal systems, Journal of Thermal Science and Engineering Applications. 10 (2018). https://doi.org/10.1115/1.4036795.

[81] M. Vakili, S.M. Hosseinalipour, S. Delfani, S. Khosrojerdi, Solar Energy Materials & Solar Cells Photothermal properties of graphene nanoplatelets nano fl uid for low-temperature direct absorption solar collectors, Solar Energy Materials and Solar Cells. 152 (2016) 187–

191. https://doi.org/10.1016/j.solmat.2016.01.038.

[82] M. Karami, M.A. Akhavan-Bahabadi, S. Delfani, M. Raisee, Experimental investigation of CuO nanofluid-based Direct Absorption Solar Collector for residential applications, Renewable and Sustainable Energy Reviews. 52 (2015) 793–801. https://doi.org/10.1016/j.rser.2015.07.131.

[83] N. Singh, V. Khullar, Efficient Volumetric Absorption Solar Thermal Platforms Employing Thermally Stable - Solar Selective Nanofluids Engineered from Used Engine Oil, Scientific Reports. 9 (2019) 1–12. https://doi.org/10.1038/s41598-019-47126-3.

[84] A.K. Kaushal, M.K. Mittal, D. Gangacharyulu, An experimental study of floating wick basin type vertical multiple effect diffusion solar still with waste heat recovery, Desalination. 414 (2017) 35–45. https://doi.org/10.1016/j.desal.2017.03.033.

[85] N. Rahbar, J.A. Esfahani, A. Asadi, An experimental investigation on productivity and performance of a new improved design portable asymmetrical solar still utilizing thermoelectric modules, Energy Conversion and Management. 118 (2016) 55–62. https://doi.org/10.1016/j.enconman.2016.03.052.

[86] G.S. Dhindsa, M.K. Mittal, Experimental study of basin type vertical multiple e ff ect di ff usion solar still integrated with mini solar pond to generate nocturnal distillate, Energy Conversion and Management. 165 (2018) 669–680. https://doi.org/10.1016/j.enconman.2018.03.100.

[87] S.W. Sharshir, G. Peng, A.H. Elsheikh, E.M.A. Edreis, M.A. Eltawil, T. Abdelhamid, A.E. Kabeel, J. Zang, N. Yang, Energy and exergy analysis of solar stills with micro/nano particles: A comparative study, Energy Conversion and Management. 177 (2018) 363–375. https://doi.org/10.1016/j.enconman.2018.09.074.

[88] Z.M. Omara, A.E. Kabeel, M.M. Younes, Enhancing the stepped solar still performance using internal and external reflectors, Energy Conversion and Management. 78 (2014) 876–881. https://doi.org/10.1016/j.enconman.2013.07.092.